p53-REGULATED HEXOKINASE 1b IS A NOVEL TARGET FOR METABOLIC THERAPY AGAINST NON–SMALL-CELL LUNG CANCER

by

YASEMİN YOZGAT

Submitted to the Graduate School of Engineering and Natural Sciences in partial fulfilment
of the requirements for the degree of Doctor of Philosophy

Sabancı University

July 2019

p53-REGULATED HEXOKINASE 1b IS A NOVEL TARGET FOR METABOLIC THERAPY AGAINST NON–SMALL-CELL LUNG CANCER

APPROVED BY:

Prof. Dr Hüveyda Başağa..
(Thesis Supervisor)

Prof. Dr. Devrim Gözüaçık...

Asst. Prof. Dr. Murat Alper Cevher ....

Prof. Dr. Ülkan Kılıç ....

Asst. Prof. Dr. Bilal Ersen Kerman ....

DATE OF APPROVAL: 19/JULY/2019

© 2019
Yasemin Yozgat

All Rights Reserved

p53-REGULATED HEXOKINASE 1b IS A NOVEL TARGET FOR METABOLIC THERAPY AGAINST NON–SMALL-CELL LUNG CANCER

YASEMİN YOZGAT

Molecular Biology, Genetics and Bioengineering, Doctor of Philosophy, July 2019

Thesis Supervisor: Prof. Dr. Hüveyda Başağa

Keywords: Non-small cell lung cancer (NSCLC), hexokinase 1b, tumor suppressor 53 (p53), glycolysis, cisplatin, drug targets, apoptosis, autophagy

ABSTRACT

Deregulation of glycolysis is common in non-small cell lung cancer (NSCLC). p53 controls the cellular metabolism pathway by activating hexokinases (HKs) to increase glycolysis. HK enzymes catalyze the phosphoryl-group-transfer in glucose metabolism. Unlike HK2, HK1 has several transcript variants. However, the functional differential roles of HK1 isoforms in glucose metabolism and the malignant tumor progression are still elusive. Here, we show that primary NSCLC patient tumor cells metabolically differ from the normal lung epithelium in that they display predominant expression of one of the HK1 isoforms, hexokinase1b (HK1b). Interestingly, we show that p53 positively regulates HK1b expression using CRISPR-Cas9 system. We utilized CRISPR-Cas9 system to selectively target specific HK1b isoform in NSCLC and show that silencing HK1b in NSCLC cells inhibits tumorigenesis through diminishing glycolysis and proliferation. Finally, HK1b deletion sensitizes NCLC cells to cisplatin treatment and the combination therapy synergistically increases both the p53- mediated apoptotic cell death by cisplatin and autophagic cell death by increased formation of LC3-II associated autophagic vesicles and myelinoid bodies in an AMPK-independent manner. Our findings reveal that targeting HK1b isoform alone or in combination with cisplatin may represent a novel strategy for NSCLC patients.

KÜÇÜK HÜCRELİ DIŞI AKCİĞER KANSERİNDE p53 TARAFINDAN REGULE EDİLEN HK1b METABOLİC TEDAVİ İÇİN YENİ BİR HEDEFTİR.

YASEMİN YOZGAT

Moleküler Biyoloji, Genetik ve Biyomühendislik, Doktora Tezi, Temmuz 2019

Tez Danışmanı: Prof. Dr. Hüveyda Başağa

Anahtar kelimeler: Küçük hücreli dışı akciğer kanseri (KHDAK), heksokinaz 1b, p53, glikoliz, cisplatin, ilaç hedefleri apoptoz, otofaji

ÖZET

Küçük hücreli dışı akciğer kanserinde (KHDAK) glikolizin deregülasyonu yagın olarak görünen kanser karakteristiklerinden biridir. p53 glikolizi arttırmak için hexokinaz (HK) enzimlerini aktive eder ve böylelikle glukoz metabolizma yolağını kontrol eder. HK enzimleri glukoz metabolizmasında fosforil-grup transferini katalize etmek için görevlidir. HK2 den farklı olarak HK1 geni birden fazla transcript varyantlarına sahiptir fakat bu HK1 izoformlarının glukoz metabolizmasında ve malign tümör gelişiminde fonksiyonel diferansiyel rolleri halen belirsizdir. Bu çalışmamızda ilk olarak KHDAK hasta tümör hücrelerinin HK1 izoformlarından biri olan HK1b izoform genin yüksek baskın ifadesi sebebi ile metabolik olarak normal akciğer epitel hücrelerinden farklı olduğunu gösterdik. Ayrıca, ilginçtirki p53 genin HK1b izoform ifadesini pozitif olarak regüle ettiğni gösterdik. KHDAK'de spesifik HK1b izoformunu seçici olarak hedeflemek ve KHDAK hücrelerinde gen ifadesi baskılanmış HK1b'nin glikolizi ve proliferasyonu azaltmasına sebep verdiğini ve böylece tümörijenezi inhibe edebildiğni göstermek amacı ile CRISPR-Cas9 sistemi kullandık. Son olarak, HK1b izoform susuturulması KHDAK hücrelerini sisplatin tedavisine karşı hassaslaştırdığını gösterdik. Kombinasyon terapisi sinerjitik olarak p53-aracılı apoptotik hücre ölümünü sisplatin aracılığı ile arttırıken diğer yandan artan LC3-II ile ilişkili otofajik kesecikler ve miyelinoid cisimlerin artması sebebi ile AMP- activated protein kinaz (AMPK)'den bağımsız olarak otofojik hücre ölümüne sebep verdiğni gösterdik. Bulgularımız, HK1b izoformunun tek başına veya sisplatin ile kombinasyon halinde KHDAK hastaları için özgün ve yeni bir ilaç tedavi strateji olabiliceğini ortaya koymuştur.

ACKNOWLEDGEMENTS

What do you secretly dream about that makes your heart beat so loud and so fast you simply can’t ignore it? What you want the most in your life becomes the biggest test in your life. This is the story of my PhD life. I have devoted most of my life to research and it was the most challenging time. I gave up of so many things. Nonetheless, I never gave up and kept plugging away for persuading my goal. This has not been a simple PhD degree for me and what I called it is a miracle. I always remember the quote from great scientist Nicole Tesla:

“I do not think there is any thrill that can go through the human heart like that felt by the inventor as he sees some creation of the brain unfolding to success… Such emotions make a man forget food, sleep, friends, love, everything.”

I would not have been able to find the strength if it were not for the help and support of mentors, professors, colleagues, friends, and of course loved ones and family. Although it is impossible to mention everyone by name, some of them deserve special mention.

I would like to thank my dissertation supervisor Prof. Dr. Hüveyda Başağa for providing indispensable advice, information and cooperation and all jury members Prof. Dr. Devrim Gözüaçık, Prof. Dr. Ülkan Kılıç Dr. Murat Alper Cevher, and Assoc. Prof. Dr. Bilal Ersan Kerman for their constructive comments, ideas, and supports.

I would also like to extend special thanks to Medipol university REMER family. First of all I would like to start with REMER director Prof. Dr. Gürkan Öztürk: thank you for your direction, understanding and your support. You were not only my mentor but also a valuable guide. Thank you for believe in me and opening all the resources for me to achieve my goal. I also want to special thanks to Prof. Dr. Ertuğrul Kılıç: you are the reason I have started my journey at Medipol University. You were my guidance but also big brother to me. I would like to thank both of you for listening to me whenever I had a question or problem, whether it had to do with my research or my future career aspirations. Thank you both of you also for pushing me to become a better scientist and a better communicator. Prof. Dr. Hasan Korkaya: you were not only my mentor but the guidance

you gave me was valuable to not only my research but to my life. Thank you helping me whenever I needed it. Prof Dr. Adil Mardinoğlu: without any hesitation you did not only opened your resources to me but you also believed in me. Thank you for all your help and giving me the motivation that I need.

How could I write an acknowledgment section and not mention my mentor and long-term dear friend, Dr. Murat Alper Cevher? Words are not enough to describe all you've done for me. Among other things, thank you for opening your lab and resources to me. I couldn't do this without your mentorship. I would like to thank to Bilkent university family. I need to special thanks to Murat Cevher lab members. Everyone at Bilkent University was very kind and helpful. They opened their labs, resources for helping me to achieve my goal. It is hard to mention everyone names. My friend Yasemin Barış: you were always by my side, helping me to go through my pain. Thank you for your support and friendship. Professor İhsan and Mayda Gürsel, Özgür Şahin, Serkan Göktuna, Tieu-Lan Chau-all your valuable work on my research were indispensable. Thank you for not only helping me but being by my side to achieve my goal.

My dear friend Emre Karakoç: words also cannot describe how much your help and friendship is valuable for me. I would never do this work without your help. Thank you for your friendship, your collaboration. It means world to me.

My extended family: Ülkan Kılıç, Arzu Şakul, and Şule Ayla you were all more than colleagues- you were my family. You were always by my side every time when I needed and anytime I fell into hopeless you gave me the strength to make me a strong person. Words are not enough to describe the appreciation and the love. I would not stay strong and encouraged without your help and support. Thank you for being in my life. To my dear friends YalçınGünal, Mehmet Ozansoy: thank you guys for listening, cheering me up and giving me the motivation that I need. I am really lucky to have you in my life.

My dear long-term friends Meral Yüce and Hasan Kurt: I don’t know how to thank you guys. You cheered me up and you gave me the strength when I needed it. You were always there to help me without any hesitation. Thank you for your all support and friendship.

I am obliged to dear friends Mihriban Karaayvaz and her husband Murat Yıldırım, who gave their pure friendship and support to me. They were able to reach me from Boston to keep me strong and gave me the motivation and help I need. I feel very lucky to have them in my life.

I am very grateful to my dear friends and collogues Özge Şensoy, Yasemin Yüksel Durmaz, and Şerif Şentürk for their not only friendship but also helping me on my research to achieve my goal. My dear friends Bilal and Özge Kerman, Deniz Atasoy and Nilüfer Sayar: During these difficult times I had great time with you guys. Thank you cheering me up, advising me when I need, and helping me without any hesitation. I really do appreciate your support and friendship.

To my lovely student Şeyma Kablan: thank you so much for your support! You helped me whenever I needed it. I really appreciate it. This project wouldn’t have gone far without your help. I know you will have an amazing future and I am so proud of you!

To Meditam family: Ekrem Özdemir, Ali Şenbahçe, Barış Cebeci, Ömer Kuzu, to all REMER family: Taha Keleştemur, Kaan Alkan, Mehmet Şerif Aydın, Burak Çağlayan, Çağlar Beker, Arda Kebapçı,, Olgu Enis Tok, Sadık Bay, Gülsena Baydaş, Büşra Batğı, Mehtap Şimşek, Bircan Kolbaşı, Emre Vatandaşlar and REMER genetic lab members: Fırat Çaralan, Nilgün Genç, Zeynep Doğru, and Aslı Güner: were immensely helpful with portions of this study. You are there for me whenever I need you with a helping hand. I am very luck to know each of you. To my dear friend Berrak Çağlayan: thank you for listening me whenever I cried. You have witnessed the most of my painful times and your help was so meaningful that no words can describe it.

Many friends provided emotional support throughout these two long years but I can only mention a few names. My childhood friend, my sister, Nazan Aykent has been there long before this journey began, and has never left my side. To my special family Havva and Cem İpek: Thank you for your pure love and friendship. Your support and unconditional love made me strong person. To another sister, Seçil Aydın and her family Naciye and İrfan Aydın: Thank you for being there for me whenever I need you. Berrin and Alaaddin Candan, – I am lucky to have known you! You were always being my family. Thank you for being in my life and giving me the strengths I need.

I must express my gratitude to my love Kevin Byrne for providing me strength in moments of doubt and for his love and unending support. I don't know how I am able to get through this process without you always by my side. Words cannot describe how much I love you. As we finish this chapter of our lives and move on to new adventures, whatever life has in store for me, I am not afraid, because I have you.

Finally, to my parents Hasan Yozgat and Nuriye Yozgat, my brother Ihsan Yozgat and his wife Zehra, my sister Pembegul Yozgat, my niece Esra Hüma Yozgat and my little nephew Hasan Selim Yozgat, my aunt Emine Aydogdu and my cousins Saime Aydoğdu and her husband Bülent Teymur: I cannot thank you enough. Thank you for your unconditional love and support. Your presence continues to give me strength. I can never reach where I am without their love and support.

Dedication

To my parents Hasan Yozgat and Nuriye Yozgat. I love you so much

ABSTRACT iv
ÖZET vi
ACKNOWLEDGEMENTS viii
LIST OF FIGURES xv
LIST OF TABLES xx
LIST OF SYMBOLS AND ABBREVIATIONS xxi
1 BACKGROUND 1
  1.1 Lung Cancer 1
  1.2 Non-small cell lung cancer 1
    1.2.1 The most common mutation seen in NSCLC patients 3
    1.2.2 Role of p53 pathway in NSCLC 4
  1.3 Cancer metabolism 7
    1.3.1 Role of PI3K/AKT signaling in cancer metabolism 10
    1.3.2 Role of MAPK/ERK signaling in cancer metabolism 13
    1.3.3 Role of p53signaling in cancer metabolism 14
  1.4 HEXOKINASES 15
2 INTRODUCTION 20
3 MATERIALS AND METHODS 23
  3.1 Chemicals, solutions antibodies and reagents 23
  3.2 Cell culture and treatment 24
    3.2.1 Cell Proliferation by FACS Analysis 24
    3.2.2 Cell viability assay 24
    3.2.3 Measurement of oxygen consumption rate and extracellular acidification rates 25
  3.3 Gene knockout in lung cancer cells 25
  3.4 Patient Tissue collection and immunohistochemical staining 25
  3.5 *In vivo intra-tracheal* xenograft tumorigenesis assay. 26
  3.6 RNA isolation and quantitative PCR 26
  3.7 Western blot analysis 27
    3.7.1 Protein extraction 27
    3.7.2 SDS-Polyacrylamidegelelectrophoresis (SDS-PAGE) 27
    3.7.3 Protein Transfer and Immunoblooting 28

3.8 The Cancer Genome Atlas NSCLC cohort analyses and GSEA analysis 28
3.9 Statistical analysis. 29
4 RESULTS 30
4.1 HK1 expression is upregulated in human NSCLCs and is associated with poor clinical outcome in patients 30
4.2 Human NSCLC cells express one of the HK1 isoforms- hexokinase1b (HK1b) as a poor prognostic factor 32
4.3 p53 positively regulates HK1b expression 38
4.4 Deletion of HK1b suppresses cell proliferation and tumorigenesis in NSCLC cells via regulating glycolytic activity 42
4.5 HK1b plays critical role in cisplatin response, metabolism, and survival in NSCLC cells .. 48
4.6 Deletion of HK1b sensitizes cells to cisplatin induced cytotoxicity via p53 mediated apoptotic and autophagic cell death. 52
5 DISCUSSION 57
6 CONCLUSION AND FUTURE WORK 61
7 BIBLIOGRAPHY 63
8 APPENDIX A SUPPLEMENTARY MATERIAL and METHOD 74
8.1 Sample Preparation for TEM 74
8.2 DNA Fragmentation analysis 74
8.3 Structure Preparation 74
8.4 Molecular Dynamics Simulations 74

LIST OF FIGURES

Figure 1.2.1 A) Frequency of driver mutations in lung ADC and B) driver mutation candidates in lung SCC 2

Figure 1.2.2 Distribution of Kras mutations in NSCLC. 3

Figure 1.2.3 Distribution of TP53 mutations in NSCLC subtypes 4

Figure 1.2.4 Scheme of p53 signaling pathway 5

Figure 1.2.5 Mutaional hotspots residues of p53 in lung cancer.. 6

Figure 1.2.6 Functions of mutant p53 during the evolution of a cancer cell transformation. 6

Figure 1.3.1 Changes in metabolic reprogramming during tumorigenesis. 9

Figure 1.3.2 Connection of metabolic reprogramming with other seven hallmarks of cancer. 10

Figure 1.3.3 GSK3β role in regulation of Mitochondrial-bound HKs (HK1 and HK2). 13

Figure 1.3.4 p53 role in regulation of metabolic pathway. 15

Figure 1.4.1 HK izosymes a) metabolic roles of HK b) structure of HK subtypes c) Tight coupling of both mtHK1 and mtHK2 to ATP generated by mitochondria. 17

Figure 1.4.2 HK1 mRNA gene expression profiles. 19

Figure 4.1.1 HK1 expression is upregulated in human NSCLC from western blot analyses. Protein was isolated from NSCLC tumor and adjacent-non tumor samples and HK1 level was determined by WB analyses **A)** protein lysates of human NSCLC tumor (n=6), normal lung (n=4); **B)** protein lysates of human NSCLC tumor (n=7), normal lung (n=6). **C)** Quantification of HK1 and HK2 levels in NSCLC tumor (n = 13) and normal lung samples (n=10). 31

Figure 4.1.2 HK1 expression is upregulated in human NSCLC from IHC analyses and is associated with a poor overall survival. **A)** Immunohistochemical staining of HK1 expression and H&E staining in representative human NSCLC tumor (left) and the surrounding normal tissue (right). Images are 40X magnification; insets are 200X magnification. Scale bars, 100 µm. **B)** the prognostic values of HK1 in NSCLC patients (n=226). Tumors were separated into two groups according to HK1 expression levels (high or low). The high expression of HK1 is correlated to worse survival (p=0.013)................ 32

Figure 4.2.1 **A)** RefSeq gene annotations of HK1 isoforms (HK1a, HK1b and HK1c) and HK2. HK1a and HK1b isoforms possess one extra exon, which is missing in HK1c. B) Structural alignment between crystal structures of HK1b and HK1c model. The extra exon in HK1b, which is shown in blue, codes for 32-amino acid long alpha-helix that is part of the small sub-domain of N-terminus. For the sake of simplicity only one monomer is shown. HK1b isoform levels were elevated in NSCLC tumors compared with normal lung tissue.. 35

Figure 4.2.2 HK1b isoform upregulation in NSCLC patients **A)** Representative semi q-PCR amplification results for HK1 isoforms, HK2 and P53 in H1299 and A549 cells. **B)** Immunoblot analysis of HK1 and HK2 in A549 and H1299 cells. **C)** Representative semi q-PCR amplification results for HK1 isoforms, HK2 and P53 in NSCLC patient tumors (n=3). **D)** RNA was extracted from NSCLC patient normal lung and tumor samples, HK1b, HK1c, HK2 (normal n=6, tumor n=6) and p53 (normal n=7, tumor n=7) levels were determined by qRT-PCR. mRNA levels were normalized to ACTB mRNA. Data are from two or three independent experiment as triplicate, presented as mean ± SEM, Student’s t test 36

Figure 4.2.3 Increased expression of the HK1b isoform is associated with worse prognosis from TCGA NSCLC patient data **A)** Kaplan–Meier plots showing the association of HK1b isoform overexpression between normal and TCGA Lung adenocarcinoma samples in patients from the TCGA cohort. Kaplan–Meier survival curves **B)** adenocarcinoma (n = 501) and **C)** squamous cell carcinoma (n = 489), patients stratified according to low or high HK1b expression levels. P values indicate significance levels from the comparison of survival curves using the Log-rank (Mantel-Cox) test.. 37

Figure 4.3.1 PCR and DNA fragmentation analysis of **A)** p53 elimination at the target loci, indicating insertion of 104 bp nucleotides resulting in a frame-shift mutation. **B)** HK1b isoform elimination at the target loci, indicating deletion of 14 bp nucleotides resulting in a frame-shift mutation... 40

Figure 4.3.2 Elimination of p53 and HK1 b isoform. A549 p53-/- and A549 WT cells were analyzed by **A)** qRT-PCR for level of HK1 b, c, HK2, and p53 in A549 p53-/- cells. Error bars indicate mean ± SEM, (n=3) or **B)** Immunoblot analysis of p53 KO in A549 cells. A549 HK1b-/- and A549 WT cells were analyzed by **C)** qRT-PCR for level of HK1 b, c, HK2, and p53 in A549. Error bars indicate mean ± SEM, (n=3) or **D)** Immunoblot analysis of HK1b KO in A549 cells. E) Immunofluorescence analysis of p53 KO and HK1b KO in A549 cells. 42

Figure 4.4.1 RMSF Plot shows four major regions fluctuating in HK1c and HK-2 while HK1b is more stable. Structure of HK1c is shown in the figure, first region (1) responsible for ligand binding in N-terminal and a part of small sub-domain (which is responsible for opening and closing of ligands binding pocket), second region (2) ligand binding site in C-terminal part of small sub-domain, third region (3) C-terminal part of large domain and involved in ATP binding, fourth region (4) near to Glucose binding site of C-terminal large domain. 44

Figure 4.4.2 Effect of HK1b knockout on metabolism and proliferation of A549 cells. Seahorse metabolic analysis **A)** of OCR values from mitochondrial stress test, and **B)** of glycolysis stress test in A549 HK1b-/- and A549 WT cells. Experiments were performed at least twice in quadruplicates for OCR and once for quintuple for ECAR. The results are presented as the mean ± SEM and means compared with Student's t test. **C)** Ki-67 proliferation flow cytometry analysis of A549 WT and A549 HK1b-/-. 45

Figure 4.4.3 Effect of HK1b knockout on tumorigenicity of A549 cells. **A)** A549 WT or A549 HK1b-/- cells were intra-tracheally injected into immunodeficient NSG male mice. Graphs on the left show tumor volume in (n=7, each) A549 WT (control) and A549 HK1b-/- (n=7) mouse and representative images of resected tumors on the left. Tumor volumes presented as mean ± SEM, two-tailed unpaired t-test. **B)** Immunohistochemical staining of HK1 expression and H&E staining in representative mouse xenograft A549WT tumor (left) and A549 HK1b-/- tumor (right). Images are 40X magnification; insets are 200X magnification. Scale bars, 100 µm. **C)** Representative photographs of Ki-67 expression in xenografts of A549 WT (left) and A549 HK1b-/- (right) stained by IHC in upper panel. Number of Ki-67 positive cells is counted per area (mm2) from 5 different fields in 8 different slides. The results are presented as the mean ± SEM and means compared with Student’s t test. 47

Figure 4.5.1HK1b KO role in cisplatin response on metabolism, **A)** OCR analysis of untreated or 6hrs cisplatin treated A549 WT and A549 HK1b-/- cells. Experiments were performed twice in quadruplicates for OCR. The results are presented as the mean ± SEM and means compared with one-way ANOVA and Tukey's post hoc test. **B)** ECAR analysis of untreated or 6hrs cisplatin treated A549 WT and A549 HK1b-/- cells. Experiments were performed once for quintuple for ECAR. The results are presented as the mean ± SEM and means compared with one-way ANOVA and Tukey's post hoc test 50

Figure 4.5.2 HK1b KO role in cisplatin response **A)** A549 WT and A549 HK1b-/- cells were treated with increasing concentrations of cisplatin (0.1 μM–100 μM) for 48 h. Dose-response curves were generated from which IC50 values were deduced (n=2). **B)** Flow cytometric quantification analysis of propidium iodide (PI) staining in A549 WT and A549 HK1b-/- cells as unstained, untreated, and treated with cisplatin (75μM and 47 μM, respectively), (n=2). 51

Figure 4.5.3 Immunoblot analysis of cells treated with cisplatin (75μM and 47 μM, respectively) or rapamycin (100μM and 47 μM, respectively). **A)** Immunoblot analysis of apoptosis markers. **B)** Immunoblot analysis of HK1 and Bcl-2. Anti-beta-actin is used as a loading control. **C)** Immunoblot analysis of AKT, GSK3β, ERK, and STAT3. 52

Figure 4.6.1 Synergetic effect HK1b ablation and cisplatin increases p53-mediated apoptotic cell death. Immunoblot analysis of cells treated with cisplatin (75μM and 47 μM, respectively) or rapamycin (100μM and 47 μM, respectively) **A)** Immunoblot analysis of p53 and H2AX **B)** Representative transmission electron microscopy (TEM) micrographs displaying characteristics of apoptosis; images are representative of two independent experiments; scale bar, 1 µm (left) and 400 nm (right). 54

Figure 4.6.2 Synergetic effect HK1b ablation and cisplatin increases autophagic cell death. Immunoblot analysis of cells treated with cisplatin (75μM and 47 μM, respectively) or rapamycin (100μM and 47 μM, respectively) **A)** Immunoblot analysis of AMPKα, LC3B I/II, Beclin-1, ATG13, mTOR. Anti-beta-actin is used as a loading control. **B)** Representative transmission electron microscopy (TEM) micrographs displaying characteristics of autophagy; images are representative of two independent experiments; scale bar, 2µm (left) and 400 nm (right). Red arrows represent autophagic vesicles, black starts represent myelinoid bodies and n refers to nuclear fragment. 56

LIST OF TABLES

Table 4-1 List of total 18 NSCLC patients’ clinical details is included in this study. 30

LIST OF SYMBOLS AND ABBREVIATIONS

18FDG	Fluoro-deoxy Glucose (18)
3D	3 Dimensions
A549	Non- small-cell Lung Carcinoma Cell Line (p53 WT)
AMPK 5'-	AMP activated kinase
ATP	Adenosine-5'-triphosphate
BAX	BCL2-Associated X Protein
BCL-2	B-cell lymphoma 2
CRISPR	Clustered Regularly Interspaced Short Palindromic Repeats
Cas	CRISPR associated
Caspases	Cysteine Proteases with Aspartate Specificity
cDNA	Complementary deoxyribonucleic acid
DNA	Deoxyribonucleic acid
EDTA	Ethylene-Diamine-Tetra-Acetic acid
ERK	Extracellular Receptor Kinase
FACS	Fluorescence Activated Cell Sorting
FBS	Fetal Bovine Serum
G6P	Glucose 6-phosphate
GFP	Green fluorescent protein
Glc	Glucose
H1299	Non- small-cell Lung Carcinoma Cell Line (p53 null)
IHC	Immunohistochemistry
MAPK	Mitogen Activated Protein Kinase
mRNA	messenger Ribonucleic acid
mTOR	Mammalian Target of Rapamycin

mtDNA	Mitochondrial DNA
NSCLC	Non–small-cell lung cancer
NADP	Nicotianamide adeninine diphosphate-oxidized
NADPH	Nicotianamide adeninine diphosphate-reduced
O2	Oxygen
PET	Positron Emission Tomography
PI3K	PhosphatidylinositolV3Vkinase
PMSF	Phenylmethylsulfonyl fluoride PPP Pentose phosphate pathway
pSer	Phosphoserine
PVDF	Polyvinylidene fluoride
PCR	Polymerase Chain Reaction
qRT-PCR	Quantitative real-time polymerase chain reaction
RPMI	Roswell Park Memorial Institute medium
RNA-Seq	RNA Sequencing
rpm	Rotation per minute
SDS PAGE	Sodium Dodecyl Sulfate Polyacrylamide Gel Electrophoresis
STAT3	Signal Transducer and Activator of Transcription 3
TCA	Tri-carboxylic acid
TCGA	The Cancer Genome Atlas Program
TEM	Transmission electron microscopy
WT	Wild type

1 BACKGROUND

1.1 Lung Cancer

Lung cancer is the most common malignancy and leading cause of cancer deaths worldwide. A total of 1.8 million new cases of lung cancer and 1.6 million related deaths were reported in 2012 [1]. The processes of lung tumor initiation and progression may be modulated by multistep carcinogenesis factors that contribute to induction of DNA damage and mutations, which occur naturally or via environmental factors [2, 3]. Although tobacco use causes 80% to 90% of all lung cancers, many other environmental exposure causes of lung cancer are identified such as arsenic, asbestos, radon, nickel [4]. The diagnostic evaluation for suspected lung cancer has three simultaneous steps includes tissue diagnosis, staging, and determination of functional capacity. Management of lung cancer patients is based on individual tumor histology, molecular diagnosis, tumor staging, and performance status [2, 5, 6]. Patient selection in lung cancer as of today is based on the recognition of both different histological subtypes and driver mutations that determine the biology of these malignancies [7, 8]. There are two main types of primary lung cancer: small-cell lung cancer (SCLC) represents about 15 to 20% of cases and non–small-cell lung cancer (NSCLC) accounts 80 to 85% of cases. Even though both cancers affect the lungs but they have several key differences, including how they are treated and their average progression time [9, 10].

1.2 Non-small cell lung cancer

Non-small-cell lung cancers (NSCLCs) is the most common type of all lung cancer, are known to have diverse pathological features. NSCLC is sub-classified based on the histological features into three types: squamous-cell lung carcinoma, lung adenocarcinoma, and large-cell lung carcinoma [8, 11].

Squamous-cell lung carcinoma (lung SCC) is made up 25–30% of all lung cancer cases. Squamous cell lung cancer begins in the squamous cells in the airway epithelial. Most squamous cell carcinomas of the lungs are located in the bronchial tubes in the center of the lungs. Lung SCC subtype is strongly correlated with cigarette smoking, accounting for approximately 95% of cases [11-13].

The most common type of lung cancer is lung adenocarcinoma (lung ADC), represents about 40% of all lung cancers. It evolves from small mucosal glands, type II alveolar cells, in the lung periphery [14]. Although most cases of lung ADC subtype is usually associated with smoking, is the most common form of lung cancer to occur in patients who have never smoked [11].

NSCLC is histologically and molecularly heterogeneous, which reflects changes in the biology and clinical implication of the disease [15]. Immunohistochemistry (IHC) is currently one the main tool to distinguish between lung SCC and lung ADC along with the observation of morphological changes. Expression of cytokeratin- 5 and cytokeratin-6 and/or the transcription factors SRY-box 2 (SOX2) and p63 are indicators of lung SCC whereas expression of thyroid transcription factor (TTF)-1 is the main indicator of lung ADC subtype [10, 16, 17]. It is generally accepted that there are different cells-of –origin, which drive the distinct phenotypes and genotypes of NSCLCs [10]. Recent advances in genomic studies of NSCLC, particularly in lung ADC, have discovered several driver mutations that potentially can be used for targeted therapy or disease progression. The most common driver genetic alterations in lung ADC and driver mutation candidates in lung SCC are shown in Figure 1.2.1 [18, 19].

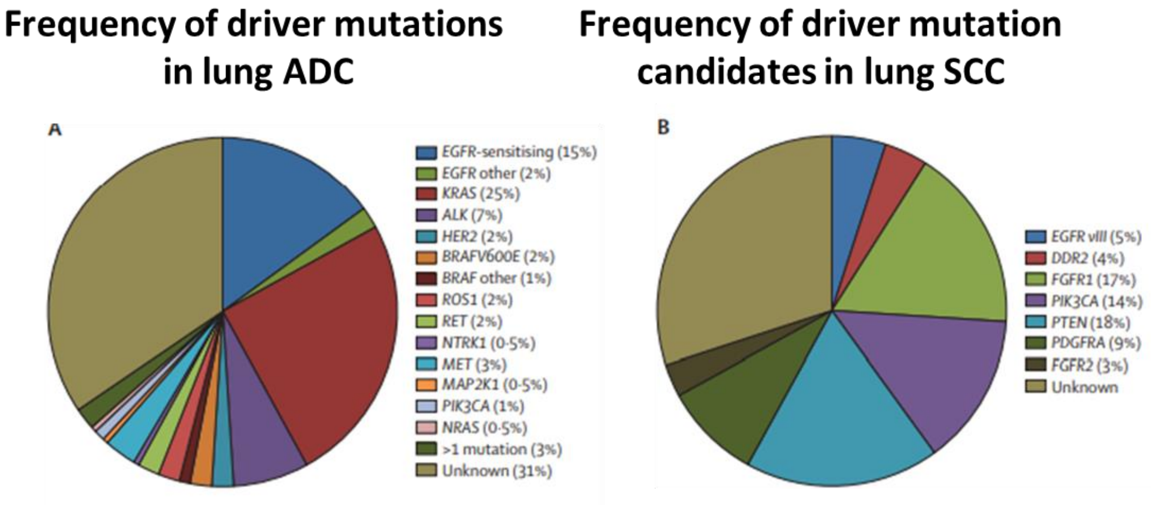

Figure 1.2.1 A) Frequency of driver mutations in lung ADC and B) driver mutation candidates in lung SCC

1.2.1 The most common mutation seen in NSCLC patients

KRAS and *EGFR* activating mutations are commonly mutated genes in lung ADC patients [8]. An anaplastic lymphoma kinase (ALK) rearrangement is only seen in lung ADC and only accounting for 7 to 8% of all lung ADC patients. *EGFR* (epidermal growth factor receptor) is mutated, in about 10 to 15% of patients with lung ADC and 5% with lung SCC. About 25% of *KRAS* -activating mutations is commonly seen in patients with lung ADC, and more than 97% of *KRAS*-mutant cases affect exon 2 and 3 (G12, G13, and Q61) (Figure 1.2.2) [8, 19, 20]. Mutations in *TP53* gene is the most common alterations seen in NSCLC and 80% of these alterations are located in the DNA binding domain as a missense mutations. The frequency TP53 mutation is 70% to 80% in lung SCC and 50% in lung ADC (Figure 1.2.3) [21, 22]. Most clinical studies suggest that TP53 alterations in patients with NSCLC displays worse prognosis and may be relatively more resistant to chemotherapy and radiation [22].

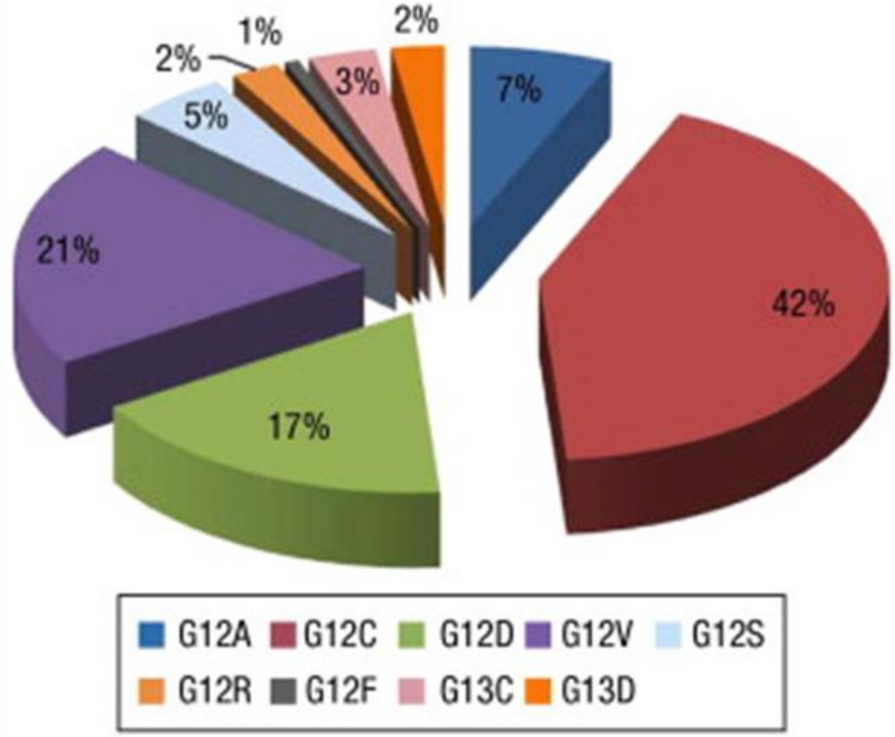

Figure 1.2.2 Distribution of Kras mutations in NSCLC.

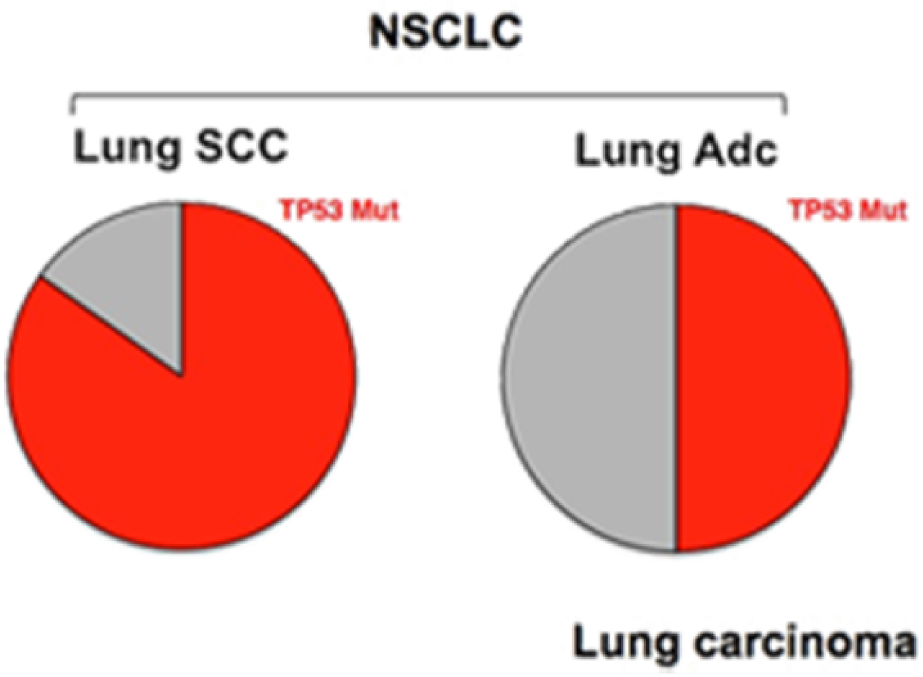

Figure 1.2.3 Distribution of TP53 mutations in NSCLC subtypes

1.2.2 Role of p53 pathway in NSCLC

Potent activator of p53 function serves as a DNA damage checkpoint [23]. In response to oncogenic cellular stresses, such as DNA damage, p53 protein acts as a transcription factor that regulates diversity of biochemical activities including transient cell cycle arrest, cellular senescence and apoptosis [24]. However, recent studies showed that p53 has also other important regulatory role in other cellular processes such as cellular metabolism [25, 26]. Upon stress signals, p53 pathway in cellular response is simplified in figure 1.2.4 [27].

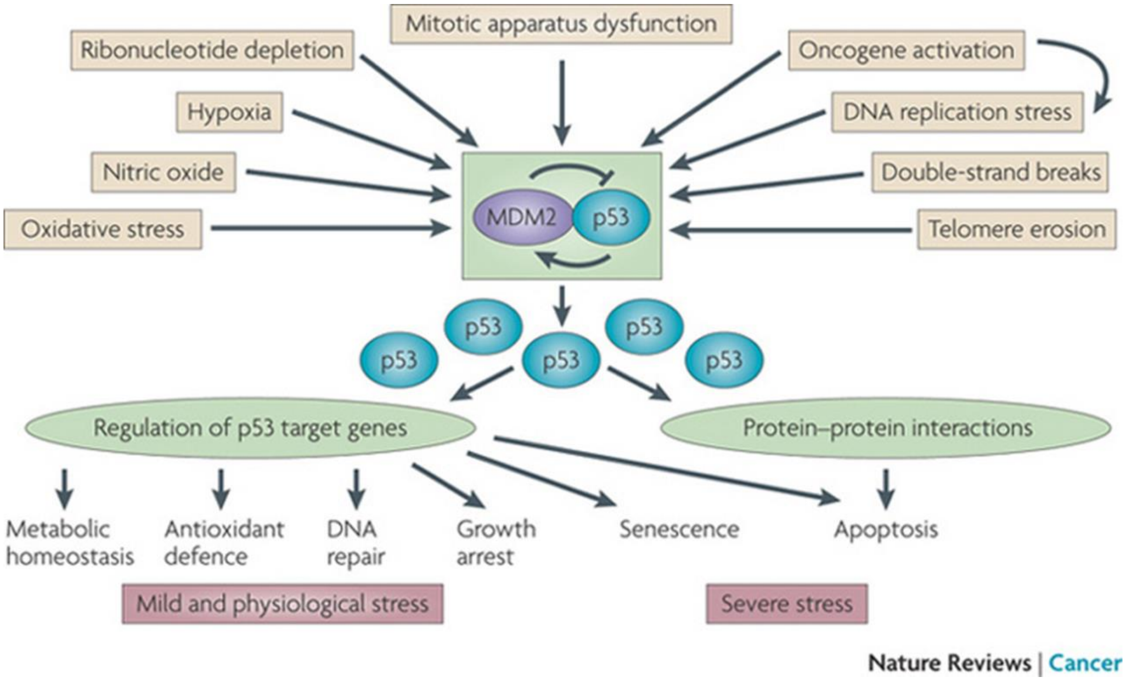
Mitotic apparatus dysfunction
Ribonucleotide depletion
Oncogene activation
Hypoxia
DNA replication stress
Nitric oxide
Double-strand breaks
Oxidative stress
Telomere erosion
MDM2
p53
Regulation of p53 target genes
Protein–protein interactions
Metabolic homeostasis
Antioxidant defence
DNA repair
Growth arrest
Senescence
Apoptosis
Mild and physiological stress
Severe stress
Nature Reviews | Cancer

Figure 1.2.4 Scheme of p53 signaling pathway

Allelic dilution of WT p53 by chromosomal deletion, along with point mutation in the remaining copy, is frequently observed in diverse human tumor types as a mechanism to bypass this critical checkpoint [28].

Interestingly, besides classic tumor suppressor functions that are lost upon mutation of the protein, both classes of mutants have also been shown to produce gain-of-function (GOF) phenotypes. p53 with GOF mutation acquires several novel oncogenic properties that promote invasion, proliferation, chemo-resistance, metastasis, and metabolic reprogramming [29-31]. The Cancer Genome Atlas (TCGA) projects on lung ADC and lung SCC revealed the spectrum of p53 mutations data. Although mutations have been found at almost all amino acid positions in the protein, several hot spot regions have been identified (V157, R158, R175, G245, R248, R249, and R273), which highlight the critical function of the core DNA-binding domain of p53 (Figure 1.2.5) [28, 32].

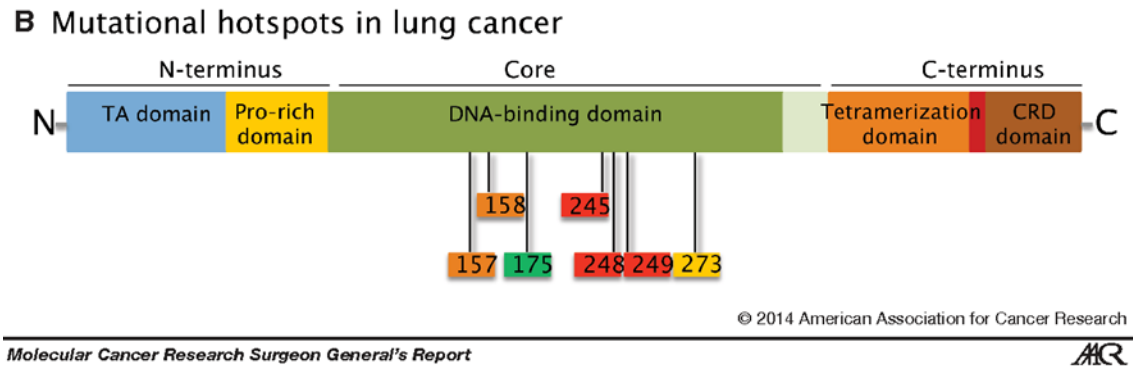
B Mutational hotspots in lung cancer
N-terminus
Core
C-terminus
N
TA domain
Pro-rich domain
DNA-binding domain
Tetramerization domain
CRD domain
C
158
245
157
175
248
249
273
© 2014 American Association for Cancer Research
Molecular Cancer Research Surgeon General's Report
AACR

Figure 1.2.5 Mutaional hotspots residues of p53 in lung cancer

In the course of evolution of a normal cell toward a cancerous one is a complex process, accompanied by multiple steps of genetic and epigenetic alterations that confer selective advantages upon the altered cells [33]. During tumorigenesis process, mutation in TP53 exerts its function on promoting tumor development. In a heterozygous situation, where both wildtype (WT) and mutant alleles exist, mutant p53 can antagonize WT p53 tumor suppressor functions in a dominant negative manner for varying time periods. At the stage of carcinogenesis/metastasis, WT p53 allele is generally lost through loss-of-heterozygosity (LOH), resulting in the sole existence of only the mutant p53 (Figure 1.2.6) [33, 34].

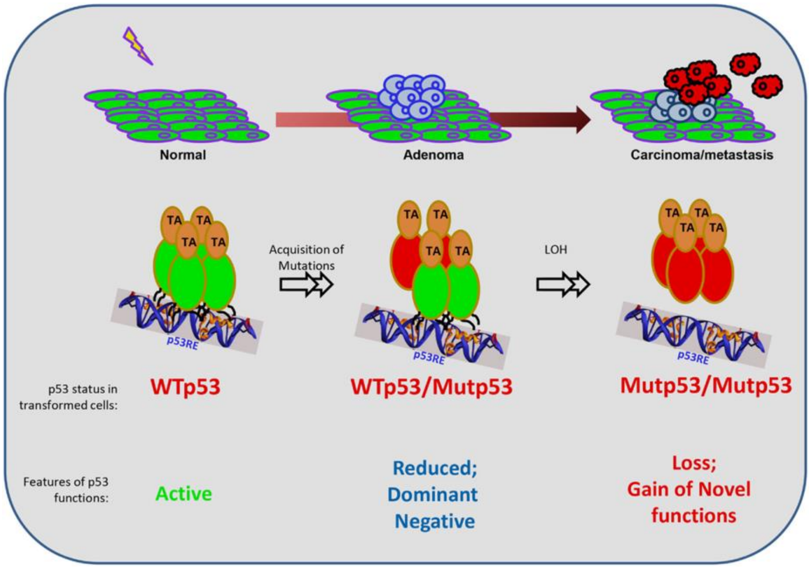
Normal
Adenoma
Carcinoma/metastasis
TA
Acquisition of Mutations
LOH
p53RE
p53 status in transformed cells:
WTp53
WTp53/Mutp53
Mutp53/Mutp53
Features of p53 functions:
Active
Reduced; Dominant Negative
Loss; Gain of Novel functions

Figure 1.2.6 Functions of mutant p53 during the evolution of a cancer cell transformation.

Most clinical studies suggest that TP53 alterations in patients with NSCLC displays worse prognosis and may be relatively more resistant to chemotherapy and radiation [35]. Several studies indicated that NSCLC patients with mutations of TP53 survived for a shorter period of time [36].

Like all cancer types, NCLC patients with p53 mutations have poor clinical outcomes and most of the patients develop eventually chemo-resistance [22, 37]. Although targeting p53 is attractive therapeutic strategy for this disease, attempts to develop drugs that target mutant p53 proteins have, so far, been unsuccessful [38, 39]. Currently, much attention is focused on p53 downstream pathways such as cancer metabolism.

1.3 Cancer metabolism

Living organisms require a constant supply of energy to maintain cell and organ function. Sufficient balance between the production of energy (catabolism) by combustion of fuel sources and the utilization of energy by synthesizing macromolecules (anabolism) is essential to maintain cellular homeostasis. These nutrients provide energy and support essential anabolic processes such as nucleic acid, protein, and lipid synthesis. In rapidly proliferating cells there is a higher demand of glucose and glutamine for generation of biosynthetic precursors to synthesize the building blocks that support anabolic processes [40-42].

In normal conditions, most mammalian tissues utilize glucose as the main source of energy. However, in tissues with high energy requirement, such as in heart and resting skeletal muscle, up to 50% of energy, in the form of ATP production generated from fatty acid beta-oxidation [43]. Glucose is oxidized in the presence of oxygen (O2) to generate 38 molecules of ATP. In this process, glycolysis produces 2 molecules of ATP and the remaining 36 are produced by oxidative phosphorylation. When oxygen availability is limited and oxidative phosphorylation is impaired, elevated glucose metabolism through glycolysis is the primary source of energy in the mammalian cell [41].

In the presence of oxygen, normal cells predominantly utilize mitochondrial oxidative phosphorylation. In contrast, cancer cells rely mainly on the glycolysis pathway-converting glucose to lactate-to fulfil their respective energetic requirements even if oxygen is available [41]. Otto Warburg, first reported that cancer cells displays a hyperactive glycolysis even in the presence of oxygen and is popularly known as the “Warburg effect” [44]. Warburg initially hypothesized that the glycolytic phenotype of cancer cells was because of the mitochondrial dysfunction, but careful observations revealed that most tumor cells have functional mitochondria, suggesting that the glycolytic phenotype is not simply an adaptation, but rather is an inherent property of tumor cells [45]. Therefore, altered energy metabolism has been accepted as hallmarks of cancer [46]

As numerous connections between signal transduction pathways and metabolic activities contribute to metabolic reprogramming of transformed cells [40]. Distinct hallmarks of tumorigenesis-associated metabolic reprogramming and their functional contribution to the establishment and maintenance of the tumorigenic state have been determined, these hallmarks are: (1) deregulated uptake of glucose and amino acids, (2) use of opportunistic systems of nutrient obtainment, (3) use of glycolysis/TCA cycle intermediates for biosynthesis and NADPH production, (4) increased demand for nitrogen, (5) alterations in metabolite-driven gene regulation, and (6) metabolic interactions with the microenvironment [47]. Schema describing the changes in metabolic reprogramming during tumorigenesis is presented in Figure 1.3.1 [48].

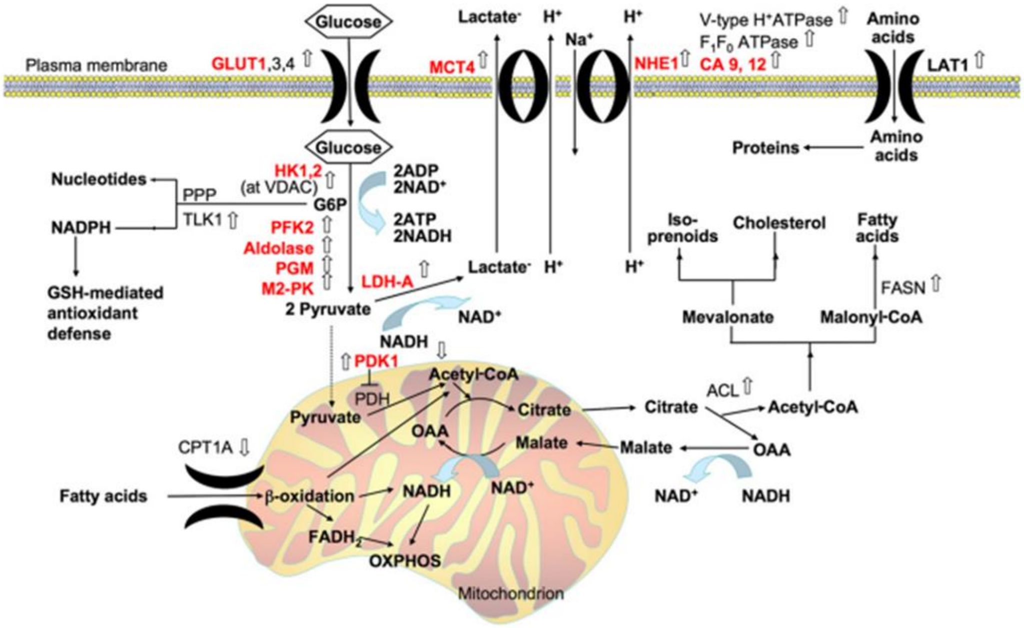
Glucose
Lactate⁻
H⁺
Na⁺
H⁺
V-type H⁺ATPase ⇧
F₁F₀ ATPase ⇧
Amino acids
Plasma membrane
GLUT1,3,4 ⇧
MCT4 ⇧
NHE1 ⇧
CA 9, 12 ⇧
LAT1 ⇧
Glucose
Proteins
Amino acids
Nucleotides
PPP
HK1,2 (at VDAC) ⇧
2ADP
2NAD⁺
G6P
TLK1 ⇧
NADPH
PFK2 ⇧
Aldolase ⇧
PGM ⇧
M2-PK ⇧
2ATP
2NADH
Iso-prenoids
Cholesterol
Fatty acids
LDH-A ⇧
Lactate⁻
H⁺
H⁺
FASN ⇧
GSH-mediated antioxidant defense
2 Pyruvate
NAD⁺
Mevalonate
Malonyl-CoA
NADH ⇩
⇧ PDK1
PDH
Acetyl-CoA
Pyruvate
Citrate
Citrate
ACL ⇧
Acetyl-CoA
OAA
CPT1A ⇩
Malate
Malate
OAA
Fatty acids
β-oxidation
NADH
NAD⁺
NAD⁺
NADH
FADH₂
OXPHOS
Mitochondrion

.

Figure 1.3.1 Changes in metabolic reprogramming during tumorigenesis.

Several studies revealed that metabolic change has linked to seven essential hallmarks of cancer that are intertwined with an altered cancer cell-intrinsic metabolism (Figure 1.3.2) [48].

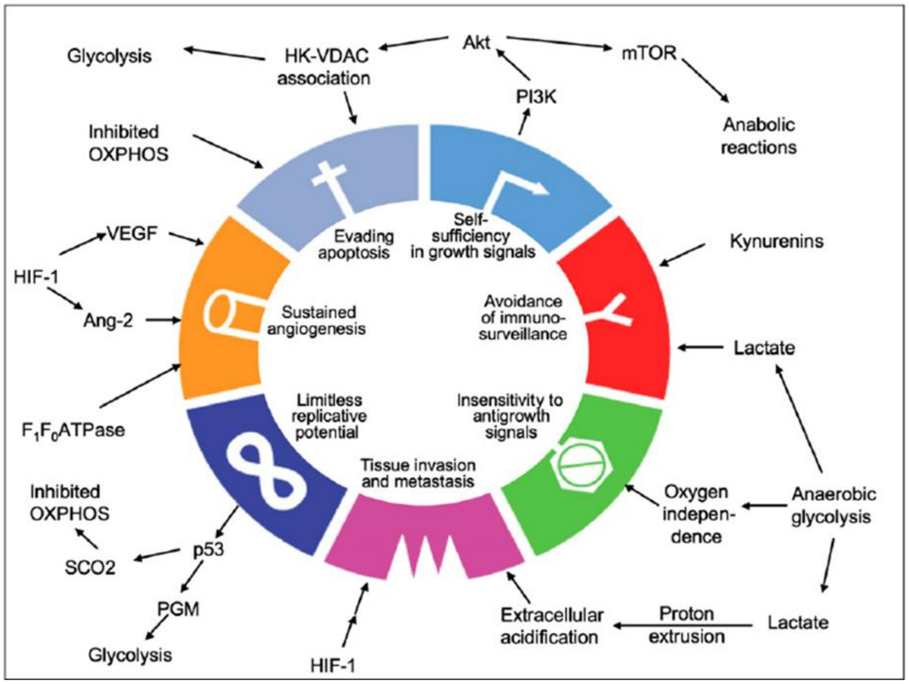
Glycolysis
HK-VDAC association
Akt
mTOR
PI3K
Anabolic reactions
Inhibited OXPHOS
Self-sufficiency in growth signals
Evading apoptosis
Kynurenins
VEGF
HIF-1
Ang-2
Sustained angiogenesis
Avoidance of immuno-surveillance
Lactate
F$_1$F$_0$ATPase
Limitless replicative potential
Insensitivity to antigrowth signals
Tissue invasion and metastasis
Inhibited OXPHOS
Oxygen indepen-dence
Anaerobic glycolysis
SCO2
p53
PGM
Glycolysis
HIF-1
Extracellular acidification
Proton extrusion
Lactate

Figure 1.3.2 Connection of metabolic reprogramming with other seven hallmarks of cancer.

Extensive studies on molecular mechanism of cancer-specific metabolic reprogramming revealed that several signaling pathways, such as phosphatidylinositol-3-kinase/serine/threonine-specific protein kinase (PI3K/Akt), mitogen-activated protein kinase/extracellular signal-regulated kinase (MAPK/Erk), and p53, are critical for maintaining the metabolism towards anabolism, thereby supporting cancer cell growth, proliferation, and survival [42, 48]. These signaling pathways regulate cancer metabolism either by inducing the expression and/or increasing the catalytic activity of several enzyme that are responsible of glycolysis [49].

1.3.1 Role of PI3K/AKT signaling in cancer metabolism

Phosphoinositide 3′-kinases (PI3K) are a family of lipid kinases. There are three classes of PI3K based on sequence homologies, lipid substrate specificity and structure including PI3K class I, PI3K class II, and PI3K class III. PI3K class I is a heterodimeric complex that is composed of a regulatory subunit (p85) and a catalytic subunit (p110). The two regulatory subunits p85α and p85β isoforms both contain two src-homolgy 2 (SH2) domains, inter-SH2 domain, SH3 domain, two proline-rich domain, and Bcr/Rac GTPaseactivating protein (GAP) homology domain. SH2 domains activate the catalytic subunit (p110) by coupling p85 isoforms to phosphorylated tyrosine of the receptor [50-52]. PI3K is activated via binding its p85 subunit to the phosphorylated receptor tyrosine kinase (RTK). There are several key downstream targets of PI3K pathway that are activated upon activation of PI3K including serine/threonine-specific protein kinase AKT, protein kinase C (PKC), mammalian target of rapamycin (mTOR), p70 S6 kinase, eukaryotic translation initiation factor 4E-binding protein 1 (4EBP1), and glycogen synthase kinase 3 beta (GSK3β) that play a key role in multiple cellular processes [53-55].

AKT is a serine/threonine-specific protein kinase. PI3K activation leads to co-localization of activated PDK1 and AKT. PDK1 phosphorylates AKT on threonine 308, leading to partial activation of AKT. AKT becomes fully activated upon phosphorylation site serine 473 by the TORC2 complex of the mTOR protein kinase. Activated AKT phosphorylate numerous substrates that control a variety of downstream processes, such as metabolism, apoptosis, cell proliferation, cell survival, and cell migration [56-58]. AKT regulates cancer metabolism via increasing glycolytic flux and upregulating glycolytic enzymes. AKT increases glycolysis in cancer cells through (1) increasing the catalytic activity of hexokinases (HK1 and HK2), (2) increasing the expression of Glucose transporters (GLUT1, GLUT2, GLUT3, and GLUT4), (3) activating phosphofructokinase-1 and 2 (PFK1 and PFK2) [49, 59].

mTOR is a serine/threonine protein kinase that is part of the PI3K –related kinase protein family. mTOR exists in two distinct multi-complexes with different protein components and downstream substrates: mTOR complex 1 (mTORC1) and mTOR complex 2 (mTORC2). The cellular balance between anabolism and catabolism is maintained by mTORC1 in response to the environmental signals such as growth factors, amino acids, and stress [60, 61]. Activation of mTORC1 induces protein synthesis by promoting ribosome biogenesis and mRNA translation by activating ribosomal S6 kinase (S6K) and the inhibitory eIF4E-binding proteins (4E-BPs) [61-63]. mTOR is downstream of AKT in PI3K pathway and mTOR is phosphorylated at Ser-2448 by AKT kinase [64]. mTOR regulates cell growth, cell proliferation, cell motility, cell survival, protein synthesis, and transcription [65]. Moreover, mTORC1 phosphorylates ULK1 and inhibits the activation of adenosine 5′-monophosphate (AMP)-activated protein kinase (AMPK) under nutrient sufficient condition, thereby blocking autophagy induction [66].

Glycogen synthase kinase 3 (GSK3) is a proline-directed serine-threonine kinase that has two isoforms: GSK-3α and GSK-3β. GSK3β is downstream of AKT in PI3K pathway and it regulates energy metabolism, cell proliferation, apoptosis, neuronal cell development, and body pattern formation [67, 68]. GSK3 activity is inhibited through phosphorylation of serine 21 in GSK-3α and serine 9 in GSK3β and is found to be phosphorylated and inactivated in multiple cancer type [69, 70]. Several studies have showed that GSK3 phosphorylation is regulated by AKT, cAMP-dependent protein kinase A, S6K1, and ERK1/2 [67, 71-73]. Glycolytic metabolism promotes proliferation of cancer cells, but it also protects them from cell death. The dynamic balance between increased glycolysis and cell death is also regulated by GSK3β. Association of HK1 and HK2 to the outer mitochondrial membrane (OMM) is enhanced when GSK-3 is inactivated through phosphorylation at Ser9 by the survival kinase AKT (Figure 1.3.3) [74].

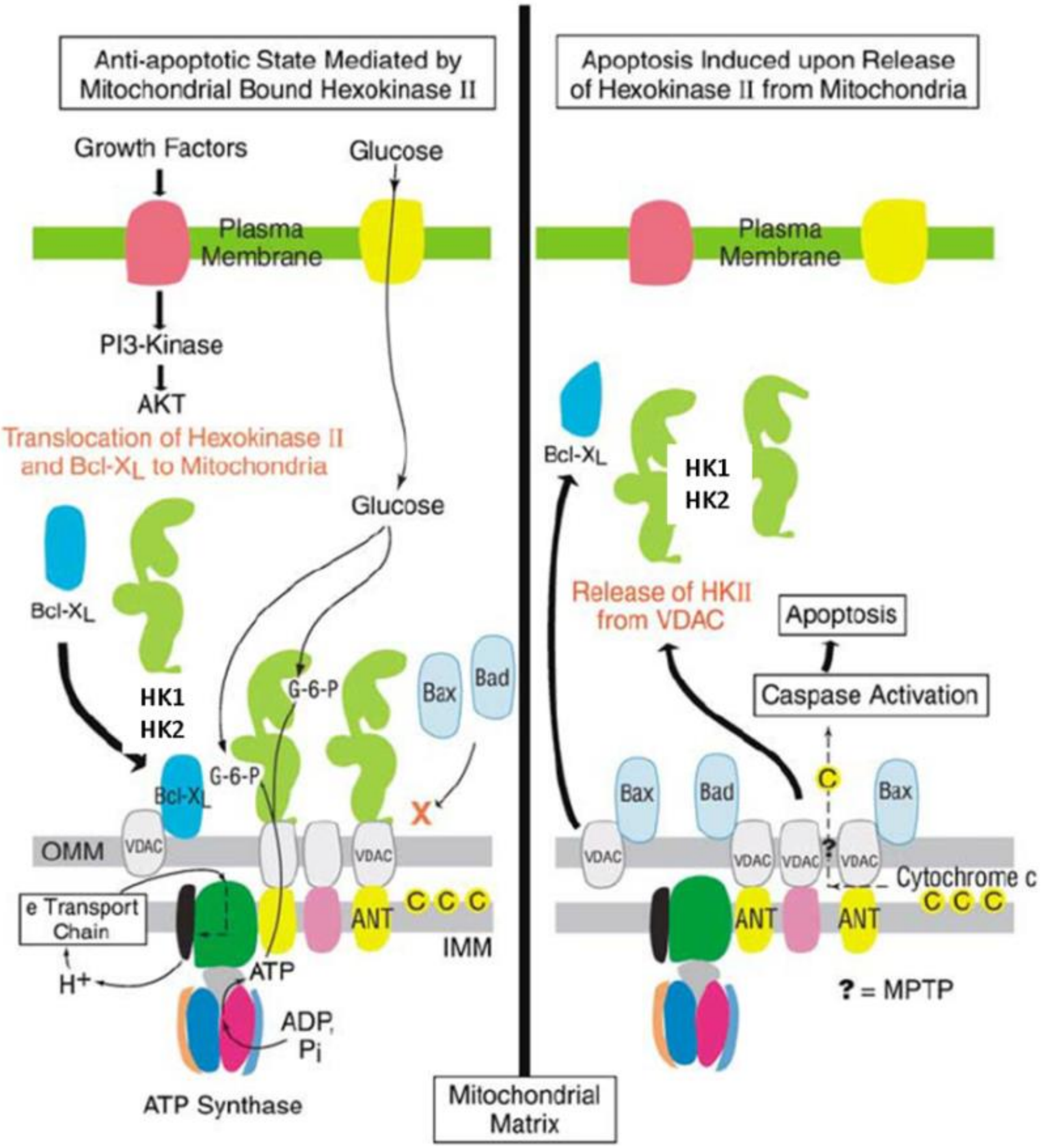
Anti-apoptotic State Mediated by Mitochondrial Bound Hexokinase II
Apoptosis Induced upon Release of Hexokinase II from Mitochondria
Growth Factors
Glucose
Plasma Membrane
PI3-Kinase
AKT
Translocation of Hexokinase II and Bcl-XL to Mitochondria
Glucose
Bcl-XL
HK1
HK2
G-6-P
G-6-P
Bax
Bad
X
Bcl-XL
OMM
VDAC
VDAC
e Transport Chain
H+
ATP
ANT
C C C
IMM
ADP, Pi
ATP Synthase
Mitochondrial Matrix
Plasma Membrane
Bcl-XL
HK1
HK2
Release of HKII from VDAC
Apoptosis
Caspase Activation
C
Bax
Bad
Bax
VDAC
VDAC
VDAC
VDAC
?
Cytochrome c
C C C
ANT
ANT
? = MPTP

Figure 1.3.3 GSK3β role in regulation of Mitochondrial-bound HKs (HK1 and HK2).

1.3.2 Role of MAPK/ERK signaling in cancer metabolism

Mitogen-activated protein kinase (MAPK) cascades are a key signaling pathway that has important role in cell division, cell survival, cell adhesion, transcription and metabolism [75]. MAPK/ERK activation starts with RAS activation. RAS is a GTP-binding protein that is activated when it is bound to GTP. RAS has two conformations: an active guanine triphosphate (GTP) bound form and an inactive guanine diphosphate (GDP) bound form, and activation is regulated by guanine nucleotide exchange factors, or GEFs

[76, 77]. Once RAS is activated, it then activates the serine/threonine kinase RAF-1 by interacting with it. Activated RAF-1 in turn activates dual-specificity kinases MEK 1 and 2 by phosphorylating them, which in turn activate the mitogen-activated protein kinases ERK1 and ERK2 through phosphorylation of Threonin202/Tyrosine204 residues.

These two isoforms (ERK1 and ERK2) are co-expressed in almost all tissues but with a variable quantity [78-80]. Phosphorylated ERKs translocate to the nucleus, where it regulates gene expression by activating transcription factors [80-82].

Several studies have showed that activation of ERK1/2 pathway promotes proliferation and aerobic glycolysis via induction of transcriptional regulators of glycolysis, the TCA cycle, and macromolecular biosynthesis [83]. ERK1/2 regulates expression levels of various glycolytic genes, including GLUT1, GLUT3, and HK1, 2 [84-86] and affects metabolic enzymes, such as PGK1, pyruvate dehydrogenase kinase (PDK) [87].

1.3.3 Role of p53signaling in cancer metabolism

Until recently, p53 tumor suppressor gene has been known to play key roles in promoting cell cycle arrest, apoptosis and senescence upon diverse stress signals, including DNA damage, hypoxia, and oncogenic activation. However, now p53 has added other important regulatory role in other cellular processes such as cellular metabolism [25, 88].

Several studies have revealed that p53 functions in balancing the use of glycolysis and oxidative phosphorylation, through transcriptional regulation of target genes. The complexity of p53 role in regulation of both glycolysis and oxidative phosphorylation is depending on the level of nutrient and oxygen levels [25, 88].

p53 has several functions in regulating oxidative phosphorylation that include: (1) suppresses the glucose uptake by inhibiting the transcription of glucose transporter GLUT 1, GLUT 3 and GLUT 4, thereby opposing the Warburg effect. (2) promotes oxidative phosphorylation by regulating IKK, IκB kinase; NF-κB, nuclear factor-κB; SCO2, synthesis of cytochrome c oxidase 2; TCA, tricarboxylic acid [25, 88].

p53 increase glycolysis under some circumstances, including (1) P53 activates phosphoglycerate mutase (PGM), (2) regulates genes that control autophagy (promote or inhibit autophagy) depending on metabolic stress that is caused by level of nutrient, (3) another important regulatory roles of p53 is to control the cellular metabolism pathway, by activating Hexokinases (HKs) to increase glycolysis depending on level of glucose and oxygen. P53 regulation of glycolysis and oxidative phosphorylation is illustrated in Figure 1.3.4 [25, 88].

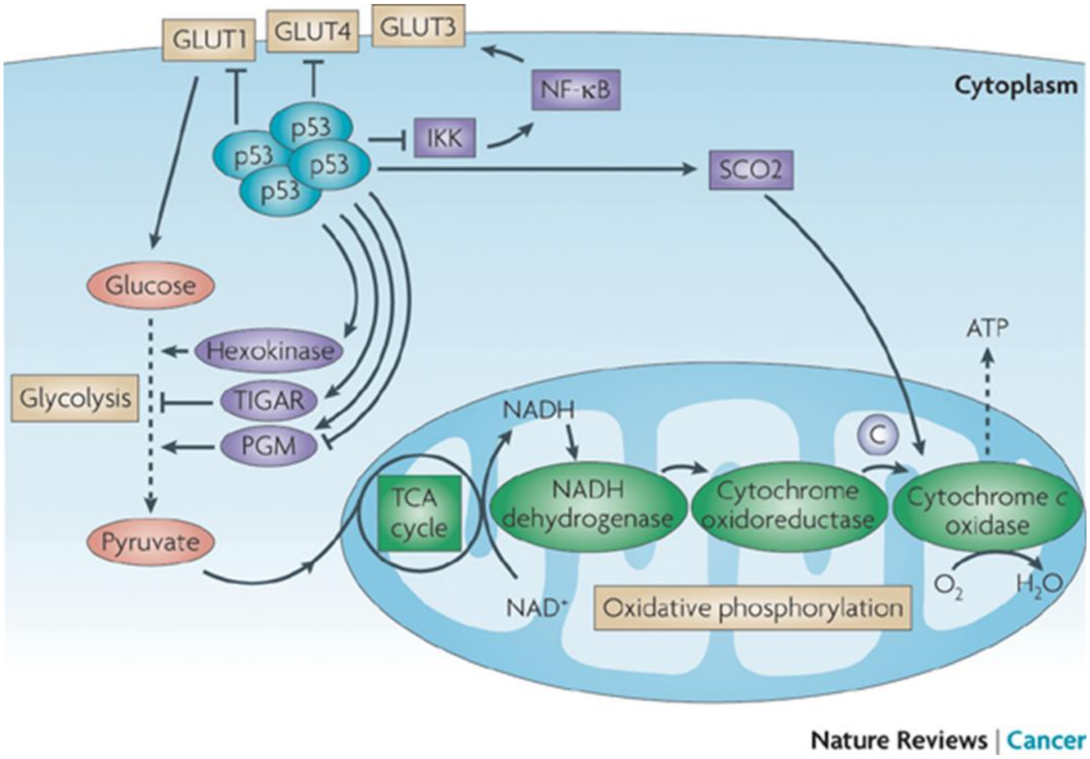
GLUT1
GLUT4
GLUT3
NF-κB
Cytoplasm
p53
IKK
SCO2
Glucose
Hexokinase
Glycolysis
TIGAR
PGM
Pyruvate
ATP
NADH
C
TCA cycle
NADH dehydrogenase
Cytochrome oxidoreductase
Cytochrome c oxidase
O_2
H_2O
NAD⁺
Oxidative phosphorylation
Nature Reviews | Cancer

Figure 1.3.4 p53 role in regulation of metabolic pathway.

Therefore, p53 with mutation not only increases cell proliferation but also promotes glycolysis and enhance anabolic pathway, key processes that promote and sustain tumor growth. Thus, identification of the enzyme(s) that catalyze the glycolysis pathway in cancer cells could be important not only to distinguish cancer cells from normal cells, but also to preferentially target cancer cells to die.

1.4 HEXOKINASES

Hexokinases (HKs) catalyze the essentially irreversible first step of glucose metabolism in cells by phosphorylating glucose to glucose-6-phosphate (G-6-P). Hexokinases play a major role in the cellular uptake and utilization of glucose thereby promoting and sustaining a concentration gradient that facilitates glucose entry into cells and the initiation of all major pathways of glucose utilization [89-91]. There are 4 isozymes of hexokinase encoded by separate genes, HK1, HK2, HK3, and HK4. HK1 is ubiquitously expressed in almost all mammalian tissues and HK2 is normally expressed in insulin-sensitive tissues such as adipose, skeletal, and cardiac muscles. HK3 is usually expressed at low levels and HK4 expression is restricted to the pancreas and liver. Among these, HK1, HK2 and HK3 have a much lower Km value for glucose, suggesting higher affinity for glucose compared to HK4. However, HK1 is the only isozyme that shows reduced inhibition by its product G6P in the presence of inorganic phosphate. Therefore, during periods of high energy demand, in which the intracellular concentration of Pi would typically increase while that of G6P decrease, the HK1 activity would increase, causing more glucose being phosphorylated by HK1 and entering downstream metabolism primarily for energy production [74, 91-93]. Among them, both HK1 and HK2 share the most similar structure that they both have N and C- terminus domain and they both bind to the outer mitochondrial membrane via a mitochondrial binding domain (Figure 1.4.1) [94].

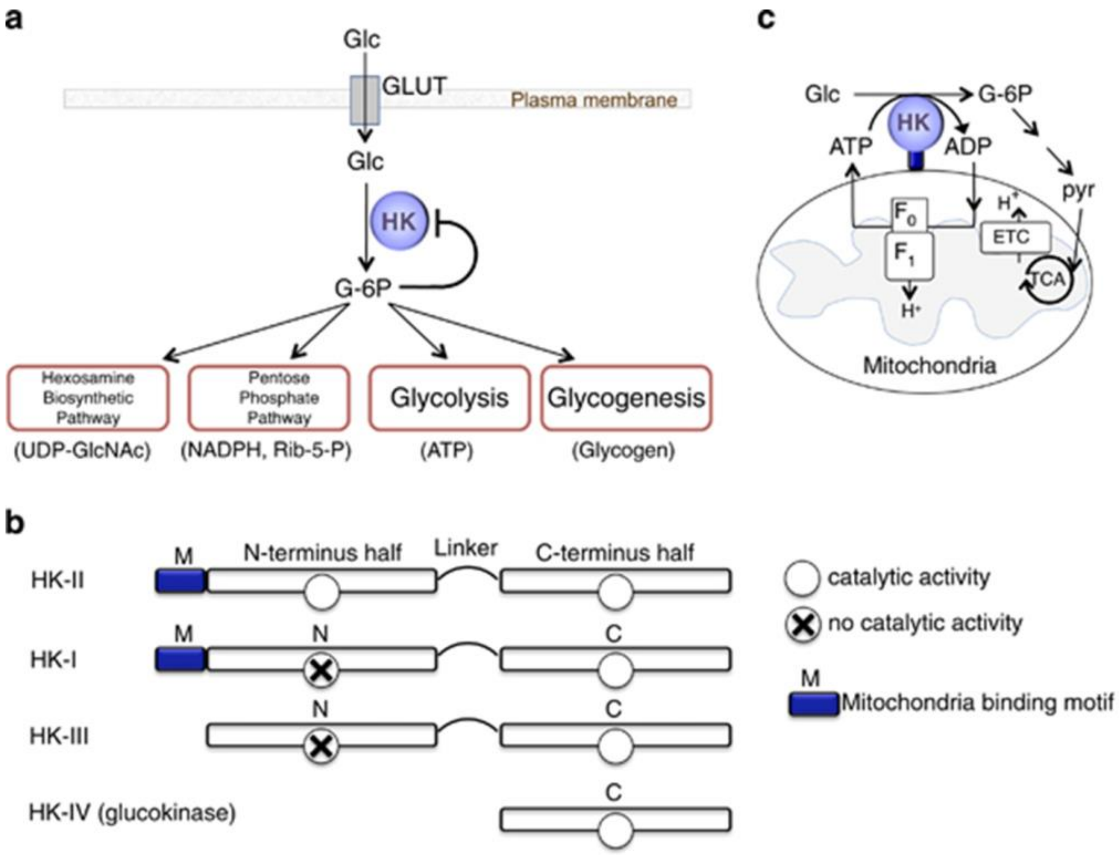
a
Glc
GLUT
Plasma membrane
Glc
HK
G-6P
Hexosamine Biosynthetic Pathway
Pentose Phosphate Pathway
Glycolysis
Glycogenesis
(UDP-GlcNAc)
(NADPH, Rib-5-P)
(ATP)
(Glycogen)
c
Glc
G-6P
HK
ATP
ADP
pyr
F_0
F_1
H^+
ETC
TCA
Mitochondria
b
M
N-terminus half
Linker
C-terminus half
HK-II
HK-I
HK-III
HK-IV (glucokinase)
N
C
catalytic activity
no catalytic activity
Mitochondria binding motif

Figure 1.4.1 HK izosymes a) metabolic roles of HK b) structure of HK subtypes c) Tight coupling of both mtHK1 and mtHK2 to ATP generated by mitochondria.

Although both HK1 and HK2 isozymes have overlapping tissue expression but they have different subcellular distribution. HK1 associated mainly with mitochondria and HK2 associated with both mitochondria and cytoplasmic compartments. John et al. found that in response to changes in glucose, subcellular translocation of HK2 dynamically directs the metabolic fate of glucose between catabolic and anabolic uses, while HK1 remains associated with mitochondria to promote glycolysis [95].

Elevated HK expression is associated with many cancer types. In recent years, both HK1 and HK2 elevated expression have been observed in malignant tumors from patients with lung, gastrointestinal and breast cancer. In the latter group, further increases in HK activity were associated with metastatic disease. In tumor cells, expression of high level of HK1 and HK2 distinguishes them from the normal differentiated cells. [95-98]. Kudryavtseva et al. showed that both HK1 and HK2 are key enzymes for glucose metabolism thereby survival of tumor cells in colorectal and melanoma cancer cells [99]. Moreover, the high level of HK expression and activity in glycolytic cancers is determined by the use of positron emission tomography (PET) to visualize the tumor growth. PET scan works using [18F] fluoro-2-deoxyglucose (FDG), fluorinated glucose analog, this is then taken up by glycolytic cancer cells and phosphorylated by hexokinase to form FDG-phosphate [100].

HK's role in cancer cell growth and proliferation via high glycolysis metabolic activity is essential and reprogramming of metabolic pathway is described as one of the hallmark of cancer [46]. It has been known that association of both mtHK1 and mtHK2 with mitochondrial outer membrane (MOM) prevents mitochondrial outer membrane permeabilization (MOMP) to block cytochrome c release, which is an essential step, for mitochondrial dependent apoptosis [101, 102]. Therefore, mtHK1 and mtHK2 binding to mitochondria induce cell death resistance, which alter cell survival signaling pathway in NSCLC.

Compared to *HK2* gene which is expressed as a single transcript, there are several transcripts of the *HK1* gene due to alternative splicing. According to the RefSeq gene annotations, which is one of the largest resources for transcript definitions, there are 10 different isoforms of the *HK1* gene. Half of these isoforms are specific to testis tissue, and are not expressed in other tissues. *HK1* gene expression is highly elevated in lung cancer, is shown in *HK1* mRNA expression profiles of multiple cancer types from TCGA and human protein atlas database (Figure 1.4.2) [103].

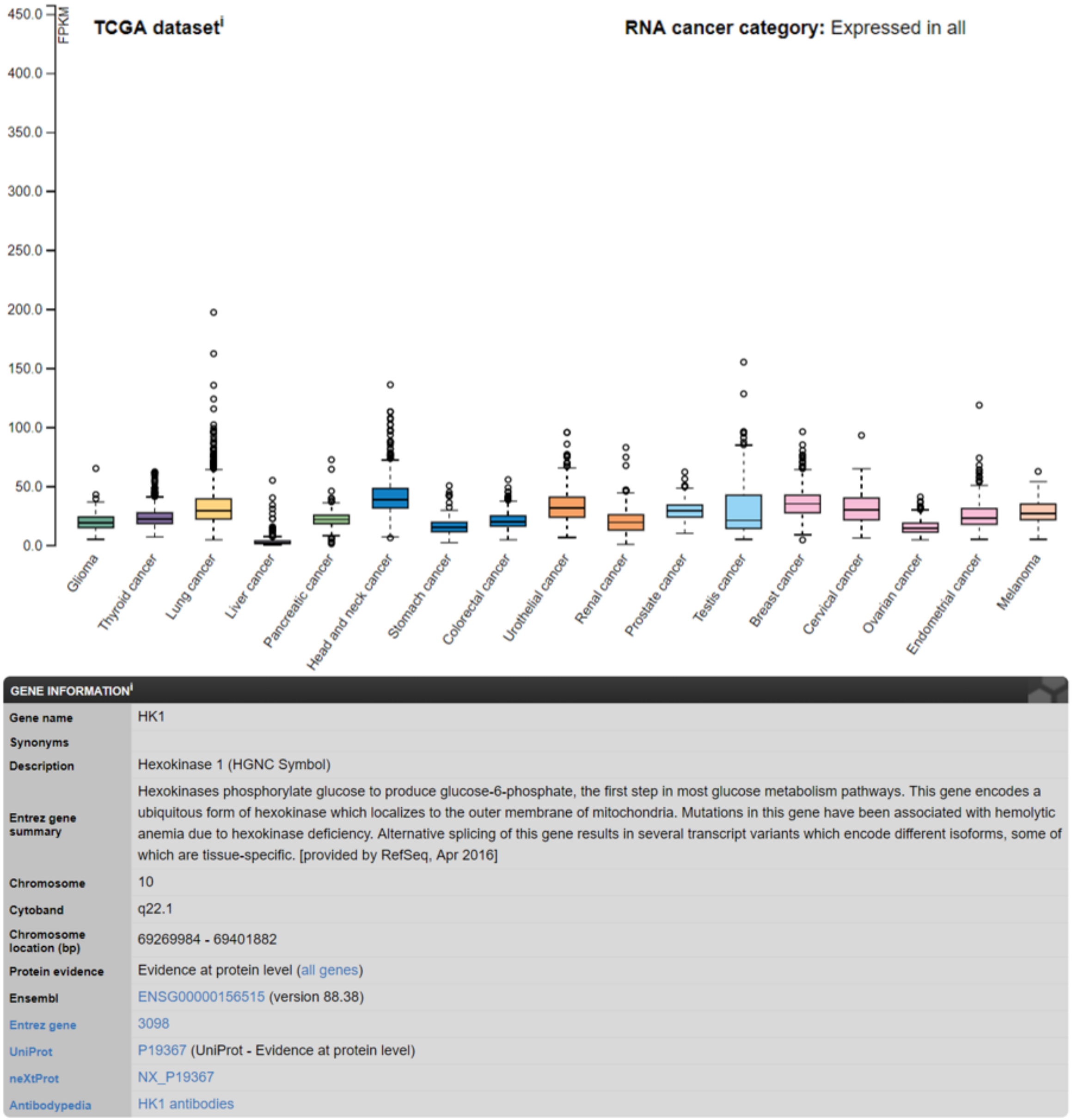
450.0
400.0
350.0
300.0
250.0
200.0
150.0
100.0
50.0
0.0
FPKM
TCGA dataset
RNA cancer category: Expressed in all
Glioma
Thyroid cancer
Lung cancer
Liver cancer
Pancreatic cancer
Head and neck cancer
Stomach cancer
Colorectal cancer
Urothelial cancer
Renal cancer
Prostate cancer
Testis cancer
Breast cancer
Cervical cancer
Ovarian cancer
Endometrial cancer
Melanoma

GENE INFORMATION

Gene name	HK1
Synonyms	
Description	Hexokinase 1 (HGNC Symbol)
Entrez gene summary	Hexokinases phosphorylate glucose to produce glucose-6-phosphate, the first step in most glucose metabolism pathways. This gene encodes a ubiquitous form of hexokinase which localizes to the outer membrane of mitochondria. Mutations in this gene have been associated with hemolytic anemia due to hexokinase deficiency. Alternative splicing of this gene results in several transcript variants which encode different isoforms, some of which are tissue-specific. [provided by RefSeq, Apr 2016]
Chromosome	10
Cytoband	q22.1
Chromosome location (bp)	69269984 - 69401882
Protein evidence	Evidence at protein level (all genes)
Ensembl	ENSG00000156515 (version 88.38)
Entrez gene	3098
UniProt	P19367 (UniProt - Evidence at protein level)
neXtProt	NX_P19367
Antibodypedia	HK1 antibodies

Figure 1.4.2 HK1 mRNA gene expression profiles.

2 INTRODUCTION

Patients with non–small-cell lung cancer (NSCLC) is often diagnosed with aggressive/metastatic disease which accounts 85% of all lung cancer, and has limited treatment options [104]. NSCLC patients with Kras-activating mutations (10–30 %) or loss of function point mutations in p53 (70 %) have poor clinical outcomes and most of the patients eventually relapse following the chemotherapies [105, 106]. Although targeting Kras or p53 is attractive therapeutic strategy for this disease, attempts to develop drugs that target mutant Kras and p53 proteins have, so far, been unsuccessful. Currently, much attention is instead focused on blocking Kras and p53 downstream elements to inhibit NSCLC progression [107, 108]. Metabolic reprogramming is one of the distinct hallmarks of cancer [46]. Unlike normal cells, cancer cells rely on increased glycolytic flux for their growth and proliferation which renders them more vulnerable to the disruption of glucose metabolism [41]. Although development of new therapies for targeting altered glucose metabolism of cancer has found some success in preclinical studies, its application in clinical settings has been limited due to induced adverse side effects [109].

Deregulation of glycolysis is common in NSCLC [110, 111]. One of the important regulatory roles of p53 is to control the cellular metabolism pathway by activating Hexokinases (HKs) to increase glycolysis depending on level of glucose and oxygen [25, 88]. Hexokinases (HKs) catalyze the essentially irreversible first step of glucose metabolism in cells by phosphorylating glucose to glucose-6-phosphate (G-6-P). The HK enzymes are encoded by four genes, HK1, HK2, HK3, and HK4. While HK1 is ubiquitously expressed in almost all mammalian tissues, HK2 is normally expressed in insulin-sensitive tissues such as adipose, skeletal, and cardiac muscles. HK3 is usually expressed at low levels while HK4 expression is restricted to pancreas and liver [74]. Among these, HK1, HK2 and HK3 have a much lower Km value for glucose, suggesting higher affinity for glucose compared to HK4. However, HK1 is the only isoform that shows reduced inhibition by its product G6P in the presence of inorganic phosphate. Therefore, during periods of high energy demand, in which the intracellular concentration of Pi would typically increase while that of G6P decrease, the HK1 activity would increase, causing more glucose being phosphorylated by HK1 and entering downstream metabolism primarily for energy production [91-93]. Moreover, both HK1 and HK2 share the most similar structure as they both have N and C- terminal domains, and they both bind to the outer mitochondrial membrane *via* a mitochondrial binding domain. Although both HK1 and HK2 have overlapping tissue expression profiles they have different subcellular distributions. While HK1 is associated mainly with mitochondria, HK2 is associated with both mitochondria and other cytoplasmic compartments [95]. The association of both HK1 and HK2 with mitochondria is regulated by Protein Kinase B (AKT) and Glycogen synthase kinase 2β (GSK3β), rendering cells resistant to apoptosis, and is therefore recognized as a key factor for survival of NSCLC cells [102].

Compared to *HK2* gene which is expressed as a single transcript, there are several transcripts of the *HK1* gene due to alternative splicing. According to the RefSeq gene annotations, which is one of the largest resources for transcript definitions, there are 10 different isoforms of the *HK1* gene. Half of these isoforms are specific to testis tissue, and are not expressed in other tissues [112, 113]. Here we focused on 3 isoforms with high sequence and structural homology: *HK1a*, *HK1b* and *HK1c*. Although these transcripts share most of their exons, some of the transcripts have certain exons that can differentiate them from the other transcripts. However, differential expression patterns of *HK1* isoforms (*HK1a*, *HK1b*, and *HK1c*) have not been studied, and their role in NSCLC tumorigenesis, cell survival, and drug response is still elusive. The identification of isoform-specific contributors to cancer cell glucose metabolism that could be selectively targeted to eliminate cancer cells without compromising systemic homeostasis or corresponding metabolic functions in normal cells could be a very attractive approach for cancer therapy.

Using cell lines and primary patient tumors, we have investigated the molecular and functional characterization of HK1 isoforms and demonstrated that HK1b isoform is a critical enzyme in glycolysis metabolism and cell survival. We showed the first time that only HK1b isoform is predominantly expressed in A549 cells and NSCLC patient tumors; this distinguishes NSCLC cells from the normal surrounding lung cells and HK1b is associated with poor NSCLC patient survival. We observed that HK1b expression was changed based on p53 status using p53 null and p53 WT NSCLC cells. In order to identify the mechanisms of HK1b regulation by p53, we deleted the p53 or HK1b isoform in human NSCLC A549 cells using CRISPR/Cas9 system. Surprisingly, we showed that p53 positively regulates HK1b. Interestingly; HK1b ablation inhibits proliferation and *in vivo* tumor growth of NSCLC cells. Finally, HK1b knockout in NSCLC cells show sensitization to cisplatin, which in turn leads to p53-mediated apoptotic and autophagic cell death. Collectively, these findings suggest that therapeutic strategies to modulate the Warburg effect, such as targeting HK1b isoform, may interfere with growth and therapeutic sensitivity of NSCLC.

3 MATERIALS AND METHODS

3.1 Chemicals, solutions antibodies and reagents

Cisplatin (50 mg/100mL) was purchased from Koçak Farma.

4x Laemmli loading buffer: Tris-HCl (pH 7.5, 62.5mM), SDS 2%, Glycerol 10%, Bromophenol Blue 0.01% and β-Mercaptoethanol 5% is added freshly.

5x Electrophoresis Running Buffer, pH 8.3: Tris base 36g**,** Glycine 172.8g**,** SDS 12g 2400ml with deionized water added.

1x Transfer Buffer: TRIS base 12.11g (25mM)**,** Glycine 57.65g (192mM)**,** Methanol 800ml**,** H2O 3200ml. Final volume 4000ml**.** Store at 4°C.

Tris-buffered Saline 10x (TBS) Stock: TRIS base 12.11g (100mM), NaCl 87.75g 1.5mM, HCl to pH 7.5. Final volume 1000ml. Store at RT.

Tris-buffered Saline 10x (TBS) Stock: TRIS base 12.11g (100mM), NaCl 87.75g 1.5mM, Tween 20 10ml (1%), HCl to pH 7.5. Final volume 1000ml. Store at RT. Tris base, Glycine, NaCl, Tris-HCl (pH 7.5), Tween 20, SDS, β-Mercaptoethanol, Methanol, HCl, Bromophenol Blue are from Fisher Scientific, USA.

Agarose Gel: For 100 ml 1% w/v gel, 1 g of agarose powder was dissolved in 100 ml 0.5X TBE buffer by heating. 0.01% (v/v) ethidium bromide was added to the solution.

Tris-Borate-EDTA (TBE) Buffer: For 1 L 10X stock solution, 104 g Tris-base, 55 g boric acid, and 40 ml 0.5M EDTA (pH 8.0) were dissolved in 1 L of ddH2O. The solution is kept at room temperature.

FACS Buffer: For 500ml 1X solution, 2.5 g bovine serum albumin (BSA) and 0.5 g sodium azide were mixed in 500 ml 1X PBS and the solution was kept at +4°C.

Plasmids: pSpCas9(BB)-2A-GFP (PX458) CRISPR Cloning plasmid, developed from Zhang Lab, purchased from Addgene.

Antibodies: Rabbit monoclonal primary antibodies against HK1 (C35C4), HK2 (C64G5), Phospho-Akt (Ser 473), total Akt, Phospho-STAT3(Tyr705), total STAT3, Cleaved PARP (Asp214) (D64E10), PARP (46D11), Cleaved Caspase-3 (Asp175) (5A1E), Caspase-3 (D3R6Y), Phospho-GSK-3β (Ser9) (D85E12), total GSK-3β (D5C5Z), Phospho-p53 (Ser15), Phospho-mTOR (Ser2448) (D9C2), Phospho-AMPKα (Thr172) (D4D6D), total AMPKα (D63G4), Atg13 (E1Y9V), β-Actin (13E5), GAPDH (D16H11) and horseradish peroxidase (HRP)-conjugated rabbit and mouse secondary antibodies purchased from Cell Signaling Technologies (USA). Mouse monoclonal primary antibodies against p53 (DO-1), Bcl-2 (C-2), MAP LC3β (G-2), and BECN1 Antibody (G-11) purchased from Santa Cruz Biotechnologies (USA). Cell culture medium (RPMI-1640), FBS, glutamine, penicillin, and streptomycin were acquired from Gibco (Grand Island, NY).

3.2 Cell culture and treatment

Human non–small cell lung cancer (NSCLC) cell lines, including A549, H1299, were obtained from Dr. Engin Ulukaya's laboratory (University of Istınye) and propagated in monolayer culture in RPMI 1640 supplemented with 10% FBS, 1% penicillin–streptomycin, and 1% L-glutamine. All cells were maintained in a humidified atmosphere containing 5% CO2 at 37°C. All cell lines were tested for Mycoplasma routinely every 3 months using MycoProbe Mycoplasma Detection Kit (R&D Systems).

3.2.1 Cell Proliferation by FACS Analysis

A549 and A549 HK1b$^{-/-}$ cells were trypsinized and harvested at 50%–70% confluency. Cells were fixed with ice-cold 70% ethanol dropwise while vortexing and incubated at minus 20 degree for a minimum of 24 hr. Fixed cells were pelleted and washed twice with PBS. Anti-Human Ki-67, FITC kit is used to stain cells according to the manufacturers' protocol (BD Biosciences). Unstained and isotype-control stained cells are shown as controls. Cells were analyzed with a FACS AriaII flow cytometer and processed using FlowJo software

3.2.2 Cell viability assay

Twenty-four hours following seeding (15,000 cells/well) in a 96-well plate, A549 and A549 HK1b$^{-/-}$ cells were treated with phosphate buffered saline, or cisplatin (0.9% NaCl w/w) with concentrations ranging from 0–100 μM/ml and the cells were incubated for a further 48 h. The cell viability was determined using the CellTiter-Blue assay kit (Promega) according to the manufacturer's instructions. IC_{50} was defined as the concentration causing a 50% reduction in absorbance relative to the negative control. IC_{50} was determined by non-linear regression analysis using Graphpad Prism v8

(Graphpad Software, CA, USA).IC50 concentration of cisplatin are used in A549 (75µM) and A549 HK1b$^{-/-}$ (47µM) cells and after 48hrs treatment cells were harvested by trypsinization, collected by centrifugation, washed once with 1 ml of PBS and stained with propidium iodide (BD Biosciences) according to the manufacturers' protocol and number of death cells was measured using fluorescence-activated cell sorting.

3.2.3 Measurement of oxygen consumption rate and extracellular acidification rates

For Seahorse XFe96 assays, cells were seeded at pre-optimized final concentration 1.5 x 10^4 cells/well onto Seahorse XF-96-well plates and glycolysis stress and mito Stress tests were performed following the manufacturer's specifications (Seahorse Bioscience, North Billerica, MA). Each datum was determined minimally in triplicate. OCR and ECAR were reported as absolute rates (pmoles/min and OCR or mpH/min for ECAR) or normalized against cell counts, or expressed as a percentage of the baseline oxygen consumption

3.3 Gene knockout in lung cancer cells

A549–HK1b isoform-knockout cells were generated by using the CRISPR/ Cas9 genome editing system. Briefly, the sgRNAs specific for *HK1b isoform only* was designed to target the 8th exon of human *HK1* gene. pX458 vector with GFP selection marker from Addgene, as described previously [19], was used to deliver Cas9 and a sgRNA targeting *HK1b* (namely sgHK1b) into the target cells. The expression of single-cell clones expressing sgHK1b were screened for HK1b isoform elimination and specific indel mutations at target loci was confirmed with PCR, DNA fragmentation analyses. The CRISPR guide sequences targeting *HK1b* were sense: GAGATTTAGAGAGAGCGCAG, antisense: CTGCGCTCTCTCTAAATCTC

3.4 Patient Tissue collection and immunohistochemical staining

This study was approved by the Ethics Committee of Istanbul Medipol University. 18 cases of clinically and immunohistologically verified frozen NSCLC primary tumor and normal lung tissue samples were collected from affiliated hospital of Istanbul Medipol University (Istanbul, Turkey), and were agreed by all patients. All studies were conducted in accordance with the Declaration of Helsinki and guidelines on Good Clinical Practice.

The sections were stained with indicated antibodies, and staining of HK1 and Ki-67 was scored pathologists based on the number of positive cells per area and staining intensity. Patients' clinical characteristics are listed in Supplementary Table 1.

3.5 *In vivo intra-tracheal* xenograft tumorigenesis assay.

NSG mice were purchased from The Jackson Laboratory and experiments were performed at the Istanbul Medipol University. All mice were maintained in a specific pathogen-free facility in a temperature-regulated room ($23\pm1^{\circ}$C) with a 12 h light/dark cycle. The protocols used were approved by the Institutional Animal Care and Use Committee of Istanbul Medipol University (Istanbul, Turkey), and performed in accordance with the provisions of the NIH Guide for the Care and Use of Laboratory 6-8 weeks old animals. $5\text{x}10^{6}$ x A549 WT and A549 $\text{HK1b}^{-/-}$ cells were *intra-tracheally* injected into the right pleural cavity of NSG male mice. Approximately 3^{rd}-4^{th} intercostal space in the midclavicular line is used for injection. *Relative t*umor volume was measured 8 weeks after implantation and, is calculated as follows: (length × width × height) × π/6. End points were reached, and mice were killed once the tumor size measured 2000 mm^{3}.

3.6 RNA isolation and quantitative PCR

RNA was isolated from human NSCLC cells and human clinical NSCLC tumor and normal samples by homogenization in Trizol reagent (Invitrogen) according to the manufacturer's instructions, followed by purification on an RNeasy column (Qiagen). RNA purity was assessed by Thermo NanoDrop 2000 (Thermo Fisher Scientific, Inc.) by standard absorbance ratios as A260/A280 ≥1.8 and A260/A230 ≥1.5. Complementary DNAs were synthesized from 2 µg of total RNA using RevertAid First Strand cDNA Synthesis Kit (Thermo Fisher Scientific, Inc.) Real time Quantitative PCR (RT-*qPCR)* results obtained with *Bio-Rad's* iTaq Universal SYBR Green Supermix..The threshold cycle (Ct) for individual reactions were identified using iCycler IQ sequence analysis software (Bio-Rad). β-actin was used for normalization of the data. All experiments were performed in triplicate.The following primers were used in this study with the following sequences:

HK1a isoform Fwd., 5'- TGGCAAGCGCTGTTCTTTGC-3'
Rev., 5'- CTGGCTCTTCAACGCAGTG-3'
HK1b isoform Fwd., 5'- CCCTGAACACGGAGATTGACA -3'
Rev, 5'- GCACCGGCACATTTCGATAG -3’
HK1c isoform Fwd, 5'- GCTCAGTGCCAGGGTGATTT-3'
Rev., 5'- TGCCAAGATAGTCCTCTTCTATTT-3'
HK2 Fwd, 5'- CATCTTCCGTGTGCTATGGG-3'
Rev., 5'- TGACACCAGGAAACTGTCGT-3'
p53 Fwd, 5'- GGACCACTAAGCGAGCACTG
Rev., 5'- TCTCGGAACATCTCGTAGCG-3',
H_β-actin Fwd, 5'- AGAGCTACGAGCTGCCTGAC -3'
Rev., 5'- AGCACTGTGTTGGCGTACAG -3'

3.7 Western blot analysis

3.7.1 Protein extraction

Cells were harvested and subjected to lysis buffer (25 mM Tris-HCl pH 7.4, 150 mM NaCl, 1% NP-40, 1 mM EDTA, 5% glycerol, 25 mM NaF), containing proteinase inhibitor cocktail and phosphatase inhibitor cocktail (Roche) and then subjected to sonication for total lysates recovery. The lysates were subjected to centrifugation at 10,000 g at 4C for 20 minutes and the supernatants removed. For immunoblotting of tissue samples, proteins were extracted in the same buffer with a tissue homogenizer after thawing frozen tissues collected by liquid nitrogen snap freezing.

3.7.2 SDS-Polyacrylamidegelelectrophoresis (SDS-PAGE)

Using SDS-PAGE, proteins were separated under denaturing conditions according to their molecular weight. 50µg of protein lysates were re-suspended in 4x Laemmli loading buffer, incubated at 100°C for 5minutes, and then allowed to cool to RT for 2 minutes. The total protein (50 µg) was fractioned by 10% SDS-PAGE Gels were run at 80V for approximately 2.5 hrs at room temperature by BioRad Mini ProteanII System (BioRad, USA).

3.7.3 Protein Transfer and Immunoblooting

0.45µM pore size (Millipore, USA) Immobilon-P transfer membranes were first dipped into methanol for 2 minutes, then washed in ddH2O for 5 minutes, and then incubated in transfer buffer for 10 minutes. After the gelelectrophoresis, gels were incubated for 5min in a cold transfer buffer. Gel and membrane were assembled in a Mini Trans-Blot Cell (BioRAD, USA) according to the manufacturer's instructions. Proteins were transferred at 90V (240mA to 400mA) for 90 minutes.

After transferred, the membrane was blocked with blocking buffer (Li-Cor) at room temperature for 1 hour, and then incubated with appropriate primary antibody at 4C overnight. After washing with TBS containing 0.05% Tween 2 (TBST), the membrane was incubated with 1:2500 dilutions of appropriate secondary antibody for 2 hours at room temperature. The membrane was washed with TBST again, and Pierce ECL Western Blotting Substrate (Thermo Scientific) was used for development of immunoreactive bands.

3.8 The Cancer Genome Atlas NSCLC cohort analyses and GSEA analysis

The publicly available Cancer Genome Atlas (TCGA) RNA-seq data on adenocarcinoma (n = 511) and SCC (n = 501) was used as an external cohort to verify DEGs between adenocarcinoma and SCC based on the RG cohort and to further analyze the expression of the HK1b isoform (transcript variant-8) between normal and TCGA Lung adenocarcinoma samples (RefSeq id NM_001322366). Lung Adenocarcinoma project contains 426 RNA sequencing of lung tumor tissues and matched with 602 normal lung tissues from the GTEx Project. For each database the supplied expected transcript read counts that are generated using the RSEM software package is used for the comparison. The read counts are normalized using the DESeq2 variance stabilized normalization method.

Gene expression data of lung cancers was extracted from the GEO database (accession number: GSE31210. Before GSEA, all lung cancer samples were divided into two groups according to their HK1 expression levels: HK1 high and HK1 low. GSEA was then performed based on normalized data using GSEA v2.0 tool (http://www.broad.mit.edu/gsea/) for identification of enriched gene sets between the HK1 high and HK1 low groups.

3.9 Statistical analysis.

Unless otherwise stated, data are expressed as mean ± SEM. GraphPad Prism 8 and SPSS 18.0 software were used for graphing and statistical analysis. After calculating normality by Shapiro-Wilk test, Student *t* or Mann-Whitney test were used to compare two samples. For multiple group comparisons, One-way ANOVA analysis and followed by Tukey's multiple comparison tests were used. Statistical parameters including exact value of n, statistical test and significance are reported in the figures and figure legends. Values of $p<0.05$ were considered statistically significant.

4 RESULTS

4.1 HK1 expression is upregulated in human NSCLCs and is associated with poor clinical outcome in patients

To validate specific upregulation of HK1 in human NSCLCs, we analyzed human NSCLC tumor tissues and adjacent non-tumor lung *tissues* for the expressions of HK1, HK2 and p53. Clinical details of patients included in this study are provided in Table 4.1. We found that in a small cohort of patients (12 tumor and 10 adjacent non-tumor samples), HK1 and HK2 were upregulated in NSCLC tumor tissues as compared to normal lung tissues as indicated with two immunoblotting assays (Fig. 4.1.1A and B). Quantification of band intensities of HK1and HK2 revealed that human NSCLC samples have significantly higher HK1 (n=12) (*p*<0001) expression than HK2 (n=12) (*p*=0037) (Fig. 4.1.1C), suggesting that HK1 is more ubiquitously overexpressed. We further confirmed *in situ* expression of HK1 in NSCLC cells by using the immunohistochemistry assay. All the noncancerous epithelium showed weak staining of HK1, while tumor cells showed moderate to strong staining of HK1 (Fig. 4.1.2A). To investigate whether gene sets that have prognostic value are enriched in *HK1*-expressing NSCLC samples, we carried out Gene Set Enrichment Analysis (GSEA) by using the GSE31210 dataset [114, 115]. Indeed, survival analysis showed that higher expression of HK1 was associated with decreased relapse-free survival (*p*=0.01; Fig. 4.1.2B), suggesting that elevated HK1 expressions associated with disease progresion.

Table 4-1 List of total 18 NSCLC patients' clinical details is included in this study.

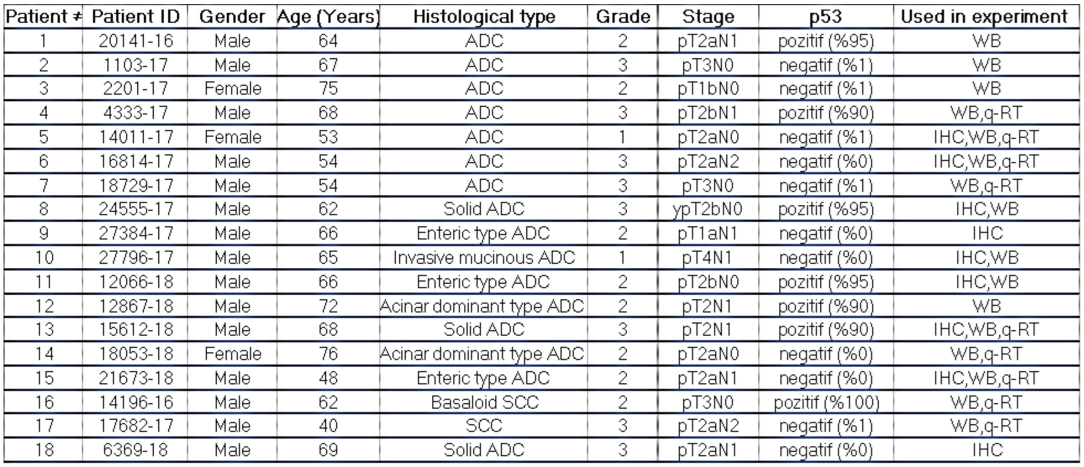

Patient #	Patient ID	Gender	Age (Years)	Histological type	Grade	Stage	p53	Used in experiment
1	20141-16	Male	64	ADC	2	pT2aN1	pozitif (%95)	WB
2	1103-17	Male	67	ADC	3	pT3N0	negatif (%1)	WB
3	2201-17	Female	75	ADC	2	pT1bN0	negatif (%1)	WB
4	4333-17	Male	68	ADC	3	pT2bN1	pozitif (%90)	WB,q-RT
5	14011-17	Female	53	ADC	1	pT2aN0	negatif (%1)	IHC,WB,q-RT
6	16814-17	Male	54	ADC	3	pT2aN2	negatif (%0)	IHC,WB,q-RT
7	18729-17	Male	54	ADC	3	pT3N0	negatif (%1)	WB,q-RT
8	24555-17	Male	62	Solid ADC	3	ypT2bN0	pozitif (%95)	IHC,WB
9	27384-17	Male	66	Enteric type ADC	2	pT1aN1	negatif (%0)	IHC
10	27796-17	Male	65	Invasive mucinous ADC	1	pT4N1	negatif (%0)	IHC,WB
11	12066-18	Male	66	Enteric type ADC	2	pT2bN0	pozitif (%95)	IHC,WB
12	12867-18	Male	72	Acinar dominant type ADC	2	pT2N1	pozitif (%90)	WB
13	15612-18	Male	68	Solid ADC	3	pT2N1	pozitif (%90)	IHC,WB,q-RT
14	18053-18	Female	76	Acinar dominant type ADC	2	pT2aN0	negatif (%0)	WB,q-RT
15	21673-18	Male	48	Enteric type ADC	2	pT2aN1	negatif (%0)	IHC,WB,q-RT
16	14196-16	Male	62	Basaloid SCC	2	pT3N0	pozitif (%100)	WB,q-RT
17	17682-17	Male	40	SCC	3	pT2aN2	negatif (%1)	WB,q-RT
18	6369-18	Male	69	Solid ADC	3	pT2aN1	negatif (%0)	IHC

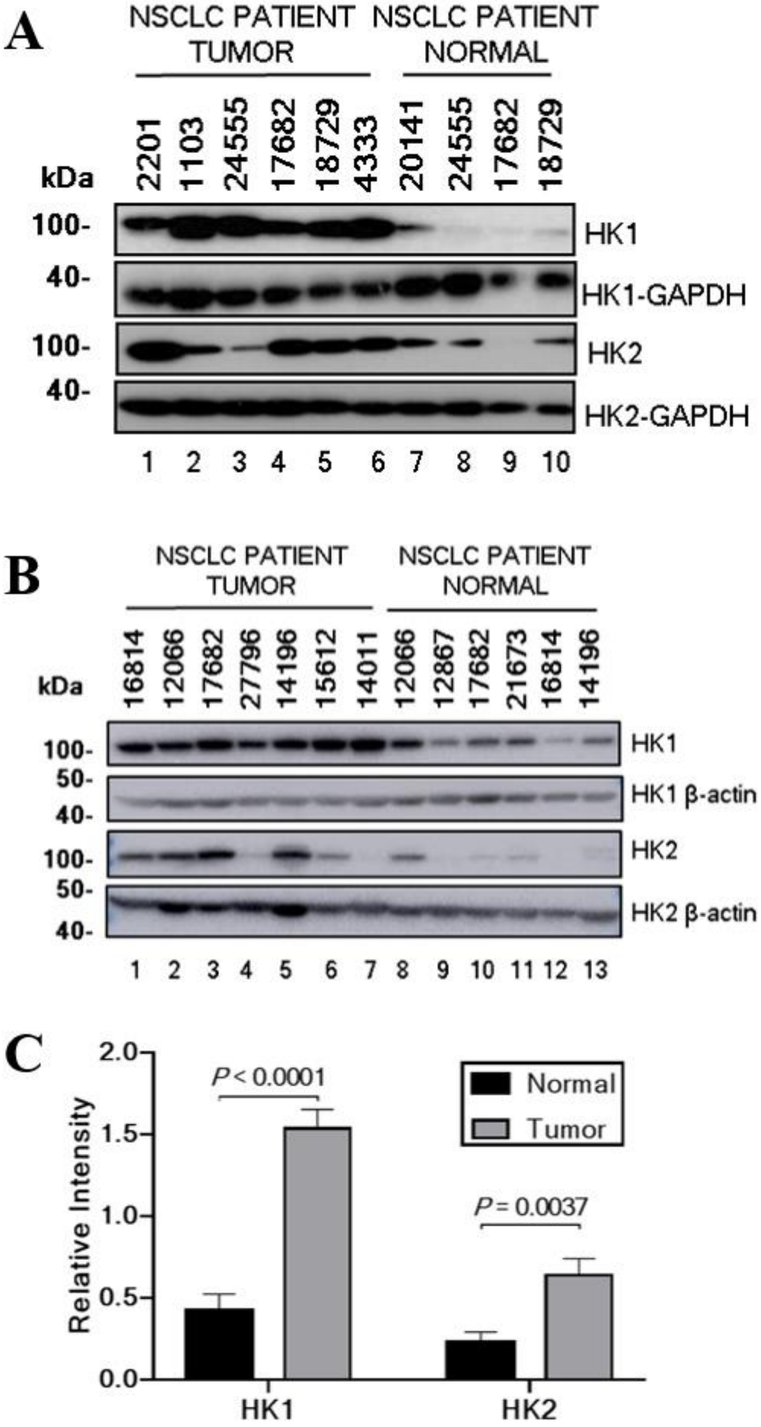

Figure 4.1.1 HK1 expression is upregulated in human NSCLC from western blot analyses. Protein was isolated from NSCLC tumor and adjacent-non tumor samples and HK1 level was determined by WB analyses **A)** protein lysates of human NSCLC tumor (n=6), normal lung (n=4); **B)** protein lysates of human NSCLC tumor (n=7), normal lung (n=6). **C)** Quantification of HK1 and HK2 levels in NSCLC tumor (n = 13) and normal lung samples (n=10).

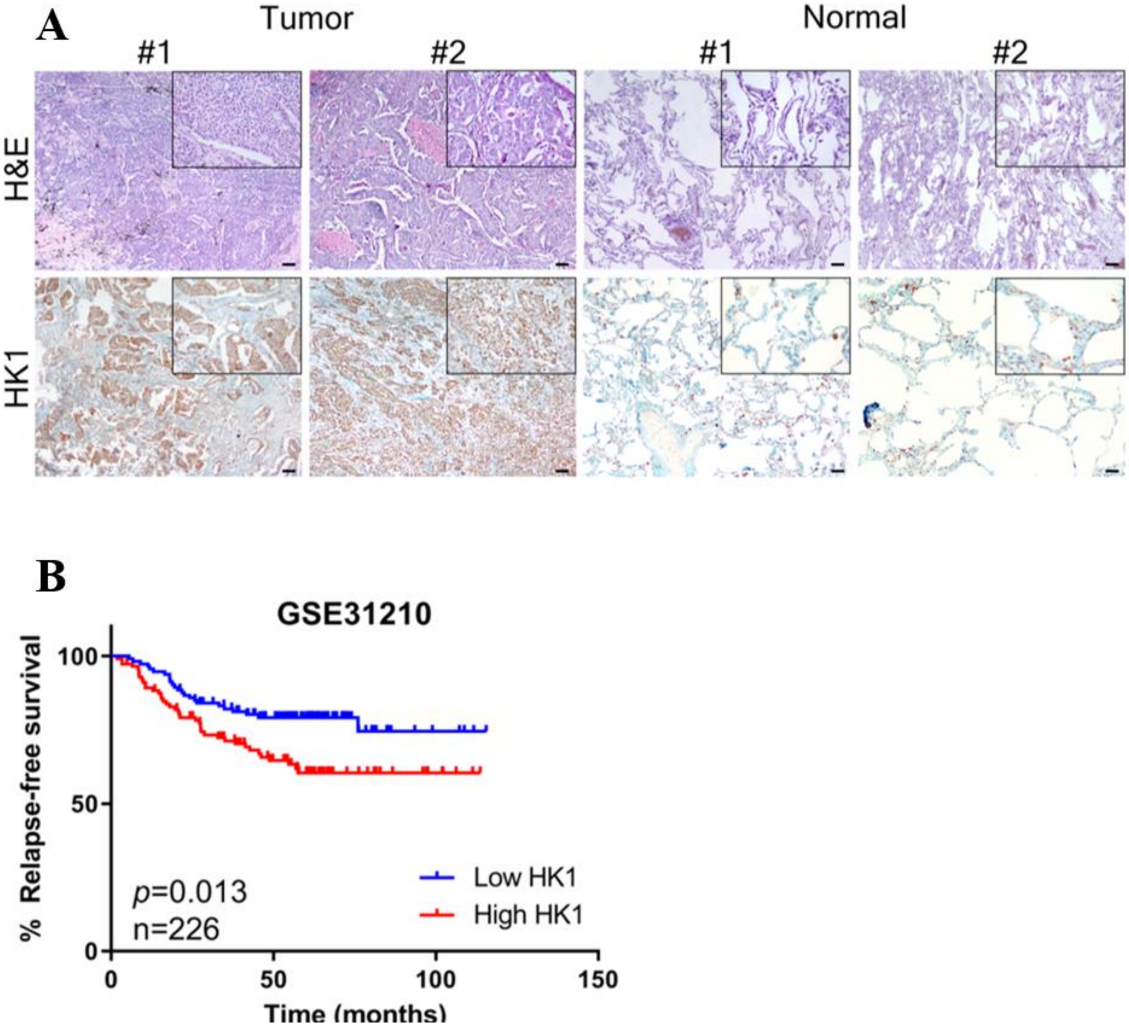

Figure 4.1.2 HK1 expression is upregulated in human NSCLC from IHC analyses and is associated with a poor overall survival. **A)** Immunohistochemical staining of HK1 expression and H&E staining in representative human NSCLC tumor (left) and the surrounding normal tissue (right). Images are 40X magnification; insets are 200X magnification. Scale bars, 100 µm. **B)** the prognostic values of HK1 in NSCLC patients (n=226). Tumors were separated into two groups according to HK1 expression levels (high or low). The high expression of HK1 is correlated to worse survival (p=0.013).

4.2 Human NSCLC cells express one of the HK1 isoforms- hexokinase1b (HK1b) as a poor prognostic factor

The HK1 gene spans approximately 131 kb and consists of 25 exons. According to RefSeq gene annotations, alternative splicing of *HK1* gene at its 5′ end produces different transcripts in different cell types. The testis-specific exons are located at approximately 15 kb upstream of the erythroid-specific exon R. The first 5 exons of the *HK1* gene encode the testis-specific sequences. The 6th exon is the erythroid-specific exon R [112]. When these tissue specific transcripts are excluded, 3 remaining transcripts are; *HK1a*, *HK1b* and *HK1c*. On the other hand the *HK2* gene has one transcript in the RefSeq gene annotations (Fig. 4.2.1A). Although, there are a few studies on the testis specific transcripts [113], the differential expressions of these three *HK1* isoforms in different tissues (including the cancer tissues) and their functional role have not been reported. When we analyze the *HK1* transcripts, it is possible to differentiate them using the differentially used exons. *HK1a* transcript contains different exons at the 5' end and therefore it is possible to distinguish this transcript. Both *HK1b* and *HK1a* isoforms possess one extra exon, which is missing in the *HK1c* isoform. Using these exon-exon junctions around this extra exon, we were able to design specific genomic probes to differentiate *HK1b* and *HK1c* isoforms. Therefore, designing specific primers for these exons will allow us to quantify the expressions of these isoforms in different tissues. Moreover, the extra exon in *HK1b* codes for 32-amino acid long alpha-helix that is part of the small sub-domain (Fig. 4.2.1B).

To identify new, HK1 isoform specific metabolic target for the treatment of NSCLC, we first analyzed HK1 isoforms (HK1a, HK1b, and HK1c) along with HK2 and p53 in NSCLC adenocarcinoma cell lines (p53 WT-A549 and p53 null-H1299). Semi-q-PCR data of both A549 and H1299 cells showed that HK1a isoform is not specific to NSCLC because of its absent expression. HK1b isoform predominantly expressed in p53 WT A549 cells, but not in p53$^{-/-}$ H1299 cells. However, we observed no difference in the levels of HK1c isoform and HK2 expressions in A549 and H1299 cells (Fig. 4.2.2A). Since there is no available isoform specific antibody to detect HK1 isoforms, we used HK1 antibody to detect the level of its expression in both A549 and H1299 cells. Therefore, we further validated the PCR results by immunoblot analysis that HK1 protein expression was higher in A549 cells than H1299 cells and HK2 expression levels were not changed in both cells (Fig. 4.2.2B), indicating that HK1b expression was specific to A549 cells. Importantly, to evaluate the clinical relevance of HK1b upregulation in human NSCL cancer, we performed semi-q-PCR and qRT-PCR analyses on tumors and adjacent non-tumor samples from NSCLC patients. In particular, HK1b was significantly (p=0.005) upregulated than HK2 transcript (p=0.03) in the NSCLC tumor when compared to normal adjacent tissue (p=0.005) (Fig. 4.2.2C and D). HK1c isoform expression was not significant, supporting the idea that Hk1b was uniquely upregulated in comparison to HK1c isoform and HK2. Interestingly, p53 expression also increased (*p*=0.005) similar to HK1b. In addition, NSCLC patient tumor cells showed no HK1a isoform expression (Fig. 4.2.2C and D). In order to further validate the increased expression of the HK1b isoform between the NSCL adenocarcinoma and the normal lung tissues, we merged the most extensive public databases TCGA (The Cancer Genome Atlas) Project and the GTEx (Genotype-Tissue Expression) Project. TCGA Lung Adenocarcinoma project contains 426 RNA sequencing of lung tumor tissues. These tumor samples, adenocarcinoma (n = 511) and SCC (n = 501), are matched with 602 normal lung tissues from the GTEx Project. Consistent with RT-PCR analyses, the comparison of the expression of the HK1b isoform (transcript variant-8) between normal and TCGA Lung adenocarcinoma samples (RefSeq id NM_001322366) showed a significant upregulation of *HK1b* in NSCLC tumor tissues compared with those in normal lung tissues (*p*= 1.85e-07) (Fig. 4.2.3A). Altogether, these data reveal that elevated HK1b expression is specific to NSCLC across a wide selection of lung cancer patients when compared to normal lung tissues. Moreover, higher expression of the HK1b isoform is associated with decreased survival probability for both adenocarcinoma (Fig. 4.2.3B) and squamous cell carcinoma (Fig. 4.2.3C) types of NSCLC, albeit the latter is not significant (*p*= 2.69e-02, *p*=9.5e-02, respectively). Collectively, our data provide compelling evidence for the specificity of HK1b isoform in NSCLC which may be utilized an attractive metabolic target.

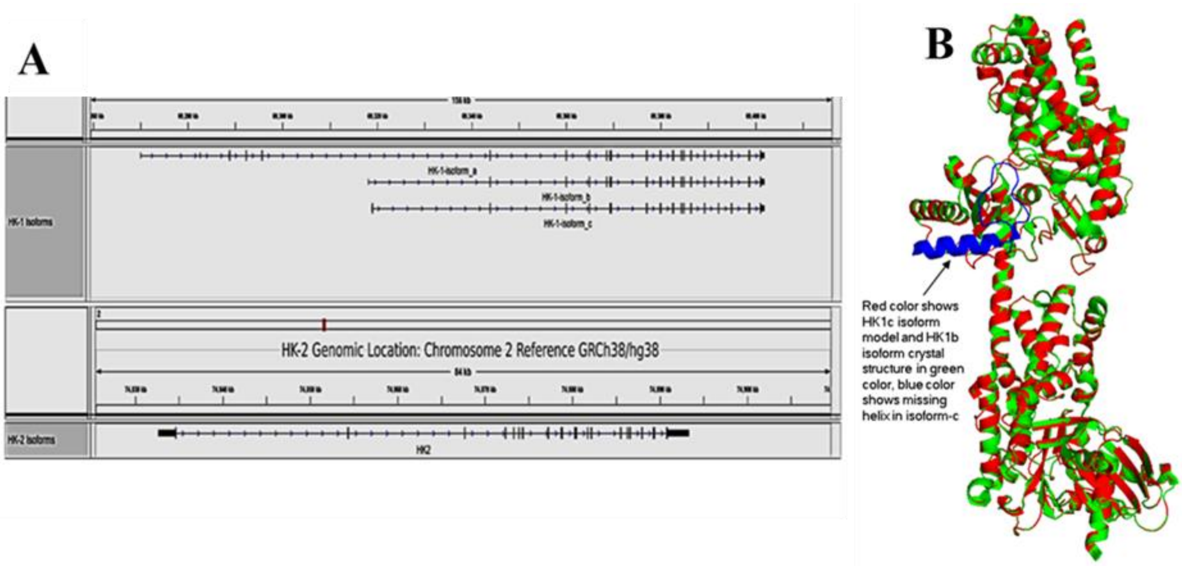
A
HK-1 isoforms
HK-1-isoform_a
HK-1-isoform_b
HK-1-isoform_c
HK-2 Genomic Location: Chromosome 2 Reference GRCh38/hg38
84 kb
HK-2 isoforms
HK2
B
Red color shows HK1c isoform model and HK1b isoform crystal structure in green color, blue color shows missing helix in isoform-c

Figure 4.2.1 **A)** RefSeq gene annotations of HK1 isoforms (HK1a, HK1b and HK1c) and HK2. HK1a and HK1b isoforms possess one extra exon, which is missing in HK1c. B) Structural alignment between crystal structures of HK1b and HK1c model. The extra exon in HK1b, which is shown in blue, codes for 32-amino acid long alpha-helix that is part of the small sub-domain of N-terminus. For the sake of simplicity only one monomer is shown. HK1b isoform levels were elevated in NSCLC tumors compared with normal lung tissue.

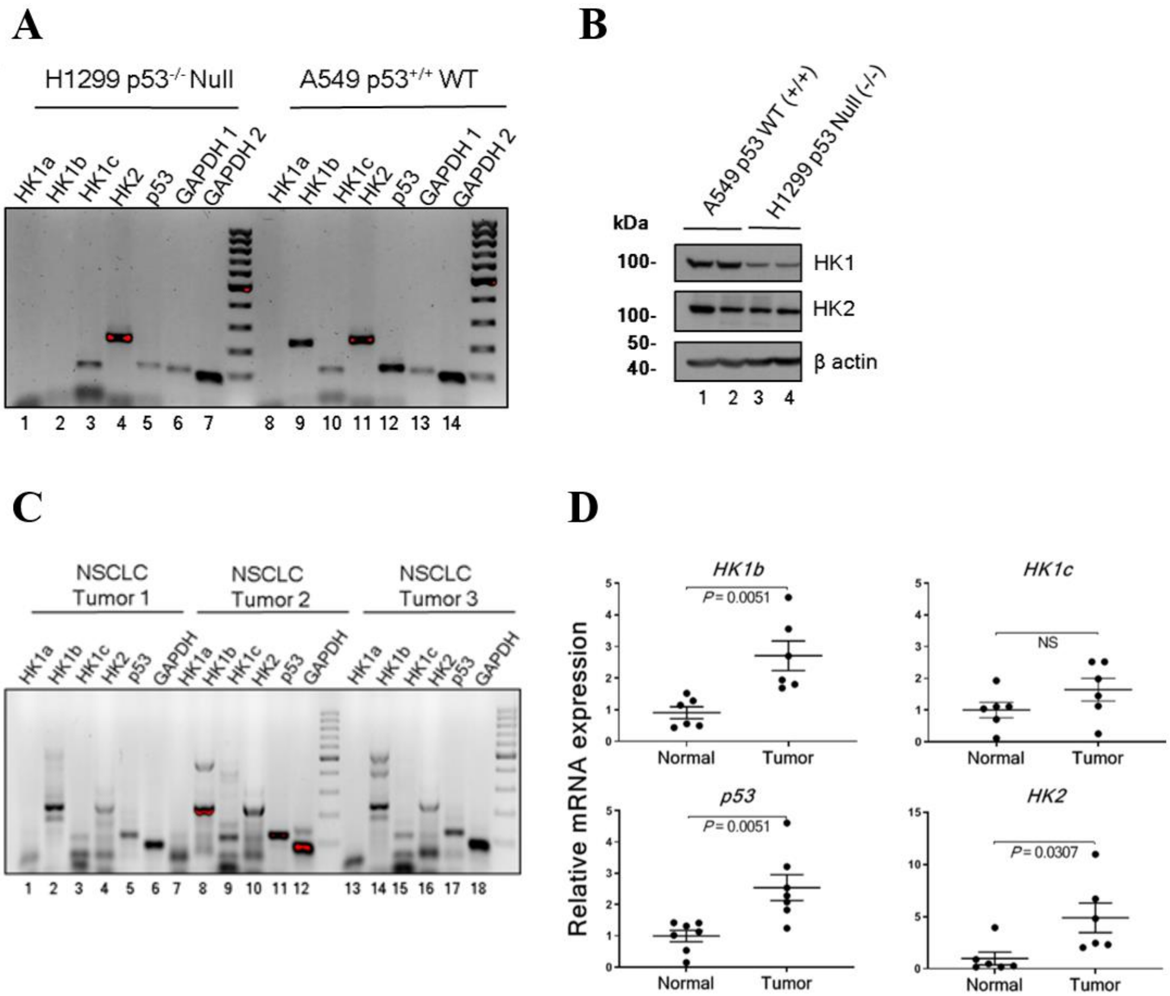

Figure 4.2.2 HK1b isoform upregulation in NSCLC patients **A)** Representative semi q-PCR amplification results for HK1 isoforms, HK2 and P53 in H1299 and A549 cells. **B)** Immunoblot analysis of HK1 and HK2 in A549 and H1299 cells. **C)** Representative semi q-PCR amplification results for HK1 isoforms, HK2 and P53 in NSCLC patient tumors (n=3). **D)** RNA was extracted from NSCLC patient normal lung and tumor samples, HK1b, HK1c, HK2 (normal n=6, tumor n=6) and p53 (normal n=7, tumor n=7) levels were determined by qRT-PCR. mRNA levels were normalized to ACTB mRNA. Data are from two or three independent experiment as triplicate, presented as mean ± SEM, Student's t test

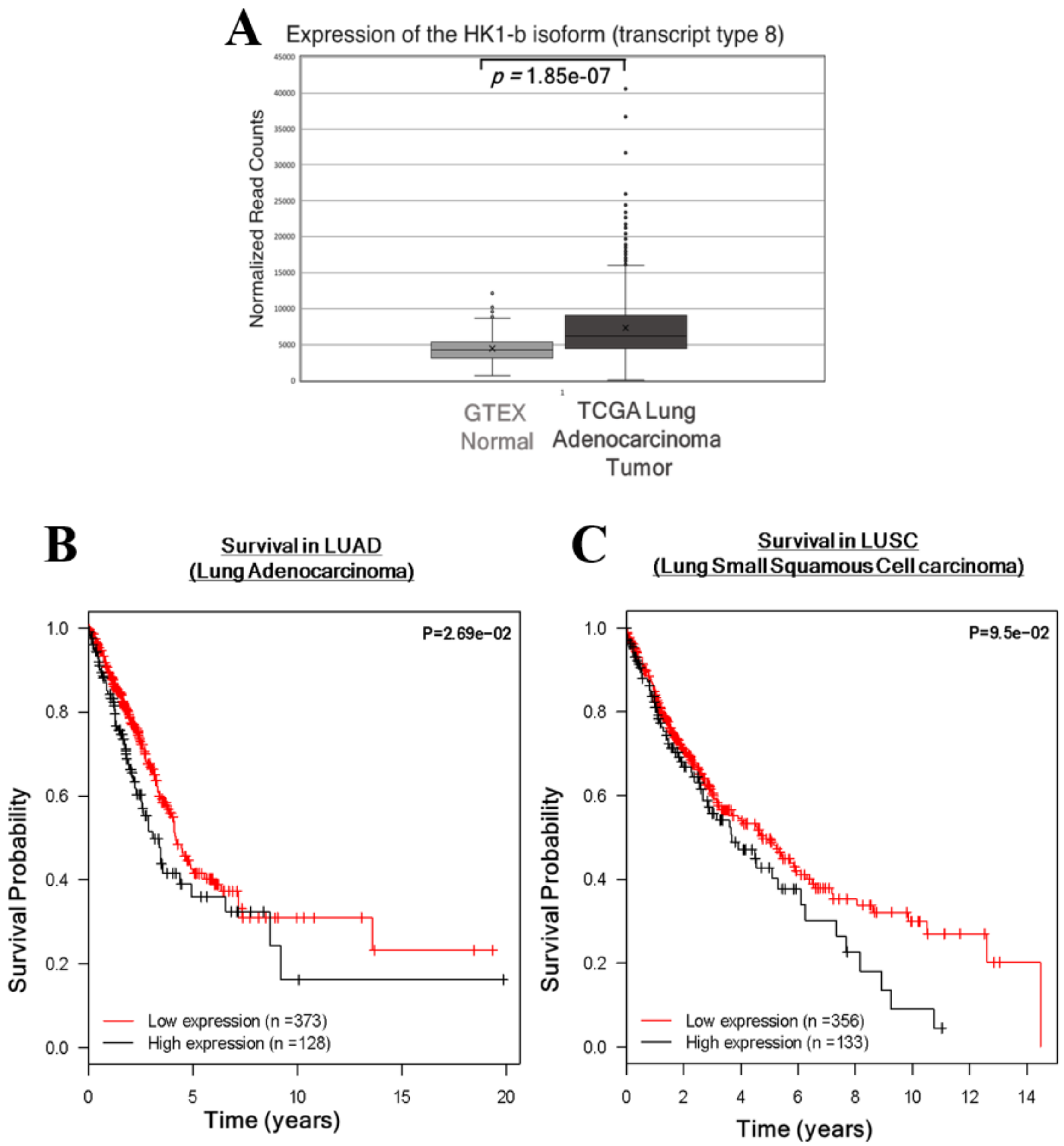

Figure 4.2.3 Increased expression of the HK1b isoform is associated with worse prognosis from TCGA NSCLC patient data **A)** Kaplan–Meier plots showing the association of HK1b isoform overexpression between normal and TCGA Lung adenocarcinoma samples in patients from the TCGA cohort. Kaplan–Meier survival curves **B)** adenocarcinoma (n = 501) and **C)** squamous cell carcinoma (n = 489), patients stratified according to low or high HK1b expression levels. P values indicate significance levels from the comparison of survival curves using the Log-rank (Mantel-Cox) test.

4.3 p53 positively regulates HK1b expression

p53 has several functions in regulating cell metabolic pathway by regulating the levels of series of gene products that balance the use of glycolysis and oxidative phosphorylation. This includes activation of hexokinase and phosphoglycerate mutase (PGM), which could increase glycolysis under some circumstances [25, 88]. We observed the change in expression of the HK1b based on p53 status of NSCLC cells. A549 NSCLC *cells* expressing WT *p53* show high levels of HK1b expression, whereas H1299 NSCLC cells that are *p53* null show absence of HK1b expression.

To understand if the association of HK1b expression with p53 is cell specific or p53 related event, we used CRISPR/Cas9 -based method to genetically disrupt p53 or HK1b isoform in human NSCLC A549 cells as an isogenic system using CRISPR/Cas9 system. While the sgRNAs specific for *p53* was designed to target the fifth exon of human *p53* gene, the sgRNAs specific for *HK1b* isoform only was designed to target the eighth exon of human *HK1* gene. pX458 vector with GFP selection marker, as described previously [116], was used to deliver Cas9 and a sgRNA targeting *p53 or HK1b* (namely sgp53 or sgHK1b) into the target cells. Single-cell clones expressing sgp53 or sgHK1b were screened for p53 or HK1b isoform elimination at the expense of specific indel mutation generation at target loci. PCR and DNA fragmentation analyses showed insertion of 104bp nucleotides in p53 (Fig. 4.3.1A) and deletion of 14 bp nucleotides in HK1b, resulting in a frame-shift mutation (Fig. 4.3.1B).

To elucidate the regulation of HK1b expression with p53, we first validated the knock-outs of p53 and particularly HK1b isoform transcriptionally. Both semi-qPCR and qRT-PCR of A549 WT and A549 p53$^{-/-}$ cells transcription analysis revealed that A549 WT cells showed absence of endogenous p53. Interestingly, as a result of p53 deletion we observed total absence of HK1b isoform expression, reduced expression of HK2, and HK1c, which was not significant (Fig. 4.3.2A). Further, both Immunoblot and immunofluorescence analyses of A549 WT and A549 p53$^{-/-}$ cells, using anti-p53 and HK1 antibodies showed the total absence of endogenous p53 and significantly decreased level of endogenous HK1 protein (Fig. 4.3.2B and E).

We further analyzed isogenic clones expressing sgHK1b with qRT-PCR. Of note, we were able to delete HK1b isoform specifically, without altering the transcriptional expressions of HK1c isoform, HK2 and p53 (Fig. 4.3.2C). Moreover, we confirmed by Immunoblot and immunofluorescence analyses that level of HK1 protein was absent due to permanent loss of HK1b isoform (Fig. 4.3.2D and E).

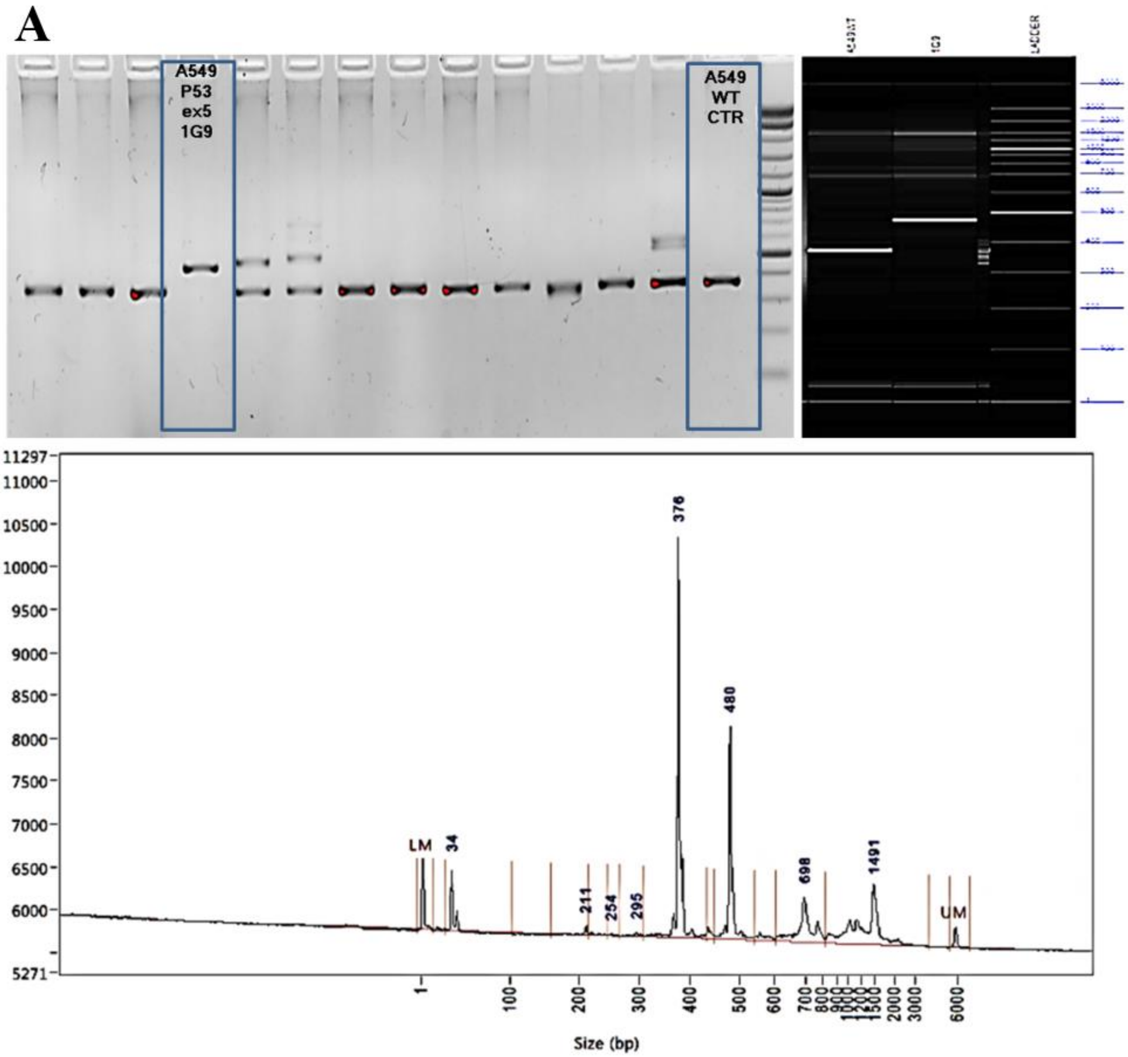

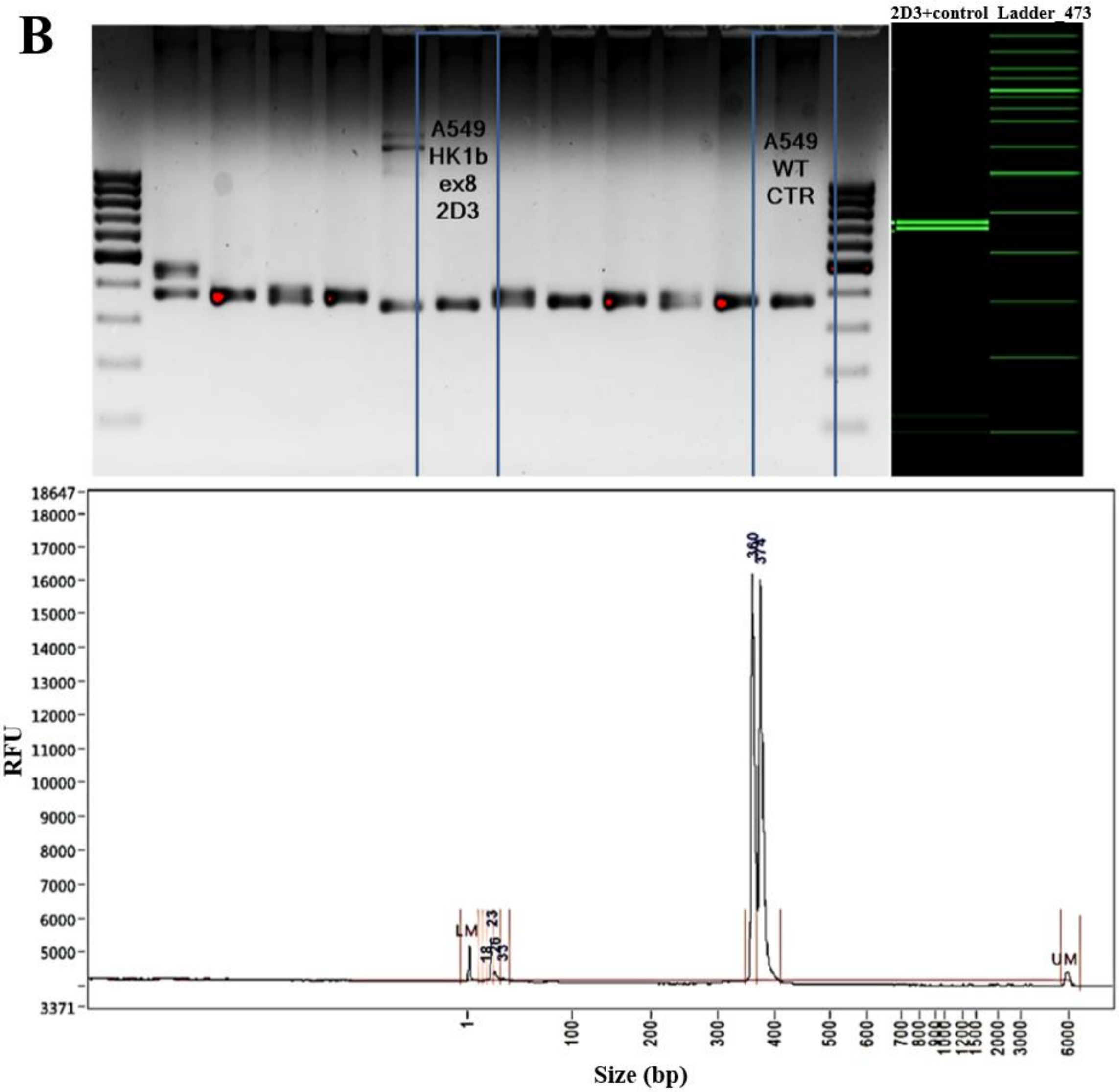

Figure 4.3.1 PCR and DNA fragmentation analysis of **A)** p53 elimination at the target loci, indicating insertion of 104 bp nucleotides resulting in a frame-shift mutation. **B)** HK1b isoform elimination at the target loci, indicating deletion of 14 bp nucleotides resulting in a frame-shift mutation.

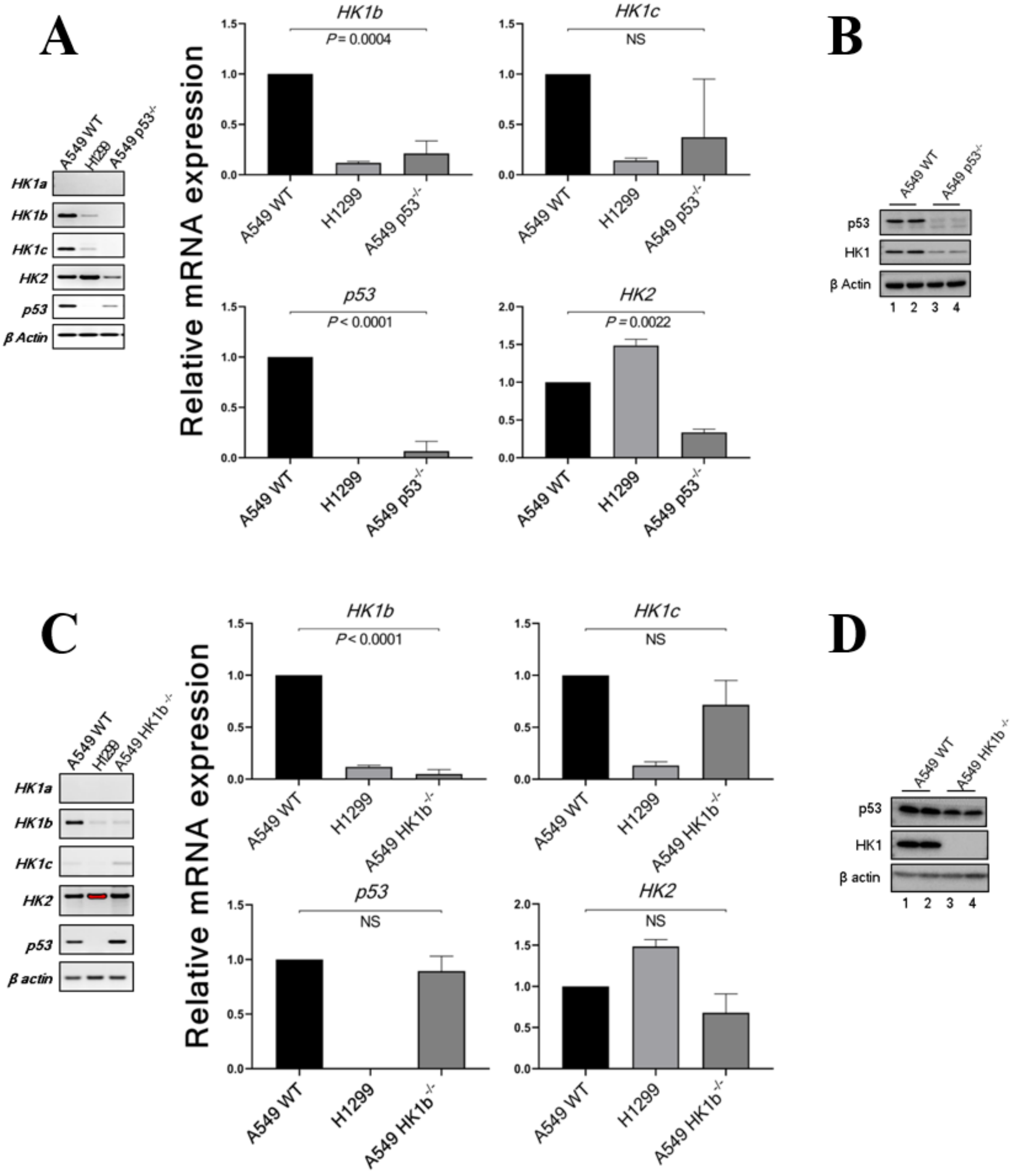
A
A549 WT
H1299
A549 p53-/-
HK1a
HK1b
HK1c
HK2
p53
β Actin
Relative mRNA expression
HK1b
P = 0.0004
HK1c
NS
p53
P < 0.0001
HK2
P = 0.0022
0.0
0.5
1.0
1.5
2.0
B
A549 WT
A549 p53-/-
p53
HK1
β Actin
1 2 3 4
C
A549 WT
H1299
A549 HK1b-/-
HK1a
HK1b
HK1c
HK2
p53
β actin
Relative mRNA expression
HK1b
P < 0.0001
HK1c
NS
p53
NS
HK2
NS
D
A549 WT
A549 HK1b-/-
p53
HK1
β actin
1 2 3 4

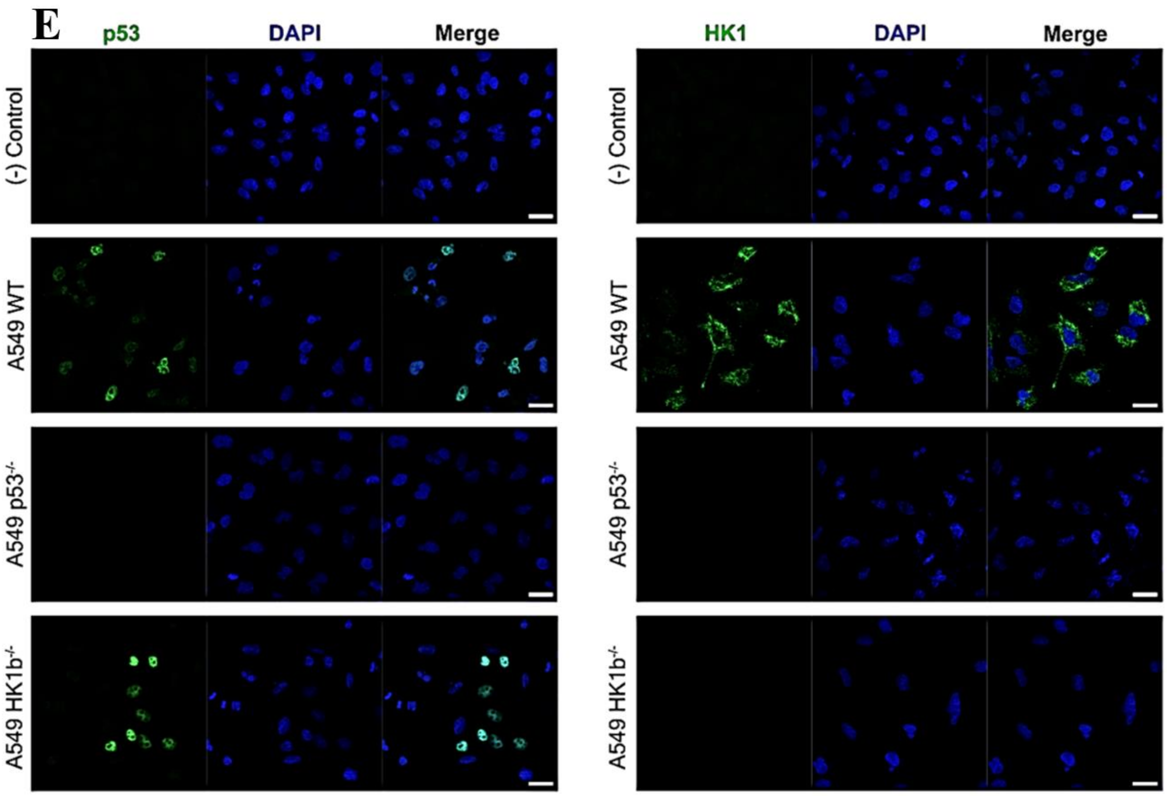

Figure 4.3.2 Elimination of p53 and HK1 b isoform. A549 p53-/- and A549 WT cells were analyzed by **A)** qRT-PCR for level of HK1 b, c, HK2, and p53 in A549 p53-/- cells. Error bars indicate mean ± SEM, (n=3) or **B)** Immunoblot analysis of p53 KO in A549 cells. A549 HK1b-/- and A549 WT cells were analyzed by **C)** qRT-PCR for level of HK1 b, c, HK2, and p53 in A549. Error bars indicate mean ± SEM, (n=3) or **D)** Immunoblot analysis of HK1b KO in A549 cells. E) Immunofluorescence analysis of p53 KO and HK1b KO in A549 cells.

4.4 Deletion of HK1b suppresses cell proliferation and tumorigenesis in NSCLC cells via regulating glycolytic activity

N-terminal domains stabilize HK1 and HK2 enzymes and are involved in their binding to the outer mitochondrial membrane [117, 118]**.** Although HK1a, b, c and HK2 have structural similarities, major differences in N-terminal sequence distinguishes from one another and thus provide distinct biochemical and functional properties in glycolytic pathway and tumor development [118-120]. We predict that an extra alpha-helix that is in the sub-domain of N-terminus of HK1b isoform might provide additional stability to the protein as shown by root-mean square fluctuation analysis (Fig. 4.4.1A). Consequently, this may impact the strength of the interaction between mitochondria and HK1b as this helix was shown to be at interface of mitochondria and the HK1 [118].

To understand the mechanism and the functional role of HK1b isoform in proliferation, survival, and tumorigenesis, we analyzed the metabolic consequences of HK1b isoform deficiency. Changes in glycolysis and respiration were measured using the Seahorse metabolic analyzer. Analysis of the mitochondrial respiration rate following HK1b knockout (KO) resulted in nonsignificant changes in oxygen consumption rate (OCR) and basal respiration (Fig. 4.4.2A), suggesting that HK1b ablation did not alter the mitochondria-driven oxidative phosphorylation (OXPHOS). However, measuring extracellular acidification rate (ECAR) showed significant reductions in glycolytic activity in HK1b isoform-deficient A549 cells (A549 HK1b$^{-/-}$) when compared to parental control cells (A549 WT) (p=0.0001) (Fig. 4.4.2B).

In order to evaluate the effect of reduced glycolysis on proliferation *in vitro*, flow cytometry analyses of Ki67 was performed and A549 HK1b$^{-/-}$ cells showed an approximately 35% decrease in Ki-67 positivity (Fig. 4.4.2C). In order to test the potential role of HK1b *in vivo*, A549 WT and A549 HK1b$^{-/-}$ cells were implanted into immunodeficient NSG male mice via intra-tracheal injection. Mice were necropsied at 8 weeks post-implantation and *relative* tumor volumes were measured. Tumor size was significantly reduced in mice bearing A549 HK1b$^{-/-}$ cells (p=0.01) (Fig. 4.4.3A). Histopathological evaluation of A549 WT or A549 HK1b$^{-/-}$ tumors confirmed that they are both NSCLC lung adenocarcinomas. HK1 staining confirmed complete depletion of HK1 expression in A549 HK1b$^{-/-}$ tumors, while A549 WT tumors expressed high levels (Fig. 4.4.3B). In situ analyses of tumor tissues showed significantly lower Ki-67 staining in A549 HK1b$^{-/-}$ tumors compared to parental control tumors (p=0.001) (Fig. 4.4.3C), indicating that HK1b KO cells have less proliferation ability. In conclusion, all these data show that inhibition of HK1b reduces cell proliferation and tumor cell growth in NSCLC and might be because of reduced glycolysis.

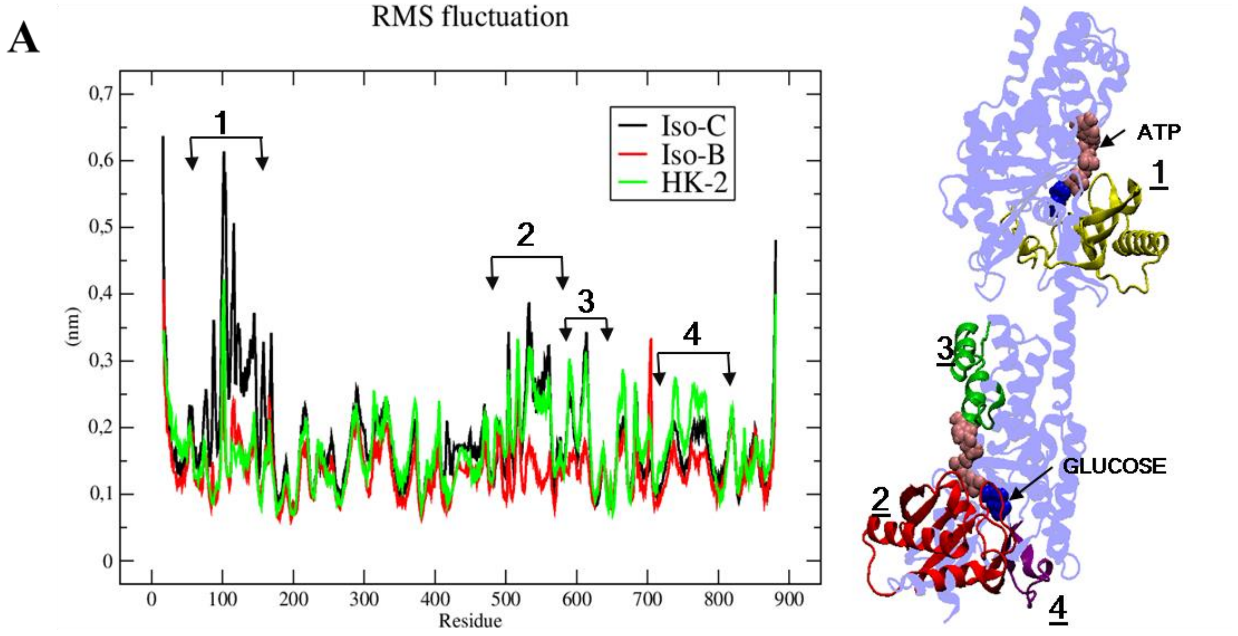

Figure 4.4.1 RMSF Plot shows four major regions fluctuating in HK1c and HK-2 while HK1b is more stable. Structure of HK1c is shown in the figure, first region (1) responsible for ligand binding in N-terminal and a part of small sub-domain (which is responsible for opening and closing of ligands binding pocket), second region (2) ligand binding site in C-terminal part of small sub-domain, third region (3) C-terminal part of large domain and involved in ATP binding, fourth region (4) near to Glucose binding site of C-terminal large domain.

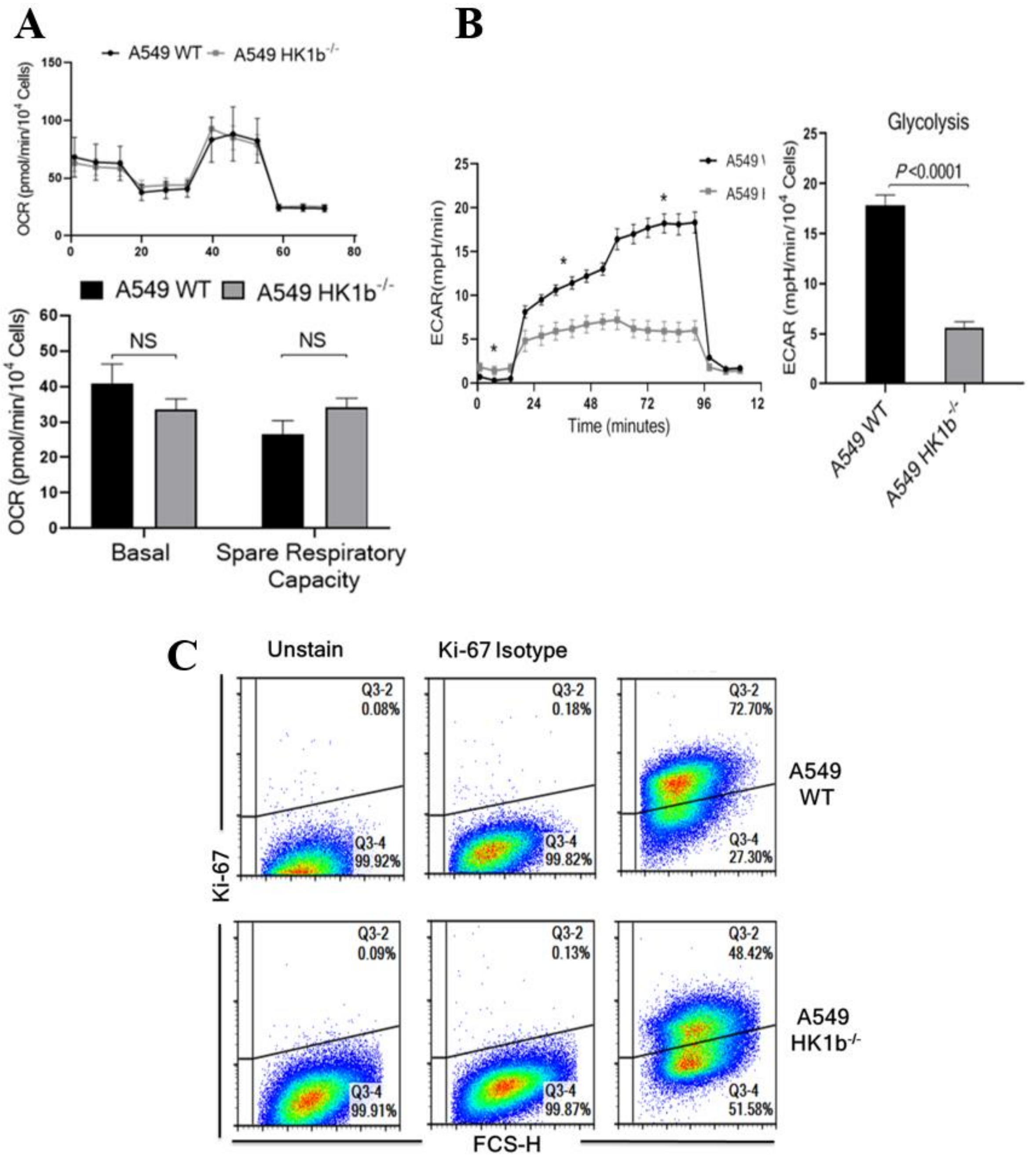

Figure 4.4.2 Effect of HK1b knockout on metabolism and proliferation of A549 cells. Seahorse metabolic analysis **A)** of OCR values from mitochondrial stress test, and **B)** of glycolysis stress test in A549 HK1b-/- and A549 WT cells. Experiments were performed at least twice in quadruplicates for OCR and once for quintuple for ECAR. The results are presented as the mean ± SEM and means compared with Student's t test. **C)** Ki-67 proliferation flow cytometry analysis of A549 WT and A549 HK1b-/-.

A

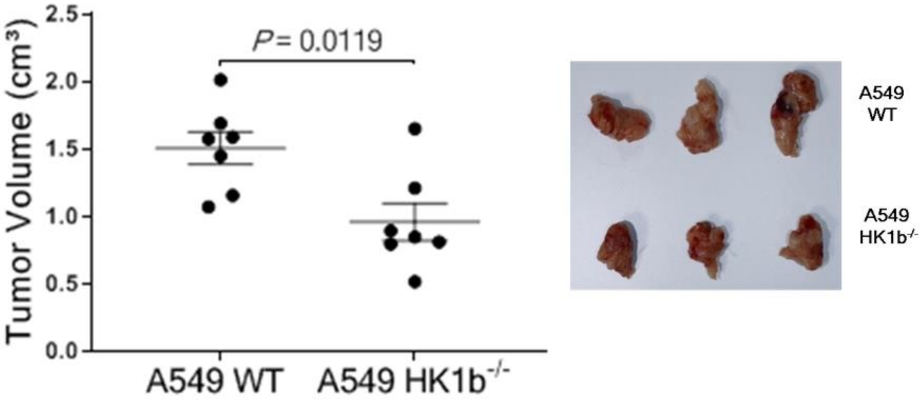

Tumor Volume (cm³)
2.5
2.0
1.5
1.0
0.5
0.0
P= 0.0119
A549 WT
A549 HK1b-/-
A549 WT
A549 HK1b-/-

B

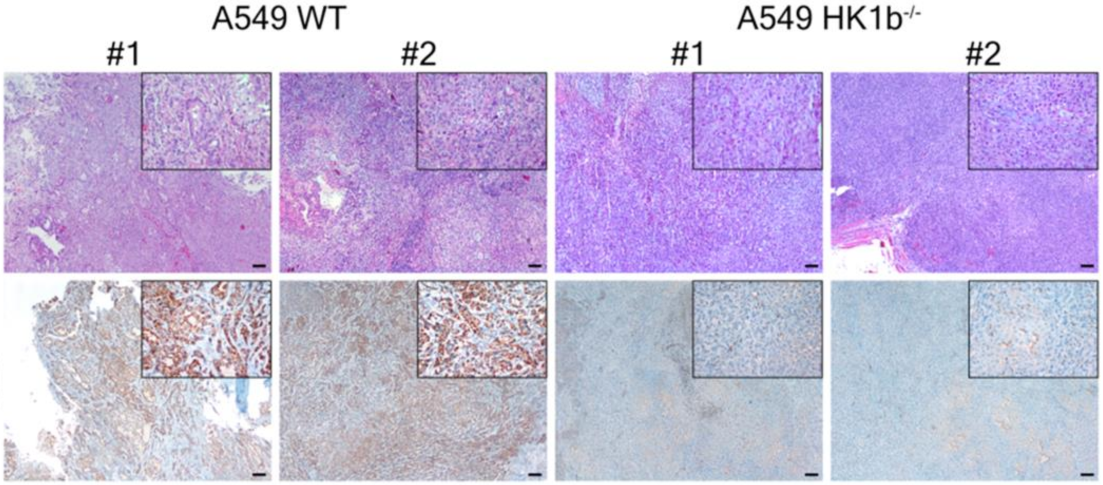

A549 WT
A549 HK1b-/-
#1
#2
#1
#2
H&E
HK1

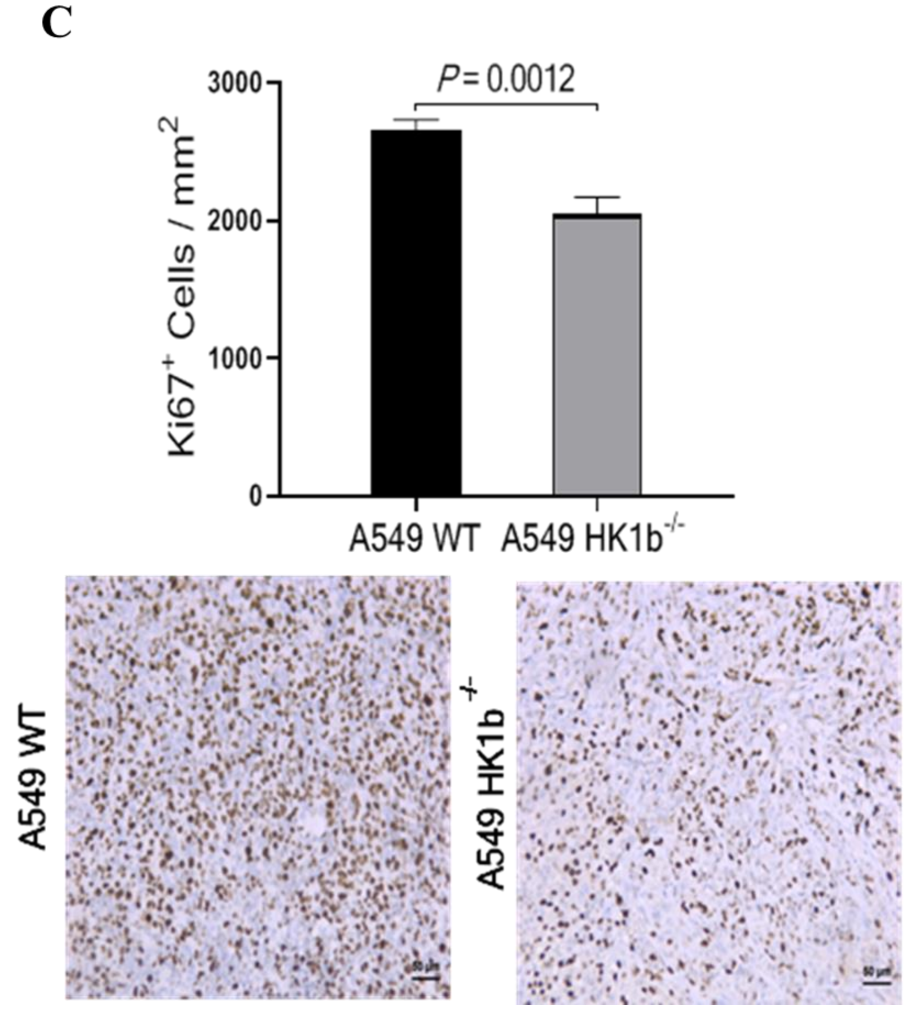

Figure 4.4.3 Effect of HK1b knockout on tumorigenicity of A549 cells. **A)** A549 WT or A549 HK1b-/- cells were intra-tracheally injected into immunodeficient NSG male mice. Graphs on the left show tumor volume in (n=7, each) A549 WT (control) and A549 HK1b-/- (n=7) mouse and representative images of resected tumors on the left. Tumor volumes presented as mean ± SEM, two-tailed unpaired t-test. **B)** Immunohistochemical staining of HK1 expression and H&E staining in representative mouse xenograft A549WT tumor (left) and A549 HK1b-/- tumor (right). Images are 40X magnification; insets are 200X magnification. Scale bars, 100 µm. **C)** Representative photographs of Ki-67 expression in xenografts of A549 WT (left) and A549 HK1b-/- (right) stained by IHC in upper panel. Number of Ki-67 positive cells is counted per area (mm2) from 5 different fields in 8 different slides. The results are presented as the mean ± SEM and means compared with Student's t test.

4.5 HK1b plays critical role in cisplatin response, metabolism, and survival in NSCLC cells

The treatment options for NSCLC are mainly based on several factors but in general, chemotherapy is often one of the first line therapies in NSCLC patients. *Cisplatin* is slightly more effective platinum-based treatment for NSCLC patients. However, cisplatin has been associated with wide range of side effects [121, 122]. Moreover, inhibitors targeting metabolic changes have been developed as a potential therapeutics and there are now several early-phase clinical trials testing metabolic inhibitors [123]. However, the efforts that have been made so far not successfull because of adverse side effect of these drugs [11]**.** Therefore, there is a clinically unmet need for identification of specific and effective metabolic targets in cancer cells to improve survival and reduce disease-related adverse events in NSCLC patients. We first hypothesized that HK1b elimination in combination with cisplatin could synergize to decrease glycolysis further that could potentially have therapeutic utility for NSCLC patients. Indeed, we observed further reduction in basal glycolysis and glycolytic capacity though not significant, and total absence of glycolytic reserve on cisplatin treated A549 HK1b$^{-/-}$ cells (Fig. 4.5.1B). No significant change of basal respiration rate was observed between both cisplatin treated A549 WT and A549 HK1b$^{-/-}$ cells, suggesting that HK1b ablation maintains the OXPHOS. However, only spare respiratory capacity was diminished in cisplatin treated A549 WT cells (p=0.02) (Fig. 4.5.1A).

We next investigated whether the HK1b deletion could sensitize NSCLC cells to cisplatin treatment. Cell viability assay was performed in A549 HK1b$^{-/-}$ cells showed significantly lower IC50 value for cisplatin (47μM) than the A549 WT control group (75μM) (Fig. 4.5.2.A). Based on these results, A549 WT and A549 HK1b$^{-/-}$ cells were treated with cisplatin at 75μM and 47μM, respectively for 48 hours. Flow cytometric quantification of cell death measured by propidium iodide *(*PI) staining. HK1b deletion when combined with cisplatin treatment significantly augmented cell death in A549 HK1b$^{-/-}$ cells (Fig. 4.5.2B). Furthermore, we found that cisplatin treatment induces cleavage of PARP and caspase 3 but induction of cleavage was significantly higher in A549 HK1b$^{-/-}$ cells (Fig. 4.5.3A). Additionally, we used rapamycin as a control and found that cisplatin but not rapamycin treatment induces apoptosis. However, cisplatin promoted greater cell death in

HK1b deleted cells (Figure 4.5.3A). Interestingly, HK1b deletion slightly induces down-regulation of Bcl-2 expression in untreated A549 HK1b$^{-/-}$ cells and further down-regulation of Bcl-2 expression was significant with the cisplatin treatment (Fig. 4.5.3B). Indeed, HK1 plays an important role in protecting against mitochondrial regulated apoptosis through direct interaction with mitochondria [124]**.** Surprisingly, HK1 expression was significantly upregulated in cisplatin treated A549 WT cells (Figure 4.5.3B). Altogether, these results suggest that loss of HK1b sensitizes NSCLC cells to cisplatin induced apoptosis.

In order to identify the underlying molecular mechanisms of synergistic apoptosis induction, we examined several signaling pathways. Upon silencing of HK1b, we detected that AKT, ERK (extracellular signal-regulated kinase), and GSK3β (Ser-9*)* phosphorylation were increased but mTOR phosphorylation was maintained in A549 HK1b$^{-/-}$ cells potentially due to glycolysis depletion in comparison to A549 WT cells (Fig. 4.5.3C and 4.6.2A). Moreover, cisplatin treatment of A549 HK1b-/- cells resulted in significant reduction of AKT phosphorylation (Fig. 4.5.3C) as well as mTOR (Fig. 4.6.2A), and STAT3 phosphorylation (Figure 4.5.3C). However, ERK and GSK3β phosphorylations were further increased by cisplatin treatment in A549 WT cells and A549 HK1b$^{-/-}$ cells (Fig. 4.5.3C). It was previously reported that AKT plays critical role in enhancing glycolysis through increasing HK activity while ERK signaling has role in promoting the aerobic glycolytic phenotype via induction of transcriptional regulators of glycolysis [73, 125, 126]. On the other hand, ERK phosphorylation might also be involved in cell death particularly when there is DNA damage [127]. Our results confirmed that cisplatin was shown to induce DNA damage as well as ERK phosphorylation. Furthermore, HK1b ablation in combination with cisplatin treatment induces greater apoptosis through down regulation of Bcl-2 by blocking its anti-apoptotic function. Taken together these results indicate that, HK1b depletion sensitizes NSCLC cells to cell death and synergizes to cisplatin.

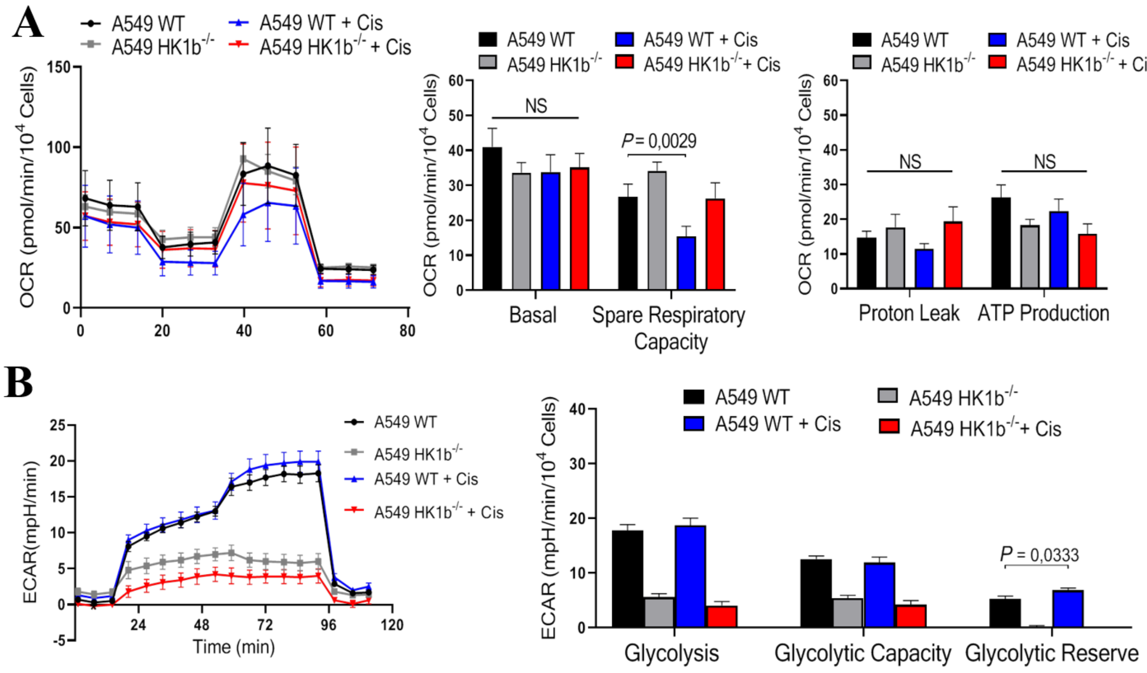

Figure 4.5.1HK1b KO role in cisplatin response on metabolism, **A)** OCR analysis of untreated or 6hrs cisplatin treated A549 WT and A549 HK1b-/- cells. Experiments were performed twice in quadruplicates for OCR. The results are presented as the mean ± SEM and means compared with one-way ANOVA and Tukey's post hoc test. **B)** ECAR analysis of untreated or 6hrs cisplatin treated A549 WT and A549 HK1b-/- cells. Experiments were performed once for quintuple for ECAR. The results are presented as the mean ± SEM and means compared with one-way ANOVA and Tukey's post hoc test

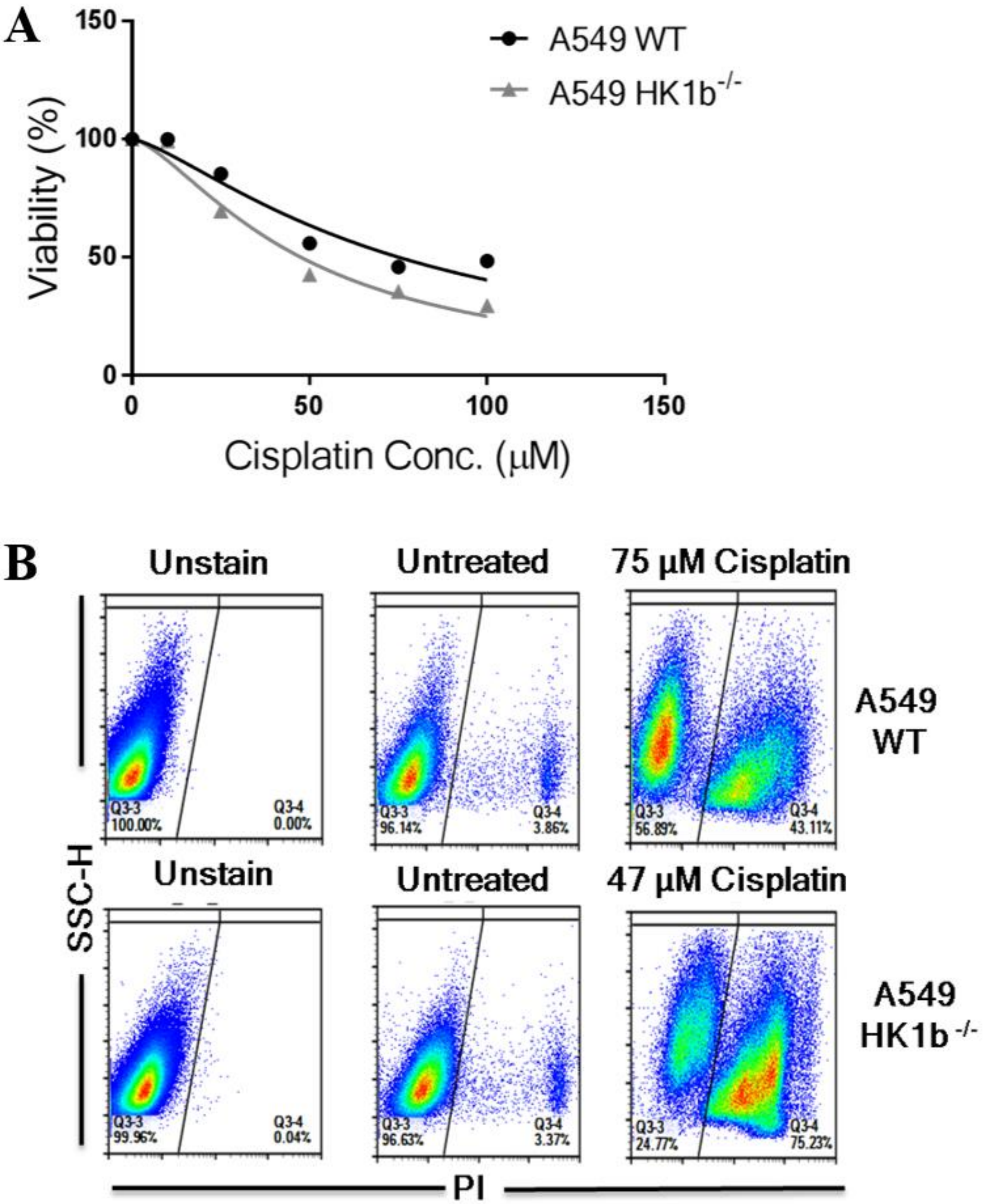

Figure 4.5.2 HK1b KO role in cisplatin response **A)** A549 WT and A549 HK1b-/- cells were treated with increasing concentrations of cisplatin (0.1 µM–100 µM) for 48 h. Dose-response curves were generated from which IC50 values were deduced (n=2). **B)** Flow cytometric quantification analysis of propidium iodide (PI) staining in A549 WT and A549 HK1b-/- cells as unstained, untreated, and treated with cisplatin (75µM and 47 µM, respectively), (n=2).

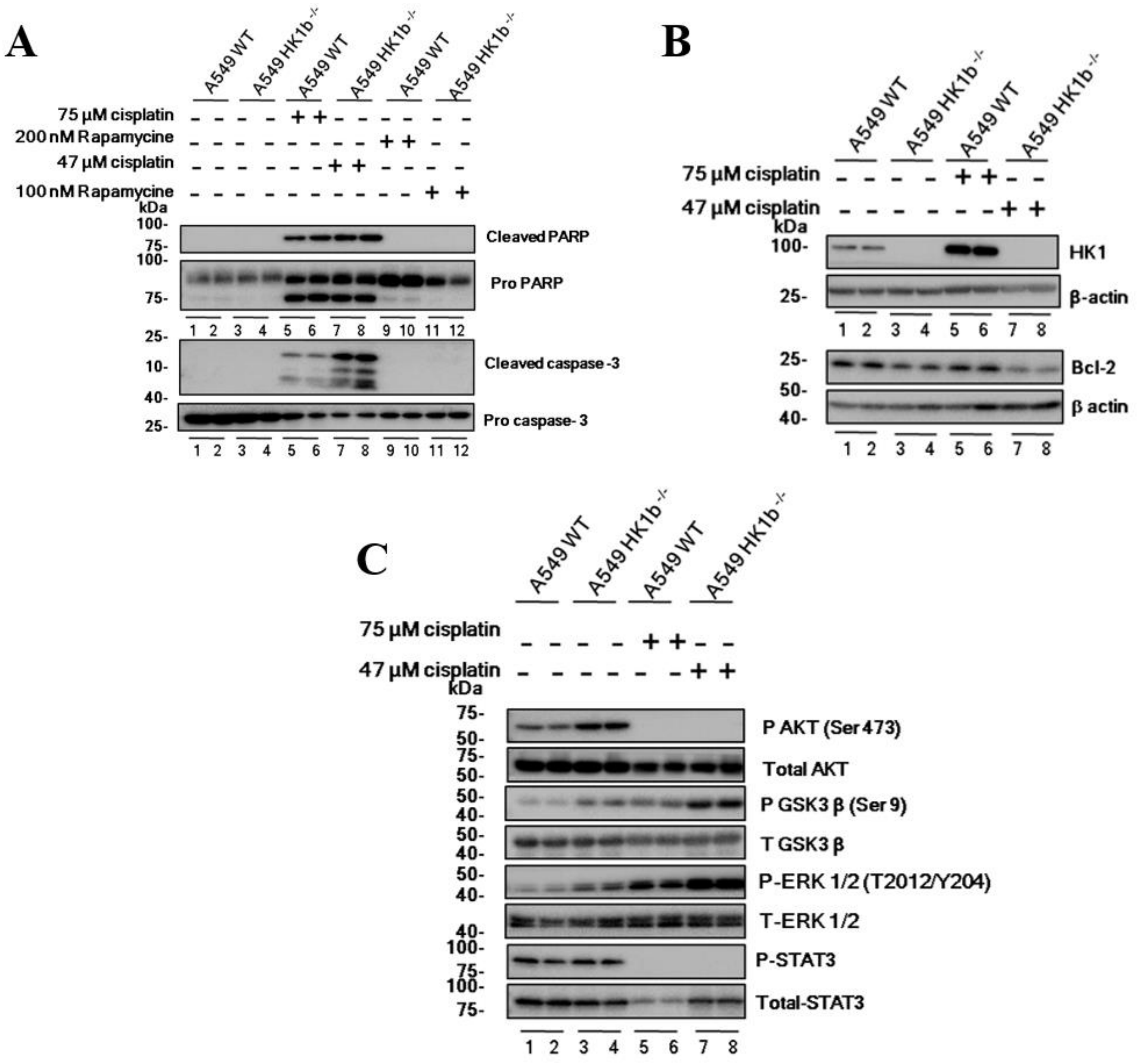
A
A549 WT
A549 HK1b -/-
75 µM cisplatin
200 nM Rapamycine
47 µM cisplatin
100 nM Rapamycine
kDa
Cleaved PARP
Pro PARP
Cleaved caspase -3
Pro caspase- 3
1 2 3 4 5 6 7 8 9 10 11 12
B
HK1
β-actin
Bcl-2
β actin
1 2 3 4 5 6 7 8
C
P AKT (Ser473)
Total AKT
P GSK3 β (Ser 9)
T GSK3 β
P-ERK 1/2 (T2012/Y204)
T-ERK 1/2
P-STAT3
Total-STAT3

Figure 4.5.3 Immunoblot analysis of cells treated with cisplatin (75µM and 47 µM, respectively) or rapamycin (100µM and 47 µM, respectively). **A)** Immunoblot analysis of apoptosis markers. **B)** Immunoblot analysis of HK1 and Bcl-2. Anti-beta-actin is used as a loading control. **C)** Immunoblot analysis of AKT, GSK3β, ERK, and STAT3.

4.6 Deletion of HK1b sensitizes cells to cisplatin induced cytotoxicity via p53 mediated apoptotic and autophagic cell death.

Because of the fact that HK1b deletion results in glycolysis reduction and synergize cells to cytotoxic cell death, we investigated the underlying mechanism of apoptotic cell death in HK1b deleted cells upon treatment with cisplatin. We found that H2AX phosphorylation is inhibited by both cisplatin and rapamycin treatments (Fig. 4.6.1A). Indeed, kinetics of H2AX phosphorylation is time dependent since cells must enter S phase in order for

H2AX stimulation [128]. We showed that cisplatin increases apoptosis through both activation through phosphorylation of Ser15 and high level of expression of p53 in HK1b deleted cells. In contrast, p53 expression was not induced by rapamycin treatment (Fig. 4.6.1A), indicating that only HK1b depletion and cisplatin synergize the induction of p53 mediated apoptosis. Furthermore, characteristics of apoptosis have been detected by electron microscopy (Fig. 4.6.1B). Recent reports suggested a complex and multifaceted relationship between autophagy and apoptosis. Moreover, glucose deprivation typically results in autophagy induction to maintain energy homeostasis [129]. However, autophagy might be growth inhibitory after a certain threshold [130]. In order to determine whether the combination of HK1b deletion and cisplatin led to the activation of autophagy in NSCLC cells, we examined the markers of autophagic signaling pathway upon treatment with cisplatin and rapamycin as a control. Expectedly, HK1b elimination induces autophagy in response to glucose deprivation since formation of LC3II significantly elevated in A549 HK1b$^{-/-}$ cells. Moreover, expression of the autophagy marker LC3-II was markedly induced in HK1b deleted cells when treated with cisplatin or rapamycin treatment in A549 HK1b$^{-/-}$ cells (Fig. 4.6.2A). Furthermore, cisplatin significantly inhibits phosphorylation of mTOR in A549 HK1b$^{-/-}$ cells (Fig. 4.6.2A). Furthermore, upon cisplatin or rapamycin treatment, AMPK phosphorylation was diminished in A549 WT cells but the phosphorylation is totally inhibited in A549 HK1b$^{-/-}$ cells (Fig. 4.6.2A). Although we observed higher LC3II expression level in cisplatin or rapamycin treated A549 HK1b$^{-/-}$ cells, expression levels of other autophagic indicators of beclin-1 and ATG13 expression levels were downregulated in both A549 WT, A549 HK1b$^{-/-}$ cells. However, concomitantly beclin-1 and ATG13 levels were not changed with rapamycin treatment (Fig. 4.6.2A). We further demonstrate that cisplatin treatment induces significant numbers of autophagic vesicles and myelinoid bodies in HK1b deleted cells as demonstrated by electron microscopy (Fig. 4.6.2B). Our findings suggest that while autophagy was induced mainly by reduction of glycolysis, apoptotic cell death was induced mainly by cisplatin. These data imply that combination of HK1b deletion with cisplatin induces greater cell death through increased activity of apoptotic and autophagic pathways.

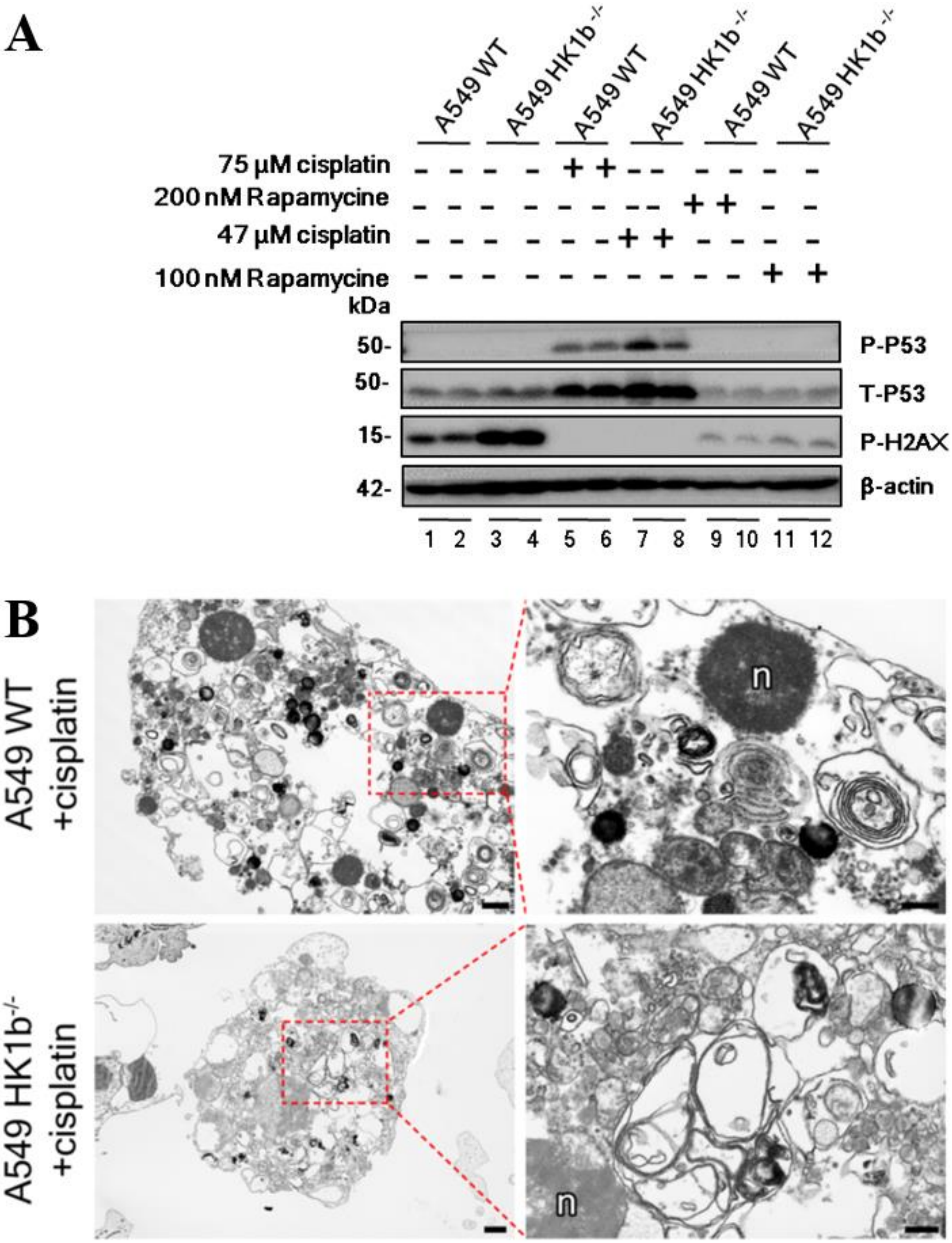
A
A549 WT
A549 HK1b -/-
A549 WT
A549 HK1b -/-
A549 WT
A549 HK1b -/-
75 µM cisplatin
200 nM Rapamycine
47 µM cisplatin
100 nM Rapamycine
kDa
50-
50-
15-
42-
P-P53
T-P53
P-H2AX
β-actin
1 2 3 4 5 6 7 8 9 10 11 12
B
A549 WT +cisplatin
A549 HK1b-/- +cisplatin
n
n

Figure 4.6.1 Synergetic effect HK1b ablation and cisplatin increases p53-mediated apoptotic cell death. Immunoblot analysis of cells treated with cisplatin (75µM and 47 µM, respectively) or rapamycin (100µM and 47 µM, respectively) **A)** Immunoblot analysis of p53 and H2AX **B)** Representative transmission electron microscopy (TEM) micrographs displaying characteristics of apoptosis; images are representative of two independent experiments; scale bar, 1µm (left) and 400 nm (right).

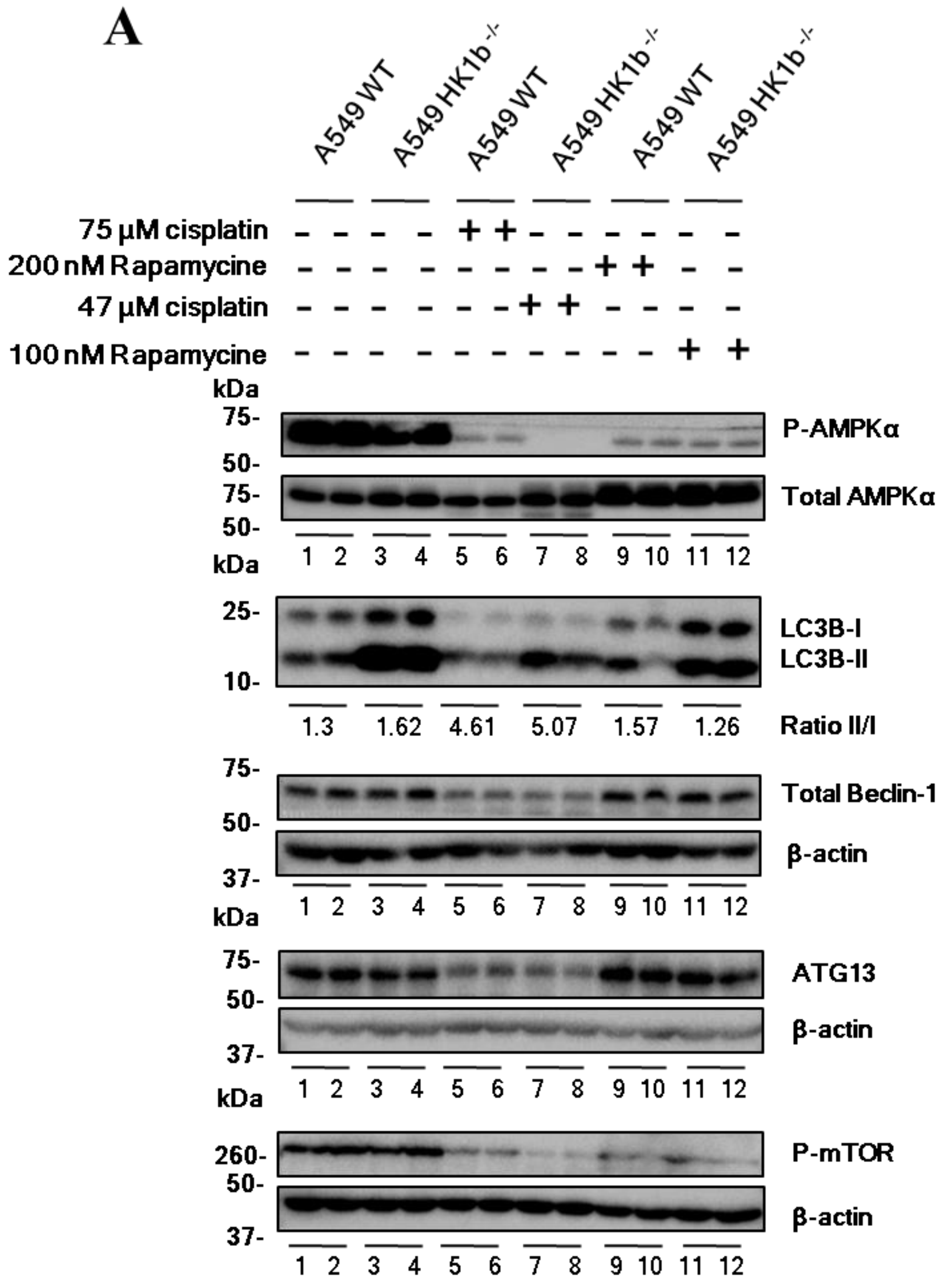
A
A549 WT
A549 HK1b -/-
A549 WT
A549 HK1b -/-
A549 WT
A549 HK1b -/-
75 µM cisplatin - - - - + + - - - - - -
200 nM Rapamycine - - - - - - - - + + - -
47 µM cisplatin - - - - - - + + - - - -
100 nM Rapamycine - - - - - - - - - - + +
kDa
75-
50-
P-AMPKα
75-
50-
Total AMPKα
1 2 3 4 5 6 7 8 9 10 11 12
kDa
25-
10-
LC3B-I
LC3B-II
1.3
1.62
4.61
5.07
1.57
1.26
Ratio II/I
75-
50-
Total Beclin-1
37-
β-actin
1 2 3 4 5 6 7 8 9 10 11 12
kDa
75-
50-
ATG13
37-
β-actin
1 2 3 4 5 6 7 8 9 10 11 12
kDa
260-
P-mTOR
50-
37-
β-actin
1 2 3 4 5 6 7 8 9 10 11 12

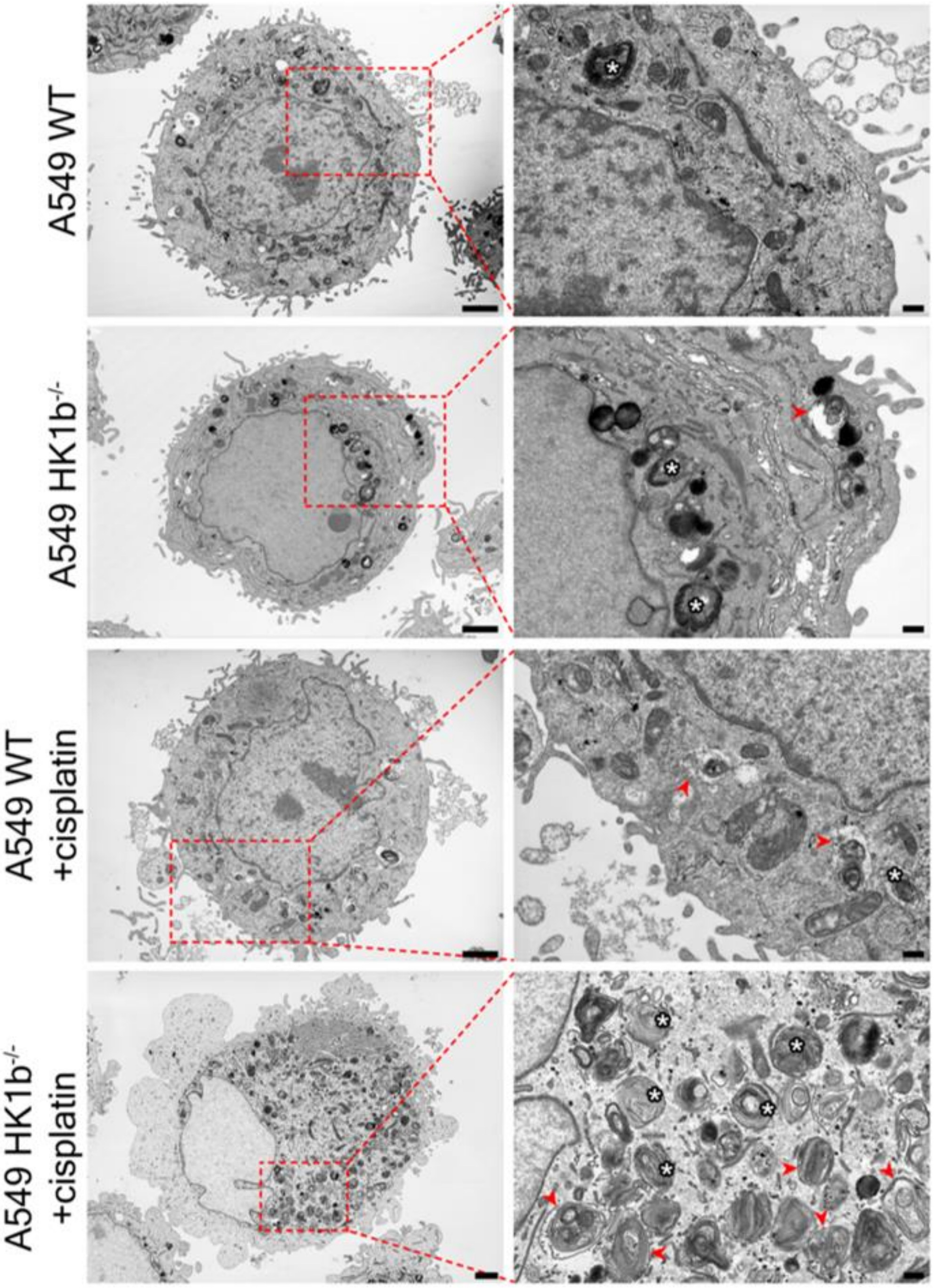

Figure 4.6.2 Synergetic effect HK1b ablation and cisplatin increases autophagic cell death. Immunoblot analysis of cells treated with cisplatin (75µM and 47 µM, respectively) or rapamycin (100µM and 47 µM, respectively) **A)** Immunoblot analysis of AMPKα, LC3B I/II, Beclin-1, ATG13, mTOR. Anti-beta-actin is used as a loading control. **B)** Representative transmission electron microscopy (TEM) micrographs displaying characteristics of autophagy; images are representative of two independent experiments; scale bar, 2µm (left) and 400 nm (right). Red arrows represent autophagic vesicles, black starts represent myelinoid bodies and n refers to nuclear fragment.

5 DISCUSSION

Like most cancers, NSCLC display comprehensive multiple metabolic alterations such as reprogramming of glucose metabolism and increased dependency on glycolysis [131, 132]. This is manifested by turning on the expression of certain enzymes such as Hexokinases (HKs) that are required for the accelerated glucose metabolism in NSCLC cells. Selective HK isoforms that regulate glucose metabolism in NSCLC cells but dispensable or absent in normal lung cells would be an attractive molecular target. In this line of work, we demonstrated that HK1 expression was significantly elevated in comparison to HK2 expression in NSCLC patient tumor samples.

It is known that alternative splicing of HK1 gene results in several transcripts encoding different isoforms, while HK2 gene has only one transcript according to RefSeq data. To the best of our knowledge, although specific HK1 isoforms has been reported in testis, there have been no reports on the role of these isoforms in other tissues (including cancer) [112]. In order to understand whether alternative isoforms tend to display distinct expression patterns, we analyzed the expression of 3 different isoforms of HK1 (HK1a, b, and c) in NSCLC cells and primary tumor tissues along with HK2, and p53. We found that only HK1b isoform was predominantly expressed in NSCLC cells and it was higher in the p53 WT A549 cells. Significantly elevated HK1b isoform in patient tumors as compared to normal tissue has also been detected, indicating a higher dependency on glycolysis and resistance to cell death in these tumor cells. Our data suggests that HK1b isoform may have therapeutic utility targeting metabolic pathway in NSCLC.

Despite several activities of p53 in cellular response, the role of p53 in the regulation of metabolism is complex. Several studies have shown that p53 regulates glycolysis by upregulating genes or increasing activity of enzymes such as hexokinases (HK1 and HK2) [25, 88]. Although, a few studies suggest that p53 might have direct connection with HK, how p53 regulates hexokinase (HK), whether is a direct regulation or not is still elusive. In reference to p53, an early study suggested that p53 increases HK2 mRNA transcription through p53-responsive elements, suggesting that p53 can promote at least some steps in glycolysis by regulating HKs [133]. Moreover, recent study found that depletion of WT p53 resulted in decreasing glycolysis and proliferation in hepatoma carcinoma cells

(HCC), suggesting that WT p53 may direct role in regulating genes that are responsible for glycolysis. Additionally, study showed that WTp53 is required to maintain growth and glycolysis by examining several different human cancer cells other than HCC cells. Altogether study revealed the oncogenic role of WTp53 in promoting the cancer metabolic switch by dominantly suppressing OXPHOS [134]. We first observed that HK1b isoform expressed in only in p53WT-A549 cells but not in p53null-H1299 cells. To find out if this finding was due to whether cell specific or p53 related event, we deleted p53 in P53WT-A549 cells using CRISPR/Cas9 system. In our study we found that p53 regulates HK1b isoform as a result of genetic disruption of *p53*.

To extent the clinical relevance of HK1b data, we examined the functional role of HK1b by deleting HK1b isoform in A549 cells using CRISPR/Cas9 system. We found that HK1b deletion inhibits proliferation and tumorigenesis *in vivo* and synergizes with cisplatin to sensitize NSCLC cells to cell death because of significant reduction of glycolysis and downregulation of the anti-apoptotic proteins. The treatment options for NSCLC patients are based mainly on several factors, including the stage of the cancer and availability of molecular markers for targeted therapy. Currently, cisplatin is widely used as a one of the main platinum-based drug, but low efficacy and considerably side effects as a single agent would not benefit NSCLC patients [122]**.** Our results provide ample evidence that the combination of cisplatin and HK1b silencing markedly increased NSCLC cell death. Cisplatin induced cytotoxicity in HK1b deleted cells is regulated by induction of p53-mediated apoptosis and increased autophagy by depletion of glycolysis. Together our data suggest that HK1b deletion could significantly synergize cells to cisplatin. The mechanism by which HK1b deletion synergizes cells to cisplatin cytotoxicity may be through blocking its binding ability to mitochondria. Our work is consistent with the previous report, suggesting that the increased expression of HK1 attenuates apoptosis in a glucose-dependent manner because of its anti-apoptotic effect and also induction of increased HK activity [124]. As previously reported, mitochondrial binding of HKs near voltage-dependent ion channel (VDAC) may be required for access to ATP to efficiently phosphorylate glucose [135].

Furthermore, we showed that N-domain of HK1b isoform is more stable around the glucose and ATP binding site compared to HK1c isoform and HK2 using molecular dynamic simulations. Our result might provide a better explanation for higher stability of HK1b over HK2 by showing that HK1b deletion induces significant depletion of glycolysis. Moreover, HK1b ablation alone or with cisplatin increases AKT, ERK, and GSK3β signaling. AKT and ERK both have role in promoting glycolysis [136]. AKT activity, particularly through the phosphorylation of T473 residue promotes glucose metabolism by stimulating the activity of hexokinase [137]. ERK increases glycolysis by upregulating transcriptional expressions of several metabolic genes [84, 138]. The inhibition of GSK3β (Ser9) is required for the stimulation of glycogen and protein synthesis and, was also suggested as a mechanism for increased resistance to apoptosis of cancer cells [139]. Recent studies strongly indicate that mitochondrial-bound HK1 and HK2 play a major role in preventing tumor apoptosis by blocking mitochondrial outer membrane permeabilization (MOMP) and the association is regulated by GSK3β [120, 140]. It has been reported that serine phosphorylation of GSK-3 is mediated by protein kinases such as AKT and ERK1/2/p90RSK [141]. Here, we found that synergetic effect of HK1b ablation and cisplatin induces higher activation of ERK inhibition of GSK3β despite the inhibition of mTOR and AKT activation because of significant reduction in glycolysis. It was suggested that, cisplatin induces DNA damage thereby activates ERK, and extensive DNA damage-induced by ERK activation causes apoptosis [142, 143]. Consistent with these studies, we also found that upregulation of HK1 in parental A549 cells upon cisplatin treatment. Furthermore, we showed downregulation of anti-apoptotic Bcl-2 upon HK1b deletion which was further reduced by cisplatin treatment. These results suggest that HK1b has an important role in not only glycolysis but also apoptotic resistance mechanism by induction of p53-mediated apoptosis.

To determine whether HK1b plays a regulatory role in autophagy under glucose deprivation, we evaluated NSCLC cells after ablation of HK1b and determined the possible change with cisplatin treatment. We found that HK1b deletion induces autophagy in A549 HK1b$^{-/-}$ cells with increased *LC3B-II* formation regardless of change in expression of AMPK, Beclin1, and ATG13. We also observed that autophagy was significantly elevated in A549 HK1b$^{-/-}$ cells in combination with cisplatin at multiple levels. Furthermore, electron microscopy images revealed significantly increased numbers of autophagic vesicles and myelinoid bodies in HK1b deleted cells upon cisplatin treatment. Interestingly, we observed inhibition of the AMPK phosphorylation and downregulation of autophagic markers such as Beclin-1 and ATG13 in NSCLC cells upon cisplatin treatment. In line with our results, it was previously reported that AMPK inhibition sensitizes several cancer cells to cisplatin via hyper-induction of p53 [144]. Taken together, our studies provide first evidence that HK1b is a compelling metabolic therapeutic target that may also potentiate the efficacy of cisplatin in NSCLCs.

6 CONCLUSION AND FUTURE WORK

The identification of isoform-specific contributors to cancer cell glucose metabolism that could be selectively targeted to eliminate cancer cells without compromising systemic homeostasis or corresponding metabolic functions in normal cells could be a very attractive approach for cancer therapy

To identify novel potential mediators and drivers of NSCLC, we analyzed HK1 isoforms (HK1a, HK1b, and HK1c) along with HK2, and p53 expression in NSCLC cell lines (A549 and H1299) and patient samples. Since there is no isoform specific antibody to detect HK1 isoforms at protein level, we first analyze the HK1 transcripts and its association to survival in clinical NSCLC tissue samples. We found that HK1 is abundantly expressed in tumors of lung cancer patients compared to their adjacent non-tumor tissues and showed that higher expression of HK1 associates with poor survival. We showed the first time that only HK1b isoform is predominantly expressed in A549 cells and NSCLC patient tumors; this distinguishes NSCLC cells from the normal surrounding lung cells and HK1b is associated with poor NSCLC patient survival.

We observed that HK1b expression was changed based on p53 status using p53 null and p53 WT NSCLC cells. In order to identify the mechanisms of HK1b regulation by p53, we deleted the p53 or HK1b isoform in human NSCLC A549 cells using CRISPR/Cas9 system. Surprisingly, we showed that p53 positively regulates HK1b. To understand the role of HK1b in NSCLC, we used HK1b knock out A549 NSCLC cells. We found that HK1b ablation inhibits glycolysis significantly, hence proliferation, and *in vivo* tumor growth of NSCLC cells. HK1b deletion caused increased in survival signaling through AKT and GSK3β to compensate significant reduction of glycolysis.

Finally, HK1b ablation and cisplatin were synergistic in decreasing glycolysis, increasing apoptosis through upregulation of p53, and inhibiting tumor growth *in vivo*. Cisplatin also synergized with HK1b deficiency to inhibit AKT, STAT3, SAPK/JNK, and mTOR in an AMPK-independent manner. Finally, HK1b deficiency with cisplatin treatment markedly increased the susceptibility to cell death by not only induction of apoptosis, but also inducing significantly increased number of autophagic vesicles and myelinoid bodies with increased LC3-II lipidation regardless of downregulation of autophagic markers such as Beclin 1 and ATG13. Collectively, these findings suggest that therapeutic strategies to modulate the Warburg effect, such as targeting HK1b isoform, may interfere with growth and therapeutic sensitivity of NSCLC.

7 BIBLIOGRAPHY

1. Wong, M.C.S., et al., *Incidence and mortality of lung cancer: global trends and association with socioeconomic status.* Sci Rep, 2017. **7**(1): p. 14300.
2. Latimer, K.M. and T.F. Mott, *Lung cancer: diagnosis, treatment principles, and screening.* Am Fam Physician, 2015. **91**(4): p. 250-6.
3. Herbst, R.S., J.V. Heymach, and S.M. Lippman, *Lung cancer.* N Engl J Med, 2008. **359**(13): p. 1367-80.
4. Alberg, A.J., et al., *Epidemiology of lung cancer: Diagnosis and management of lung cancer, 3rd ed: American College of Chest Physicians evidence-based clinical practice guidelines.* Chest, 2013. **143**(5 Suppl): p. e1S-e29S.
5. Schwartz, A.M. and M.K. Rezaei, *Diagnostic surgical pathology in lung cancer: Diagnosis and management of lung cancer, 3rd ed: American College of Chest Physicians evidence-based clinical practice guidelines.* Chest, 2013. **143**(5 Suppl): p. e251S-e262S.
6. Radzikowska, E., P. Glaz, and K. Roszkowski, *Lung cancer in women: age, smoking, histology, performance status, stage, initial treatment and survival. Population-based study of 20 561 cases.* Ann Oncol, 2002. **13**(7): p. 1087-93.
7. West, L., et al., *A novel classification of lung cancer into molecular subtypes.* PLoS One, 2012. **7**(2): p. e31906.
8. Herbst, R.S., D. Morgensztern, and C. Boshoff, *The biology and management of non-small cell lung cancer.* Nature, 2018. **553**(7689): p. 446-454.
9. Molina, J.R., et al., *Non-small cell lung cancer: epidemiology, risk factors, treatment, and survivorship.* Mayo Clin Proc, 2008. **83**(5): p. 584-94.
10. Chen, Z., et al., *Non-small-cell lung cancers: a heterogeneous set of diseases.* Nat Rev Cancer, 2014. **14**(8): p. 535-46.
11. Zappa, C. and S.A. Mousa, *Non-small cell lung cancer: current treatment and future advances.* Transl Lung Cancer Res, 2016. **5**(3): p. 288-300.
12. Sher, T., G.K. Dy, and A.A. Adjei, *Small cell lung cancer.* Mayo Clin Proc, 2008. **83**(3): p. 355-67.
13. Gandara, D.R., et al., *Squamous cell lung cancer: from tumor genomics to cancer therapeutics.* Clin Cancer Res, 2015. **21**(10): p. 2236-43.
14. Myers, D.J. and J.M. Wallen, *Cancer, Lung Adenocarcinoma*, in *StatPearls*. 2019, StatPearls Publishing

StatPearls Publishing LLC.: Treasure Island (FL).

15. Larsen, J.E. and J.D. Minna, *Molecular biology of lung cancer: clinical implications.* Clin Chest Med, 2011. **32**(4): p. 703-40.
16. Kadota, K., et al., *Reevaluation and reclassification of resected lung carcinomas originally diagnosed as squamous cell carcinoma using immunohistochemical analysis.* Am J Surg Pathol, 2015. **39**(9): p. 1170-80.
17. Bernardi, F.D.C., et al., *Lung cancer biopsy: Can diagnosis be changed after immunohistochemistry when the H&E-Based morphology corresponds to a specific tumor subtype?* Clinics (Sao Paulo), 2018. **73**: p. e361.
18. Brainard, J. and C. Farver, *The diagnosis of non-small cell lung cancer in the molecular era.* Mod Pathol, 2019.
19. Hirsch, F.R., et al., *New and emerging targeted treatments in advanced non-small-cell lung cancer.* Lancet, 2016. **388**(10048): p. 1012-24.
20. Karachaliou, N., et al., *KRAS mutations in lung cancer.* Clin Lung Cancer, 2013. **14**(3): p. 205-14.
21. Atlas of Genetics and Cytogenetics in Oncology and Haematology. *TP53 mutations in lung cancer*. 2019, July 8; Available from: http://atlasgeneticsoncology.org/Genes/P53ID88.html.
22. Mogi, A. and H. Kuwano, *TP53 mutations in nonsmall cell lung cancer.* J Biomed Biotechnol, 2011. **2011**: p. 583929.
23. Williams, A.B. and B. Schumacher, *p53 in the DNA-Damage-Repair Process.* Cold Spring Harb Perspect Med, 2016. **6**(5).
24. Bieging, K.T., S.S. Mello, and L.D. Attardi, *Unravelling mechanisms of p53-mediated tumour suppression.* Nat Rev Cancer, 2014. **14**(5): p. 359-70.
25. Vousden, K.H. and K.M. Ryan, *p53 and metabolism.* Nat Rev Cancer, 2009. **9**(10): p. 691-700.
26. Napoli, M. and E.R. Flores, *The p53 family orchestrates the regulation of metabolism: physiological regulation and implications for cancer therapy.* Br J Cancer, 2017. **116**(2): p. 149-155.
27. Levine, A.J. and M. Oren, *The first 30 years of p53: growing ever more complex.* Nat Rev Cancer, 2009. **9**(10): p. 749-58.

28. Gibbons, D.L., L.A. Byers, and J.M. Kurie, *Smoking, p53 mutation, and lung cancer.* Mol Cancer Res, 2014. **12**(1): p. 3-13.

29. Tanaka, N., et al., *Gain-of-function mutant p53 promotes the oncogenic potential of head and neck squamous cell carcinoma cells by targeting the transcription factors FOXO3a and FOXM1.* Oncogene, 2018. **37**(10): p. 1279-1292.

30. Oren, M. and V. Rotter, *Mutant p53 gain-of-function in cancer.* Cold Spring Harb Perspect Biol, 2010. **2**(2): p. a001107.

31. Schulz-Heddergott, R. and U.M. Moll, *Gain-of-Function (GOF) Mutant p53 as Actionable Therapeutic Target.* Cancers (Basel), 2018. **10**(6).

32. Chang, J.T., Y.M. Lee, and R.S. Huang, *The impact of the Cancer Genome Atlas on lung cancer.* Transl Res, 2015. **166**(6): p. 568-85.

33. Rivlin, N., et al., *Mutations in the p53 Tumor Suppressor Gene: Important Milestones at the Various Steps of Tumorigenesis.* Genes Cancer, 2011. **2**(4): p. 466-74.

34. Sabapathy, K., *The Contrived Mutant p53 Oncogene - Beyond Loss of Functions.* Front Oncol, 2015. **5**: p. 276.

35. Campling, B.G. and W.S. el-Deiry, *Clinical implications of p53 mutations in lung cancer.* Methods Mol Med, 2003. **75**: p. 53-77.

36. Gu, J., et al., *TP53 mutation is associated with a poor clinical outcome for non-small cell lung cancer: Evidence from a meta-analysis.* Mol Clin Oncol, 2016. **5**(6): p. 705-713.

37. Horio, Y., et al., *Prognostic significance of p53 mutations and 3p deletions in primary resected non-small cell lung cancer.* Cancer Res, 1993. **53**(1): p. 1-4.

38. Mantovani, F., D. Walerych, and G.D. Sal, *Targeting mutant p53 in cancer: a long road to precision therapy.* Febs j, 2017. **284**(6): p. 837-850.

39. Kogan, S. and D. Carpizo, *Pharmacological targeting of mutant p53.* Transl Cancer Res, 2016. **5**(6): p. 698-706.

40. Schulze, A. and A.L. Harris, *How cancer metabolism is tuned for proliferation and vulnerable to disruption.* Nature, 2012. **491**(7424): p. 364-73.

41. Vander Heiden, M.G., L.C. Cantley, and C.B. Thompson, *Understanding the Warburg effect: the metabolic requirements of cell proliferation.* Science, 2009. **324**(5930): p. 1029-33.

42. Gomes, A.P. and J. Blenis, *A nexus for cellular homeostasis: the interplay between metabolic and signal transduction pathways.* Curr Opin Biotechnol, 2015. **34**: p. 110-7.

43. Jaswal, J.S., et al., *Targeting fatty acid and carbohydrate oxidation--a novel therapeutic intervention in the ischemic and failing heart.* Biochim Biophys Acta, 2011. **1813**(7): p. 1333-50.

44. Warburg, O., *On the origin of cancer cells.* Science, 1956. **123**(3191): p. 309-14.

45. Zu, X.L. and M. Guppy, *Cancer metabolism: facts, fantasy, and fiction.* Biochem Biophys Res Commun, 2004. **313**(3): p. 459-65.

46. Hanahan, D. and R.A. Weinberg, *Hallmarks of cancer: the next generation.* Cell, 2011. **144**(5): p. 646-74.

47. Pavlova, N.N. and C.B. Thompson, *The Emerging Hallmarks of Cancer Metabolism.* Cell Metab, 2016. **23**(1): p. 27-47.

48. Kroemer, G. and J. Pouyssegur, *Tumor cell metabolism: cancer's Achilles' heel.* Cancer Cell, 2008. **13**(6): p. 472-82.

49. Nagarajan, A., P. Malvi, and N. Wajapeyee, *Oncogene-directed alterations in cancer cell metabolism.* Trends Cancer, 2016. **2**(7): p. 365-377.

50. Lennartsson, J., et al., *Normal and oncogenic forms of the receptor tyrosine kinase kit.* Stem Cells, 2005. **23**(1): p. 16-43.

51. Escobedo, J.A., et al., *A phosphatidylinositol-3 kinase binds to platelet-derived growth factor receptors through a specific receptor sequence containing phosphotyrosine.* Mol Cell Biol, 1991. **11**(2): p. 1125-32.

52. Kavanaugh, W.M., et al., *Tyrosine 508 of the 85-kilodalton subunit of phosphatidylinositol 3-kinase is phosphorylated by the platelet-derived growth factor receptor.* Biochemistry, 1994. **33**(36): p. 11046-50.

53. Aoki, M., E. Blazek, and P.K. Vogt, *A role of the kinase mTOR in cellular transformation induced by the oncoproteins P3k and Akt.* Proc Natl Acad Sci U S A, 2001. **98**(1): p. 136-41.

54. Rossi, F., et al., *Oncogenic Kit signaling and therapeutic intervention in a mouse model of gastrointestinal stromal tumor.* Proc Natl Acad Sci U S A, 2006. **103**(34): p. 12843-8.

55. Srivastava, A.K. and S.K. Pandey, *Potential mechanism(s) involved in the regulation of glycogen synthesis by insulin.* Mol Cell Biochem, 1998. **182**(1-2): p. 135-41.

56. Alessi, D.R., et al., *Characterization of a 3-phosphoinositide-dependent protein kinase which phosphorylates and activates protein kinase Balpha.* Curr Biol, 1997. **7**(4): p. 261-9.

57. Arcaro, A. and A.S. Guerreiro, *The phosphoinositide 3-kinase pathway in human cancer: genetic alterations and therapeutic implications.* Curr Genomics, 2007. **8**(5): p. 271-306.

58. Kauffmann-Zeh, A., et al., *Suppression of c-Myc-induced apoptosis by Ras signalling through PI(3)K and PKB.* Nature, 1997. **385**(6616): p. 544-8.

59. Robey, R.B. and N. Hay, *Is Akt the "Warburg kinase"?-Akt-energy metabolism interactions and oncogenesis.* Semin Cancer Biol, 2009. **19**(1): p. 25-31.

60. Kim, E., et al., *Regulation of TORC1 by Rag GTPases in nutrient response.* Nat Cell Biol, 2008. **10**(8): p. 935-45.

61. Mao, Z. and W. Zhang, *Role of mTOR in Glucose and Lipid Metabolism.* Int J Mol Sci, 2018. **19**(7).

62. Saxton, R.A. and D.M. Sabatini, *mTOR Signaling in Growth, Metabolism, and Disease.* Cell, 2017. **168**(6): p. 960-976.

63. Cornu, M., V. Albert, and M.N. Hall, *mTOR in aging, metabolism, and cancer.* Curr Opin Genet Dev, 2013. **23**(1): p. 53-62.

64. Chiang, G.G. and R.T. Abraham, *Phosphorylation of mammalian target of rapamycin (mTOR) at Ser-2448 is mediated by p70S6 kinase.* J Biol Chem, 2005. **280**(27): p. 25485-90.

65. Vogt, P.K., *PI 3-kinase, mTOR, protein synthesis and cancer.* Trends Mol Med, 2001. **7**(11): p. 482-4.

66. Kim, J., et al., *AMPK and mTOR regulate autophagy through direct phosphorylation of Ulk1.* Nat Cell Biol, 2011. **13**(2): p. 132-41.

67. Fang, X., et al., *Phosphorylation and inactivation of glycogen synthase kinase 3 by protein kinase A.* Proc Natl Acad Sci U S A, 2000. **97**(22): p. 11960-5.

68. Li, J., et al., *Glycogen synthase kinase 3beta induces apoptosis in cancer cells through increase of survivin nuclear localization.* Cancer Lett, 2008. **272**(1): p. 91-101.

69. Cohen, P. and S. Frame, *The renaissance of GSK3.* Nat Rev Mol Cell Biol, 2001. **2**(10): p. 769-76.

70. Ma, C., et al., *The role of glycogen synthase kinase 3beta in the transformation of epidermal cells.* Cancer Res, 2007. **67**(16): p. 7756-64.

71. Cross, D.A., et al., *The inhibition of glycogen synthase kinase-3 by insulin or insulin-like growth factor 1 in the rat skeletal muscle cell line L6 is blocked by wortmannin, but not by rapamycin: evidence that wortmannin blocks activation of the mitogen-activated protein kinase pathway in L6 cells between Ras and Raf.* Biochem J, 1994. **303 (Pt 1)**: p. 21-6.

72. Zhang, H.H., et al., *S6K1 regulates GSK3 under conditions of mTOR-dependent feedback inhibition of Akt.* Mol Cell, 2006. **24**(2): p. 185-97.

73. Ding, Q., et al., *Erk associates with and primes GSK-3beta for its inactivation resulting in upregulation of beta-catenin.* Mol Cell, 2005. **19**(2): p. 159-70.

74. Mathupala, S.P., Y.H. Ko, and P.L. Pedersen, *Hexokinase II: cancer's double-edged sword acting as both facilitator and gatekeeper of malignancy when bound to mitochondria.* Oncogene, 2006. **25**(34): p. 4777-86.

75. Roskoski, R., Jr., *ERK1/2 MAP kinases: structure, function, and regulation.* Pharmacol Res, 2012. **66**(2): p. 105-43.

76. Molina, J.R. and A.A. Adjei, *The Ras/Raf/MAPK pathway.* J Thorac Oncol, 2006. **1**(1): p. 7-9.

77. Vetter, I.R. and A. Wittinghofer, *The guanine nucleotide-binding switch in three dimensions.* Science, 2001. **294**(5545): p. 1299-304.

78. Cargnello, M. and P.P. Roux, *Activation and function of the MAPKs and their substrates, the MAPK-activated protein kinases.* Microbiol Mol Biol Rev, 2011. **75**(1): p. 50-83.

79. Dhanasekaran, N. and E. Premkumar Reddy, *Signaling by dual specificity kinases.* Oncogene, 1998. **17**(11 Reviews): p. 1447-55.

80. Force, T. and J.V. Bonventre, *Growth factors and mitogen-activated protein kinases.* Hypertension, 1998. **31**(1 Pt 2): p. 152-61.

81. Davis, R.J., *Transcriptional regulation by MAP kinases.* Mol Reprod Dev, 1995. **42**(4): p. 459-67.

82. Maik-Rachline, G., A. Hacohen-Lev-Ran, and R. Seger, *Nuclear ERK: Mechanism of Translocation, Substrates, and Role in Cancer.* Int J Mol Sci, 2019. **20**(5).

83. Parmenter, T.J., et al., *Response of BRAF-mutant melanoma to BRAF inhibition is mediated by a network of transcriptional regulators of glycolysis.* Cancer Discov, 2014. **4**(4): p. 423-33.

84. Caunt, C.J., et al., *MEK1 and MEK2 inhibitors and cancer therapy: the long and winding road.* Nat Rev Cancer, 2015. **15**(10): p. 577-92.

85. Falck Miniotis, M., et al., *MEK1/2 inhibition decreases lactate in BRAF-driven human cancer cells.* Cancer Res, 2013. **73**(13): p. 4039-49.

86. Rowe, I., et al., *Defective glucose metabolism in polycystic kidney disease identifies a new therapeutic strategy.* Nat Med, 2013. **19**(4): p. 488-93.

87. Li, X., et al., *Mitochondria-Translocated PGK1 Functions as a Protein Kinase to Coordinate Glycolysis and the TCA Cycle in Tumorigenesis.* Mol Cell, 2016. **61**(5): p. 705-719.

88. Puzio-Kuter, A.M., *The Role of p53 in Metabolic Regulation.* Genes Cancer, 2011. **2**(4): p. 385-91.

89. Katzen, H.M., D.D. Soderman, and C.E. Wiley, *Multiple forms of hexokinase. Activities associated with subcellular particulate and soluble fractions of normal and streptozotocin diabetic rat tissues.* J Biol Chem, 1970. **245**(16): p. 4081-96.

90. McGarry, T. and U. Fearon, *Cell metabolism as a potentially targetable pathway in RA.* Nat Rev Rheumatol, 2019. **15**(2): p. 70-72.

91. Robey, R.B. and N. Hay, *Mitochondrial hexokinases, novel mediators of the antiapoptotic effects of growth factors and Akt.* Oncogene, 2006. **25**(34): p. 4683-96.

92. Rose, I.A. and J.V. Warms, *Mitochondrial hexokinase. Release, rebinding, and location.* J Biol Chem, 1967. **242**(7): p. 1635-45.

93. Wilson, J.E., *Isozymes of mammalian hexokinase: structure, subcellular localization and metabolic function.* J Exp Biol, 2003. **206**(Pt 12): p. 2049-57.

94. Roberts, D.J. and S. Miyamoto, *Hexokinase II integrates energy metabolism and cellular protection: Akting on mitochondria and TORCing to autophagy.* Cell Death Differ, 2015. **22**(2): p. 248-57.

95. John, S., J.N. Weiss, and B. Ribalet, *Subcellular localization of hexokinases I and II directs the metabolic fate of glucose.* PLoS One, 2011. **6**(3): p. e17674.

96. Mathew, J., et al., *Keratin 8/18 regulation of glucose metabolism in normal versus cancerous hepatic cells through differential modulation of hexokinase status and insulin signaling.* Exp Cell Res, 2013. **319**(4): p. 474-86.

97. Smith, T.A., *Mammalian hexokinases and their abnormal expression in cancer.* Br J Biomed Sci, 2000. **57**(2): p. 170-8.

98. Warmoes, M.O. and J.W. Locasale, *Heterogeneity of glycolysis in cancers and therapeutic opportunities.* Biochem Pharmacol, 2014. **92**(1): p. 12-21.

99. Kudryavtseva, A.V., et al., *Effect of lentivirus-mediated shRNA inactivation of HK1, HK2, and HK3 genes in colorectal cancer and melanoma cells.* BMC Genet, 2016. **17**(Suppl 3): p. 156.

100. Burt, B.M., et al., *Using positron emission tomography with [(18)F]FDG to predict tumor behavior in experimental colorectal cancer.* Neoplasia, 2001. **3**(3): p. 189-95.

101. Rathmell, J.C., et al., *Akt-directed glucose metabolism can prevent Bax conformation change and promote growth factor-independent survival.* Mol Cell Biol, 2003. **23**(20): p. 7315-28.

102. Majewski, N., et al., *Hexokinase-mitochondria interaction mediated by Akt is required to inhibit apoptosis in the presence or absence of Bax and Bak.* Mol Cell, 2004. **16**(5): p. 819-30.

103. THE HUMAN PROTEIN ATLAS. *HK1*. 2018, November 15; Available from: https://www.proteinatlas.org/ENSG00000156515-HK1/pathology.

104. Ali, A., et al., *Survival of patients with non-small-cell lung cancer after a diagnosis of brain metastases.* Curr Oncol, 2013. **20**(4): p. e300-6.

105. Wang, H., et al., *Erratum to: Inhibition of glycolytic enzyme hexokinase II (HK2) suppresses lung tumor growth.* Cancer Cell Int, 2016. **16**: p. 38.

106. Linardou, H., et al., *Assessment of somatic k-RAS mutations as a mechanism associated with resistance to EGFR-targeted agents: a systematic review and meta-analysis of studies in advanced non-small-cell lung cancer and metastatic colorectal cancer.* Lancet Oncol, 2008. **9**(10): p. 962-72.

107. Stephen, A.G., et al., *Dragging ras back in the ring.* Cancer Cell, 2014. **25**(3): p. 272-81.

108. Desilet, N., T.N. Campbell, and F.Y. Choy, *p53-based anti-cancer therapies: An empty promise?* Curr Issues Mol Biol, 2010. **12**(3): p. 143-6.

109. Luengo, A., D.Y. Gui, and M.G. Vander Heiden, *Targeting Metabolism for Cancer Therapy.* Cell Chem Biol, 2017. **24**(9): p. 1161-1180.

110. Goodwin, J., et al., *The distinct metabolic phenotype of lung squamous cell carcinoma defines selective vulnerability to glycolytic inhibition.* Nat Commun, 2017. **8**: p. 15503.

111. Christofk, H.R., et al., *The M2 splice isoform of pyruvate kinase is important for cancer metabolism and tumour growth.* Nature, 2008. **452**(7184): p. 230-3.

112. Mori, C., et al., *Testis-specific expression of mRNAs for a unique human type 1 hexokinase lacking the porin-binding domain.* Mol Reprod Dev, 1996. **44**(1): p. 14-22.

113. Mori, C., et al., *Unique hexokinase messenger ribonucleic acids lacking the porin-binding domain are developmentally expressed in mouse spermatogenic cells.* Biol Reprod, 1993. **49**(2): p. 191-203.

114. Zhao, Y., et al., *A P53-Deficiency Gene Signature Predicts Recurrence Risk of Patients with Early-Stage Lung Adenocarcinoma.* Cancer Epidemiol Biomarkers Prev, 2018. **27**(1): p. 86-95.

115. Okayama, H., et al., *Identification of genes upregulated in ALK-positive and EGFR/KRAS/ALK-negative lung adenocarcinomas.* Cancer Res, 2012. **72**(1): p. 100-11.

116. Ran, F.A., et al., *Genome engineering using the CRISPR-Cas9 system.* Nat Protoc, 2013. **8**(11): p. 2281-2308.

117. Arzoine, L., et al., *Voltage-dependent anion channel 1-based peptides interact with hexokinase to prevent its anti-apoptotic activity.* J Biol Chem, 2009. **284**(6): p. 3946-55.

118. Rosano, C., *Molecular model of hexokinase binding to the outer mitochondrial membrane porin (VDAC1): Implication for the design of new cancer therapies.* Mitochondrion, 2011. **11**(3): p. 513-9.

119. Pastorino, J.G. and J.B. Hoek, *Regulation of hexokinase binding to VDAC.* J Bioenerg Biomembr, 2008. **40**(3): p. 171-82.

120. Schindler, A. and E. Foley, *Hexokinase 1 blocks apoptotic signals at the mitochondria.* Cell Signal, 2013. **25**(12): p. 2685-92.

121. Olaussen, K.A., et al., *DNA repair by ERCC1 in non-small-cell lung cancer and cisplatin-based adjuvant chemotherapy.* N Engl J Med, 2006. **355**(10): p. 983-91.

122. Dasari, S. and P.B. Tchounwou, *Cisplatin in cancer therapy: molecular mechanisms of action.* Eur J Pharmacol, 2014. **740**: p. 364-78.

123. Sborov, D.W., B.M. Haverkos, and P.J. Harris, *Investigational cancer drugs targeting cell metabolism in clinical development.* Expert Opin Investig Drugs, 2015. **24**(1): p. 79-94.

124. Gottlob, K., et al., *Inhibition of early apoptotic events by Akt/PKB is dependent on the first committed step of glycolysis and mitochondrial hexokinase.* Genes Dev, 2001. **15**(11): p. 1406-18.

125. Altomare, D.A., et al., *AKT and mTOR phosphorylation is frequently detected in ovarian cancer and can be targeted to disrupt ovarian tumor cell growth.* Oncogene, 2004. **23**(34): p. 5853-7.

126. Eldar-Finkelman, H., et al., *Inactivation of glycogen synthase kinase-3 by epidermal growth factor is mediated by mitogen-activated protein kinase/p90 ribosomal protein S6 kinase signaling pathway in NIH/3T3 cells.* J Biol Chem, 1995. **270**(3): p. 987-90.

127. Mebratu, Y. and Y. Tesfaigzi, *How ERK1/2 activation controls cell proliferation and cell death: Is subcellular localization the answer?* Cell Cycle, 2009. **8**(8): p. 1168-75.

128. Olive, P.L. and J.P. Banath, *Kinetics of H2AX phosphorylation after exposure to cisplatin.* Cytometry B Clin Cytom, 2009. **76**(2): p. 79-90.

129. Doherty, J. and E.H. Baehrecke, *Life, death and autophagy.* Nat Cell Biol, 2018. **20**(10): p. 1110-1117.

130. Mathew, R., V. Karantza-Wadsworth, and E. White, *Role of autophagy in cancer.* Nat Rev Cancer, 2007. **7**(12): p. 961-7.

131. Liu, P.P., et al., *Metabolic regulation of cancer cell side population by glucose through activation of the Akt pathway.* Cell Death Differ, 2014. **21**(1): p. 124-35.

132. Porporato, P.E., et al., *Mitochondrial metabolism and cancer.* Cell Res, 2018. **28**(3): p. 265-280.

133. Mathupala, S.P., C. Heese, and P.L. Pedersen, *Glucose catabolism in cancer cells. The type II hexokinase promoter contains functionally active response elements for the tumor suppressor p53.* J Biol Chem, 1997. **272**(36): p. 22776-80.

134. Kim, J., et al., *Wild-Type p53 Promotes Cancer Metabolic Switch by Inducing PUMA-Dependent Suppression of Oxidative Phosphorylation.* Cancer Cell, 2019. **35**(2): p. 191-203.e8.

135. Cesar Mde, C. and J.E. Wilson, *Further studies on the coupling of mitochondrially bound hexokinase to intramitochondrially compartmented ATP, generated by oxidative phosphorylation.* Arch Biochem Biophys, 1998. **350**(1): p. 109-17.

136. Papa, S., P.M. Choy, and C. Bubici, *The ERK and JNK pathways in the regulation of metabolic reprogramming.* Oncogene, 2019. **38**(13): p. 2223-2240.

137. Roberts, D.J., et al., *Akt phosphorylates HK-II at Thr-473 and increases mitochondrial HK-II association to protect cardiomyocytes.* J Biol Chem, 2013. **288**(33): p. 23798-806.

138. Yang, W., et al., *ERK1/2-dependent phosphorylation and nuclear translocation of PKM2 promotes the Warburg effect.* Nat Cell Biol, 2012. **14**(12): p. 1295-304.

139. Frame, S. and P. Cohen, *GSK3 takes centre stage more than 20 years after its discovery.* Biochem J, 2001. **359**(Pt 1): p. 1-16.

140. Pastorino, J.G., J.B. Hoek, and N. Shulga, *Activation of glycogen synthase kinase 3beta disrupts the binding of hexokinase II to mitochondria by phosphorylating voltage-*

dependent anion channel and potentiates chemotherapy-induced cytotoxicity. Cancer Res, 2005. **65**(22): p. 10545-54.

141. Liang, M.H. and D.M. Chuang, *Regulation and function of glycogen synthase kinase-3 isoforms in neuronal survival.* J Biol Chem, 2007. **282**(6): p. 3904-17.
142. Tang, D., et al., *ERK activation mediates cell cycle arrest and apoptosis after DNA damage independently of p53.* J Biol Chem, 2002. **277**(15): p. 12710-7.
143. Wang, X., J.L. Martindale, and N.J. Holbrook, *Requirement for ERK activation in cisplatin-induced apoptosis.* J Biol Chem, 2000. **275**(50): p. 39435-43.
144. Kim, H.S., et al., *Withdrawal: Inhibition of AMP-activated protein kinase sensitizes cancer cells to cisplatin-induced apoptosis via hyper-induction of p53.* J Biol Chem, 2018. **293**(46): p. 18015.

8 APPENDIX A SUPPLEMENTARY MATERIAL and METHOD

8.1 Sample Preparation for TEM

Cells were fixed with fixative mixture (0.08 M cacodylate pH 7.4, 2.5% paraformaldehyde, 1.25% glutaraldehyde and 2 mM calcium chloride) for 2 h at 4 °C washed and, were post-fixed in 2% OsO_4 aqueous solution for 20 min. Cells were incubated in 2.5% ferrocyanide for 20 min. Sequentially, the cells were incubated in 1% thiocarbohydrazide at 40 °C for 15 min, 2% OsO_4 for 20 min and 1% uranyl acetate at 4 °C for 30 min. Cells were warmed up to 50 °C for 30 min in uranyl acetate, washed twice in nanopure filtered water, were incubated in lead aspartate at 50 °C for 20 min. The samples were then dehydrated with graded alcohol series and then embedded in epoxy resin. After sectioning using an ultramicrotome (Leica EM UC7), samples were analyzed using an electron microscope (Carl Zeiss, Gemini 500).

8.2 DNA Fragmentation analysis

Standard Sensitivity NGS Fragment Analysis Kit (DNF-473-0500) is used for DNA fragmentation experiment and for dsDNA 905 Reagent Kit ((DNF-905-K0500) is used for visualization of 1-500bp PCR (Advanced Analytical Technologies, Inc., USA), according to manuscript protocol.

8.3 Structure Preparation

We used crystal structures of HK1b (PDB ID: 1QHA) and HK2 (PDB ID: 2NZT), whereas HK1c was modeled using SWISS-Homology-Modeling-Software. Unresolved parts of the crystal structures were modeled with Swiss-Modeller, and loop regions were refined with ModLoop. The protonation states of residues were determined using PROPKA. Glucose was used in beta conformation. ATP and Mg2+ were translated to each system from crystal structure of Glucokinase (PDB ID: 3FGU).

8.4 Molecular Dynamics Simulations

MD simulations were performed with GROMACS 5.1.4 employing CHARMM 36 force-field. Systems were subjected minimized using a conjugate gradient algorithm. All systems were energy relaxed with 1000 steps of steepest-descent. The systems were equilibrated using NVT ensemble with Berendsen- algorithm. The final structures were run in NPT ensemble at 1 atm and 310 K. MD simulations were run for 300-ns. All coordinates were saved at 2-ps intervals for analysis. Long-range electrostatic forces were handled using PME, and Van der Waals forces treated with a 0.9-nm-cut-off. Water molecules were modelled with TIP3P model.